

Supporting Information

Design and synthesis of new 1,2,4-Oxadiazole/Quinazoline-4-one hybrids with antiproliferative activity as multitargeted inhibitors

Amira M. Mohamed¹, Ola F. Abou-Ghadir¹, Yaser A. Mostafa¹, Kholood A. Dahlous², Stefan Bräse^{3*}, Bahaa G. M. Youssif^{1*}

¹Pharmaceutical Organic Chemistry Department, Faculty of Pharmacy, Assiut University, Assiut 71526, Egypt; ²Department of Chemistry, College of Science, King Saud University, Riyadh 11451, Saudi Arabia; ³Institute of Biological and Chemical Systems, IBCS-FMS, Karlsruhe Institute of Technology, 76131 Karlsruhe, Germany

**To whom correspondence should be addressed:*

Bahaa G. M. Youssif, Ph.D. Pharmaceutical Organic Chemistry Department, Faculty of Pharmacy, Assiut University, Assiut 71526, Egypt.

Tel.: (002)-01098294419

E-mail address: bgyoussif2@gmail.com, bahaa.youssif@pharm.aun.edu.eg

Stefan Bräse

Institute of Biological and Chemical Systems, IBCS-FMS, Karlsruhe Institute of Technology, 76131 Karlsruhe, Germany. E-mail: braese@kit.edu

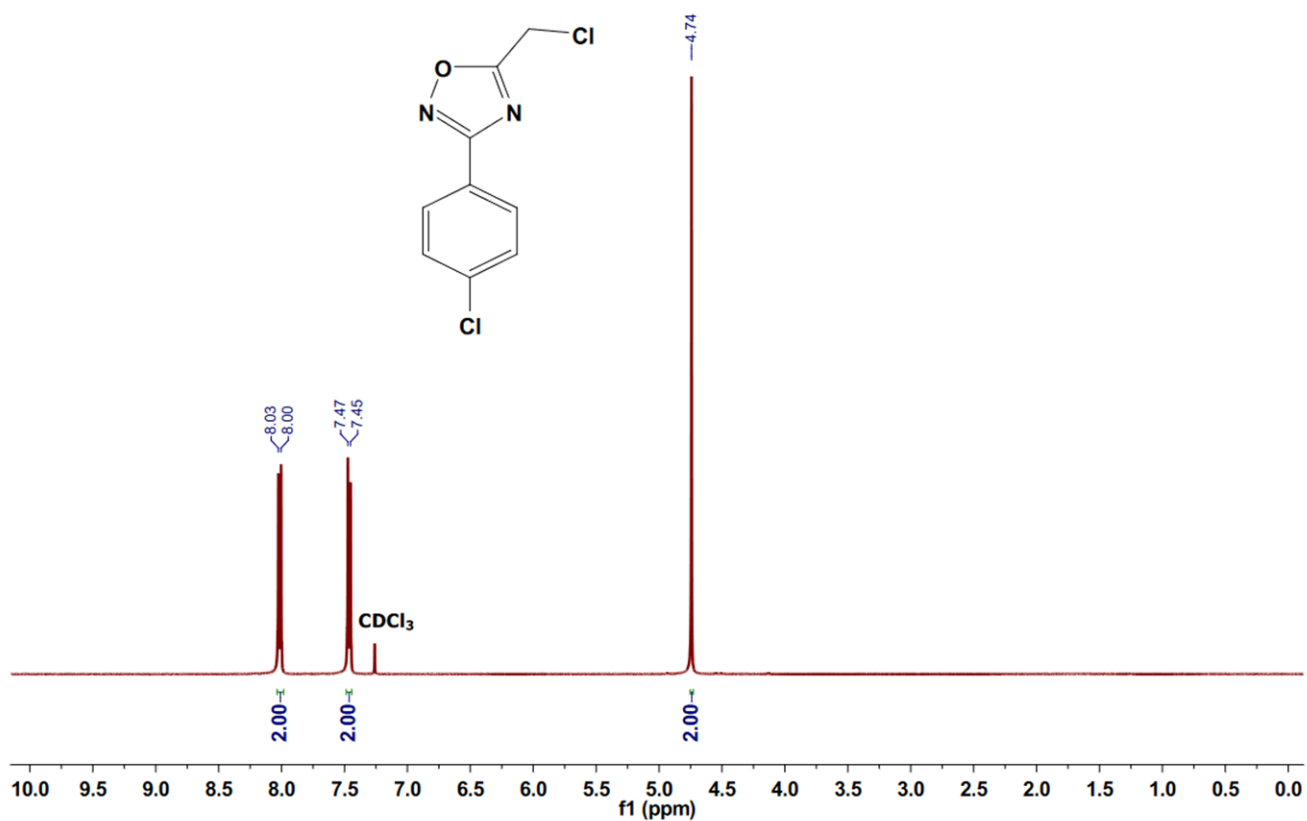


Figure S1: ¹H NMR spectrum (400 MHz, CDCl₃) of compound **8b**

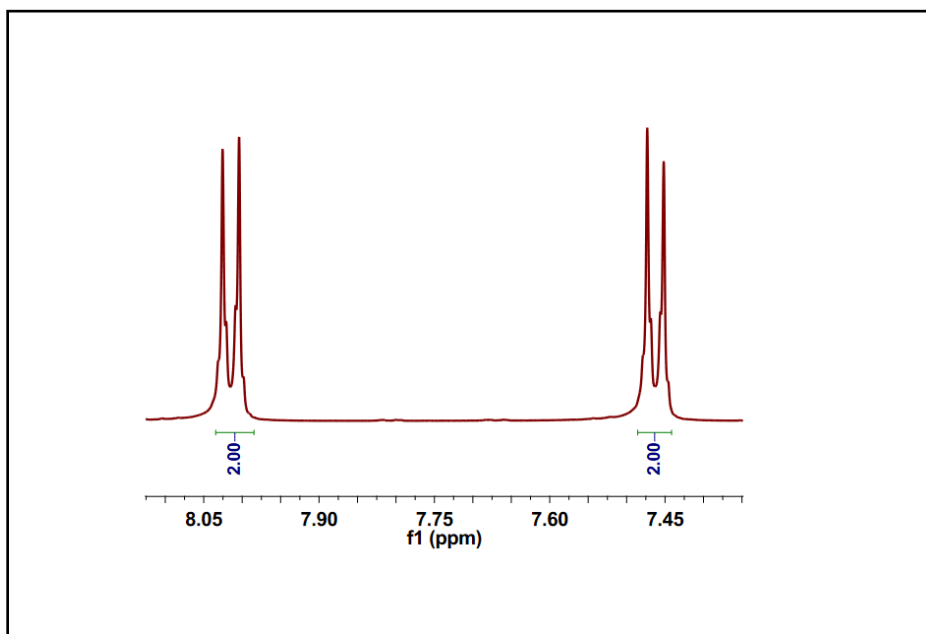


Figure S2: Expanded aromatic region of ¹H NMR spectrum (400 MHz, CDCl₃) of compound **8b**

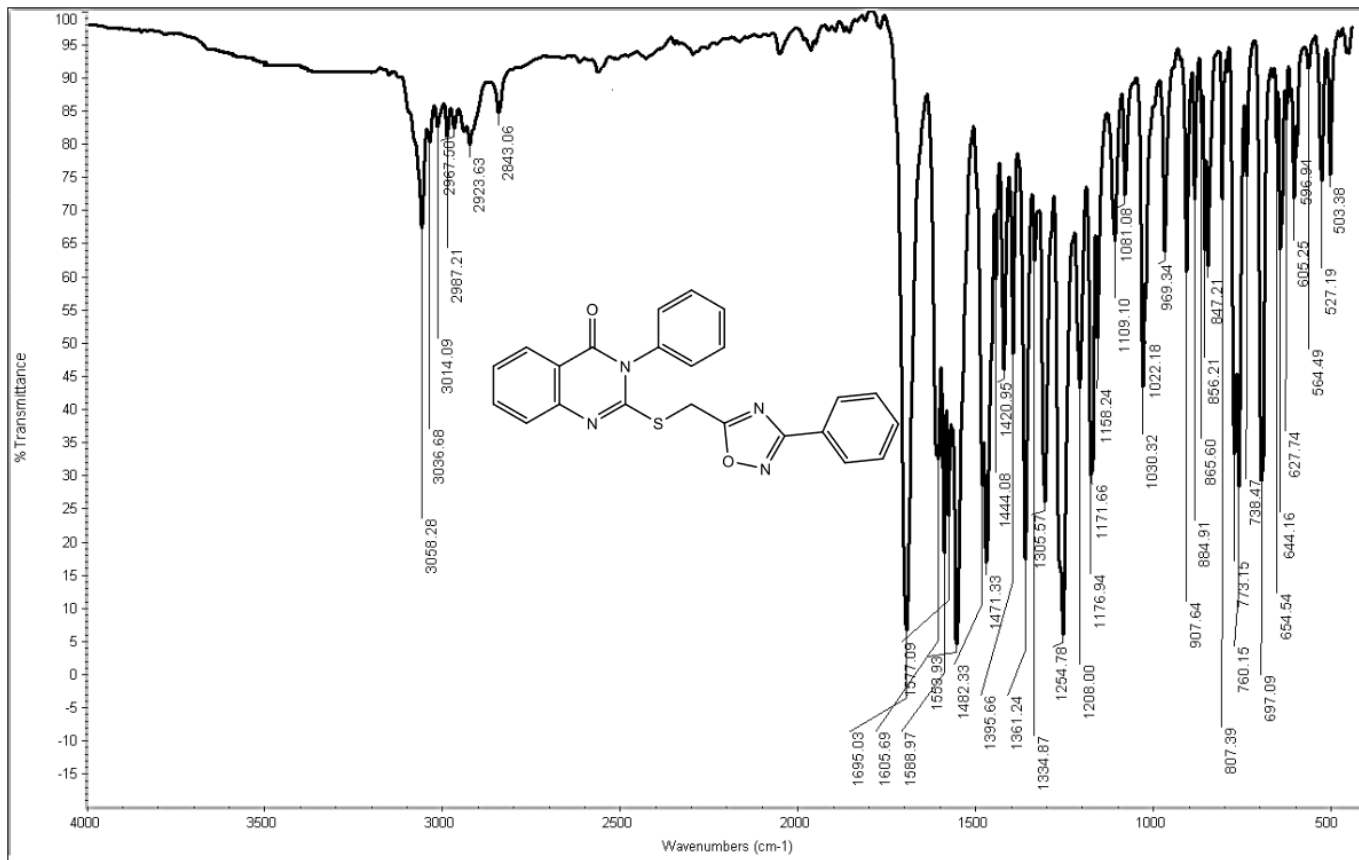


Figure S3: FTIR spectrum of compound 9a

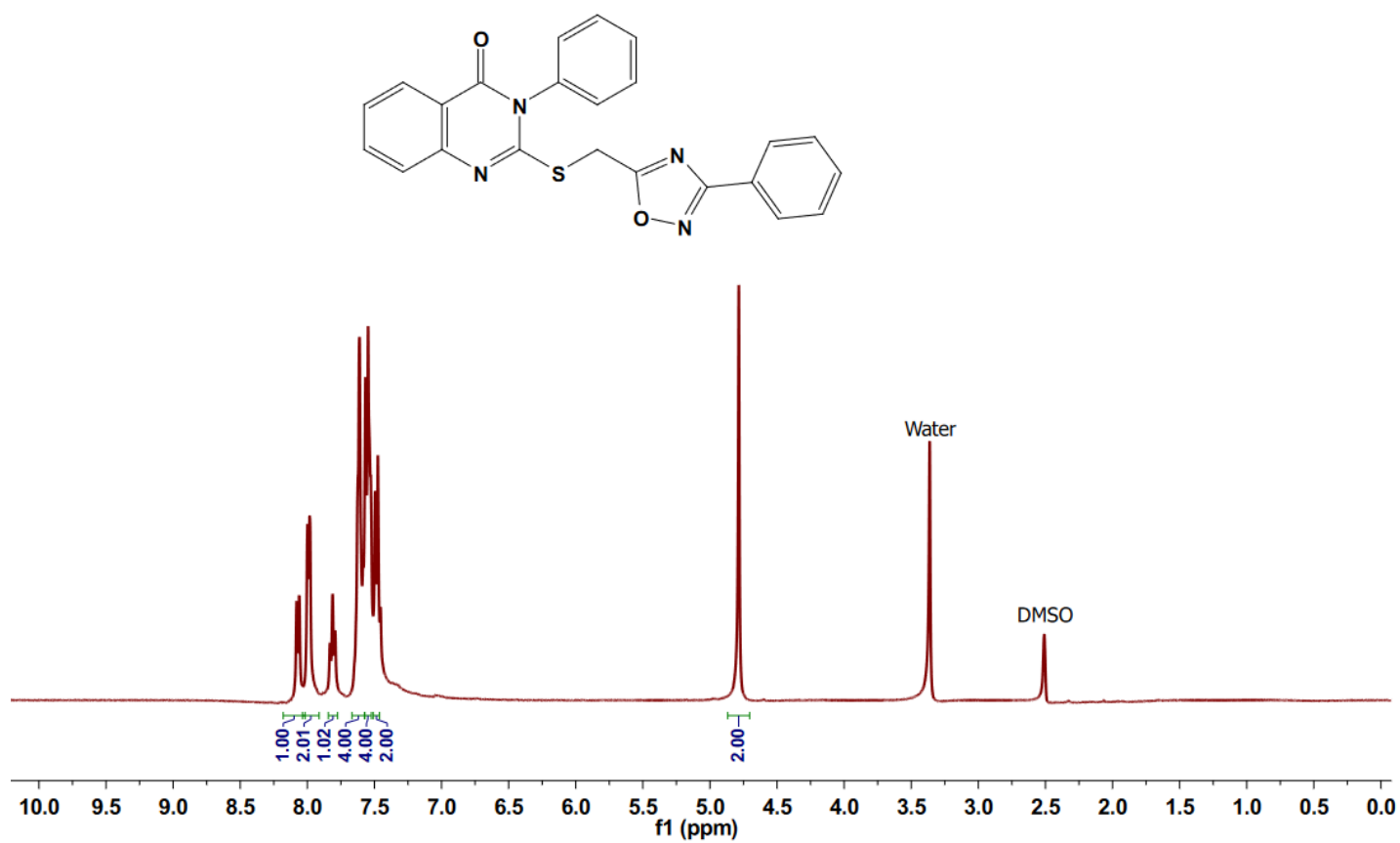


Figure S4: ¹H NMR spectrum (400 MHz, DMSO-*d*₆) of compound **9a**

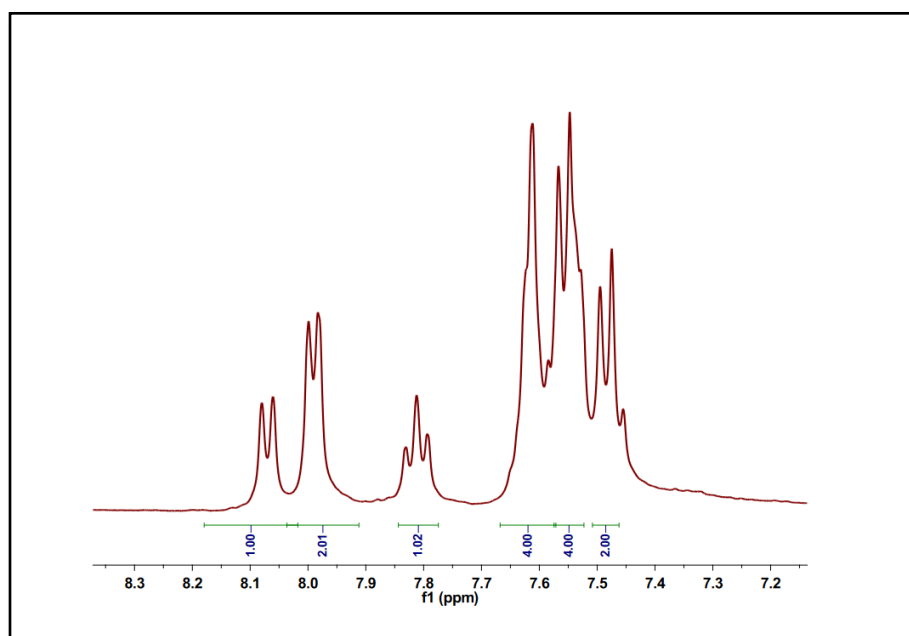


Figure S5: Expanded aromatic region of ¹H NMR spectrum (400 MHz, DMSO-*d*₆) of compound **9a**

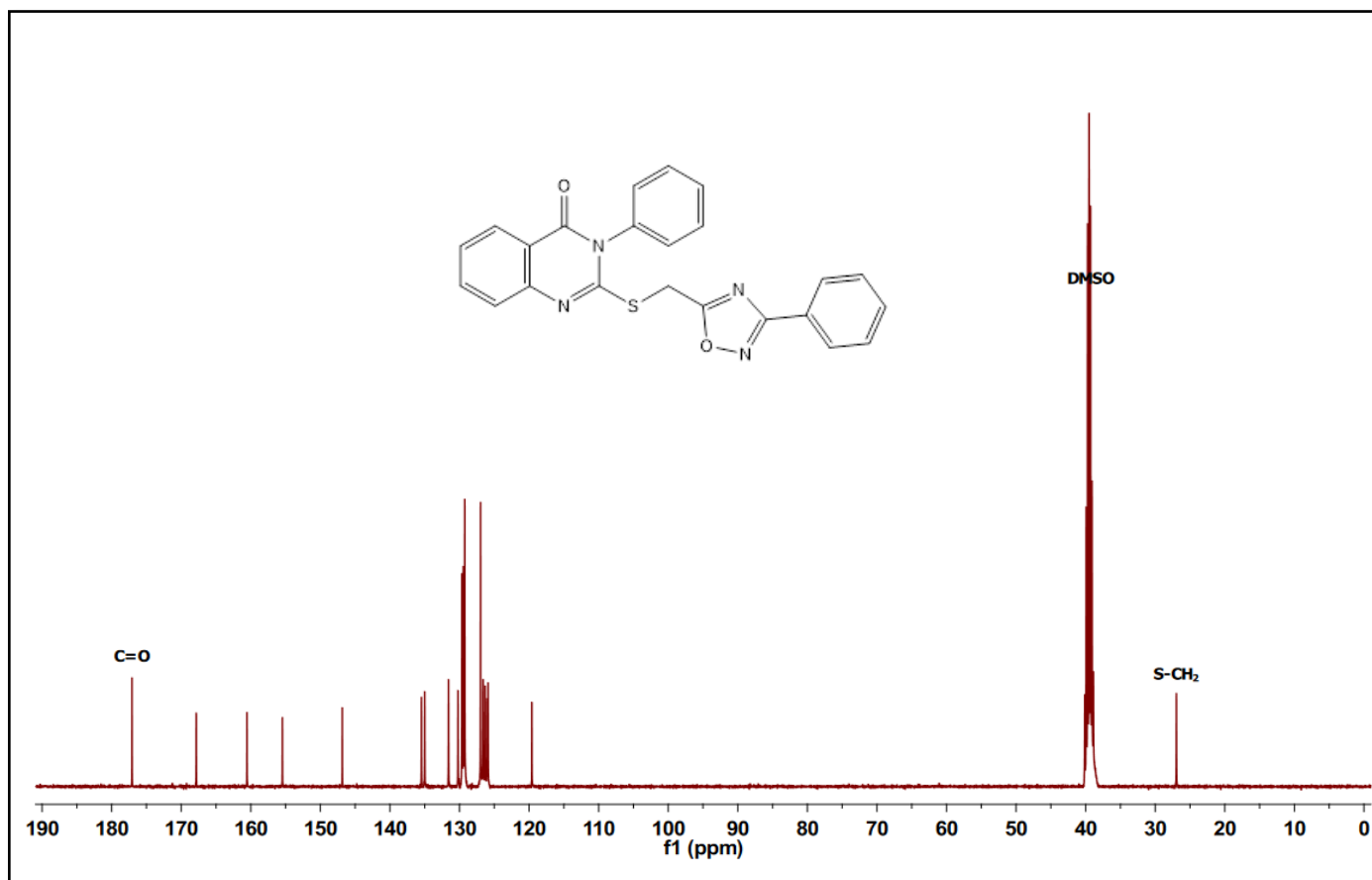


Figure S6: ^{13}C NMR spectrum (100 MHz, $\text{DMSO-}d_6$) of compound **9a**

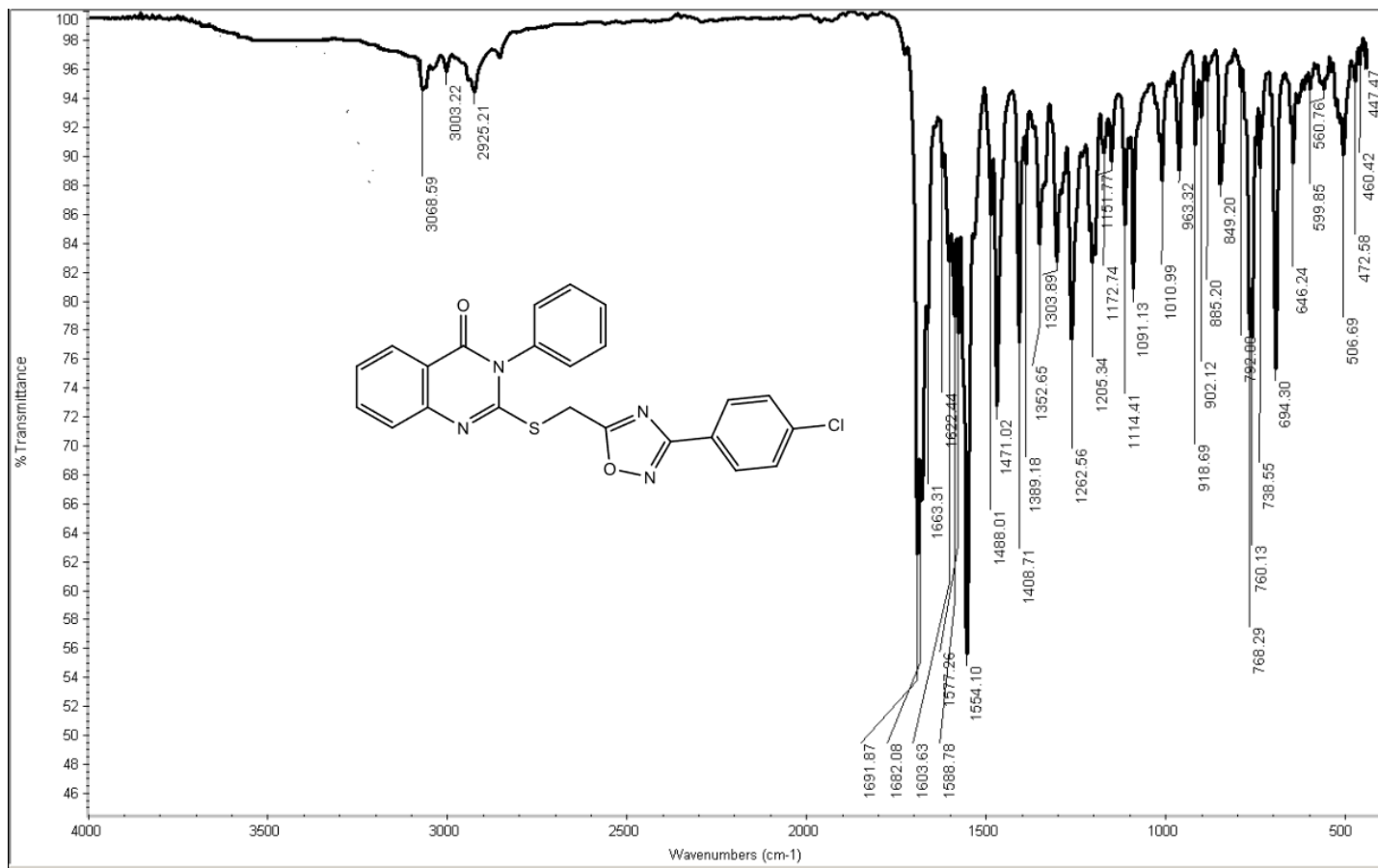


Figure S7: FTIR spectrum of compound 9b

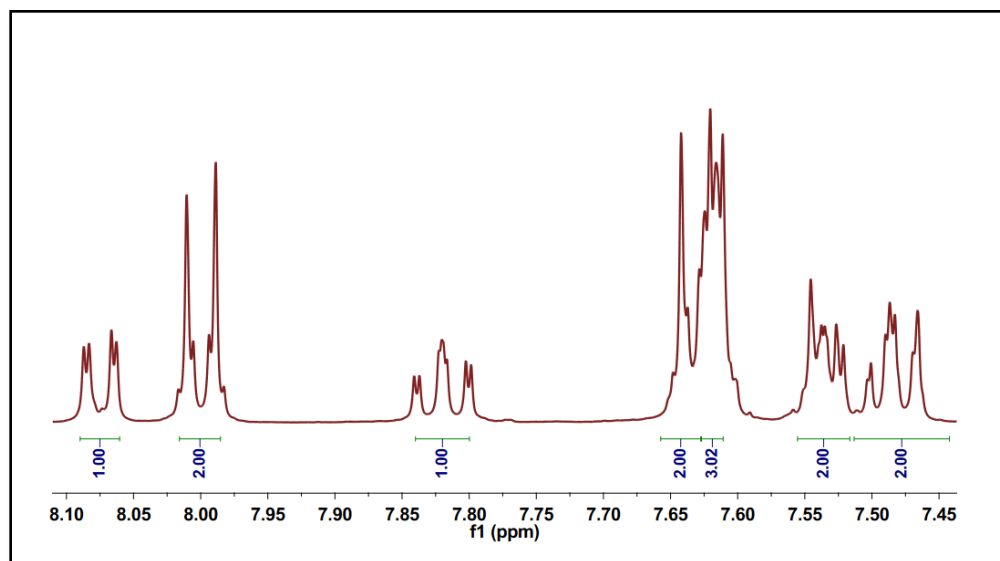
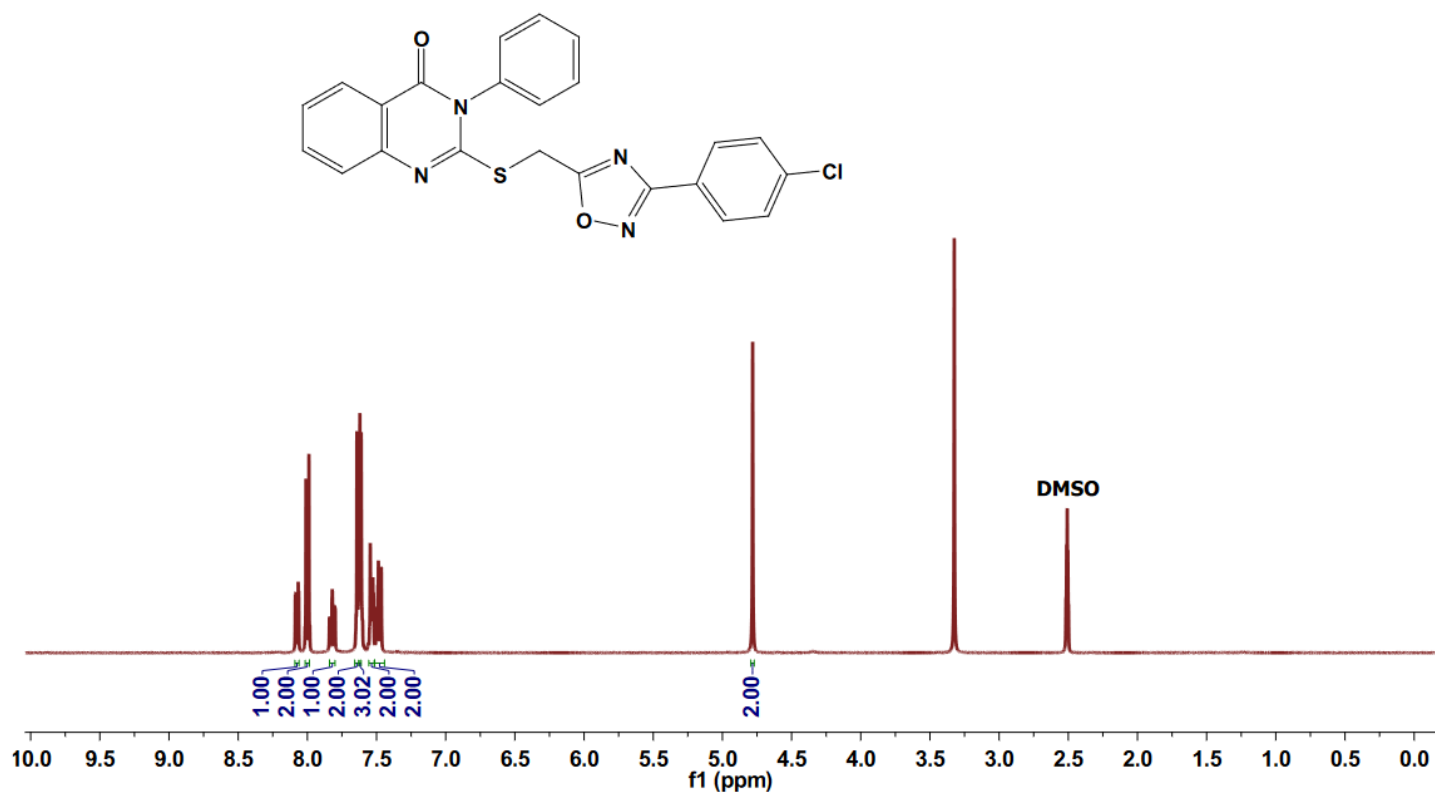
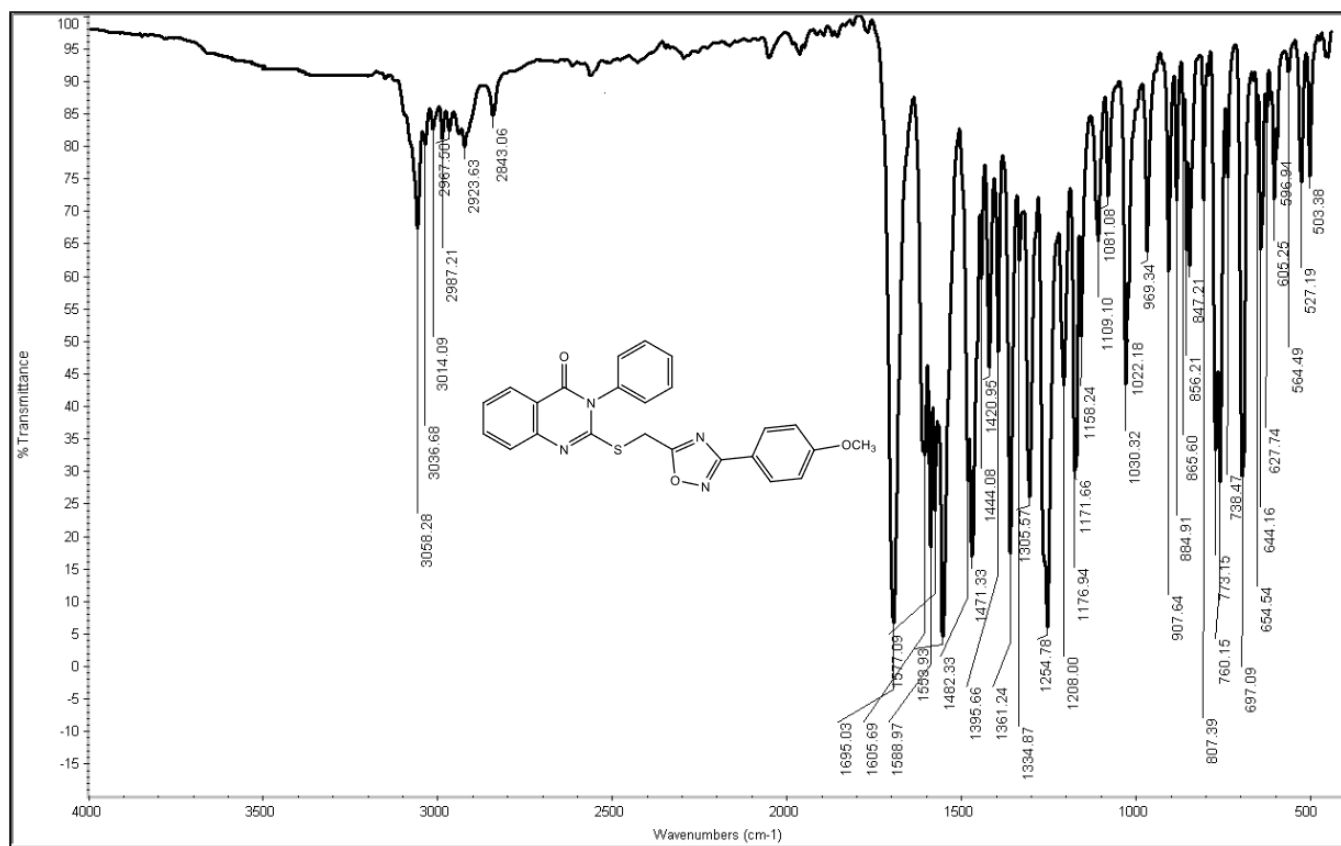
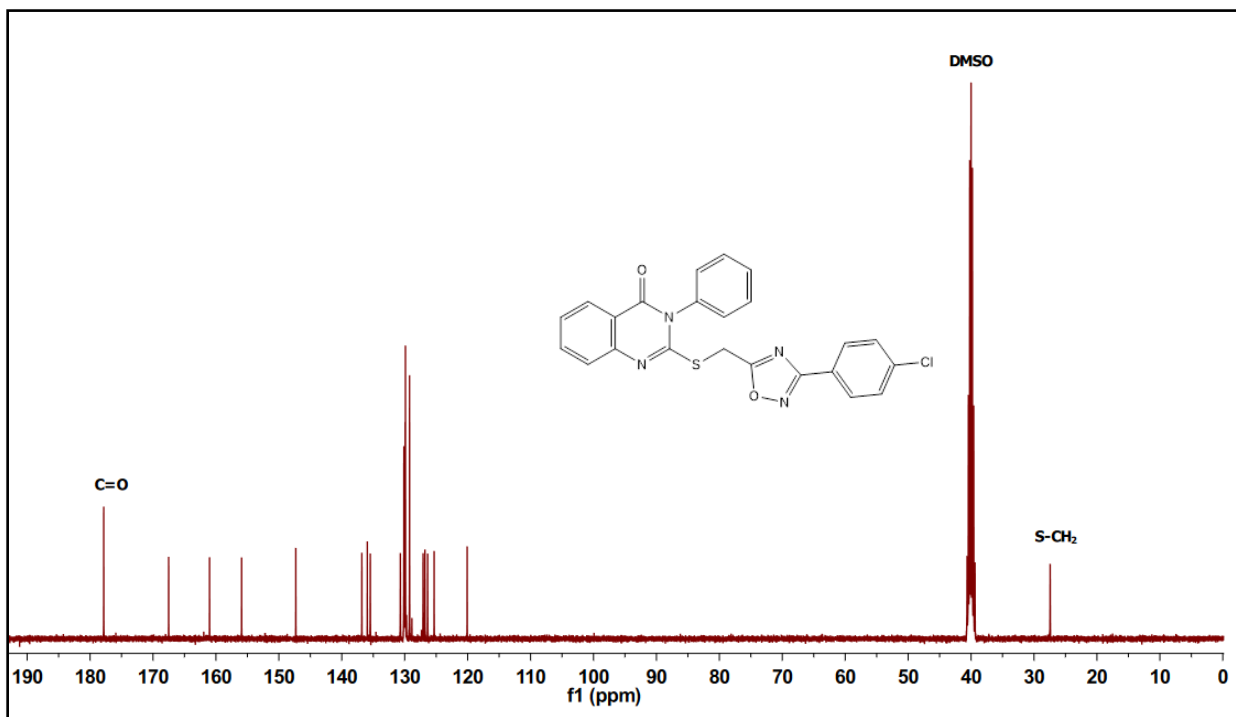


Figure S9: Expanded aromatic region of ^1H NMR spectrum (400 MHz, $\text{DMSO-}d_6$) of compound **9b**



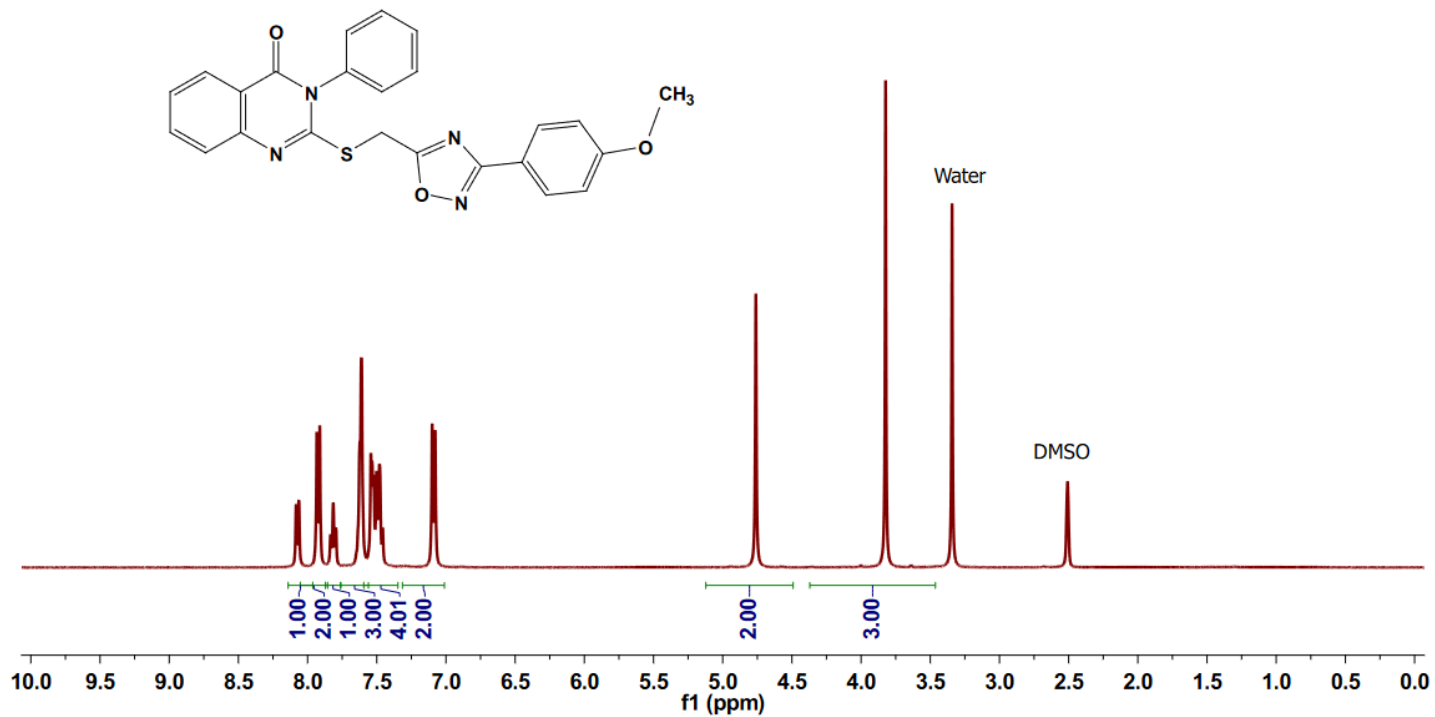


Figure S12: ¹H NMR spectrum (400 MHz, DMSO-*d*₆) of compound **9c**

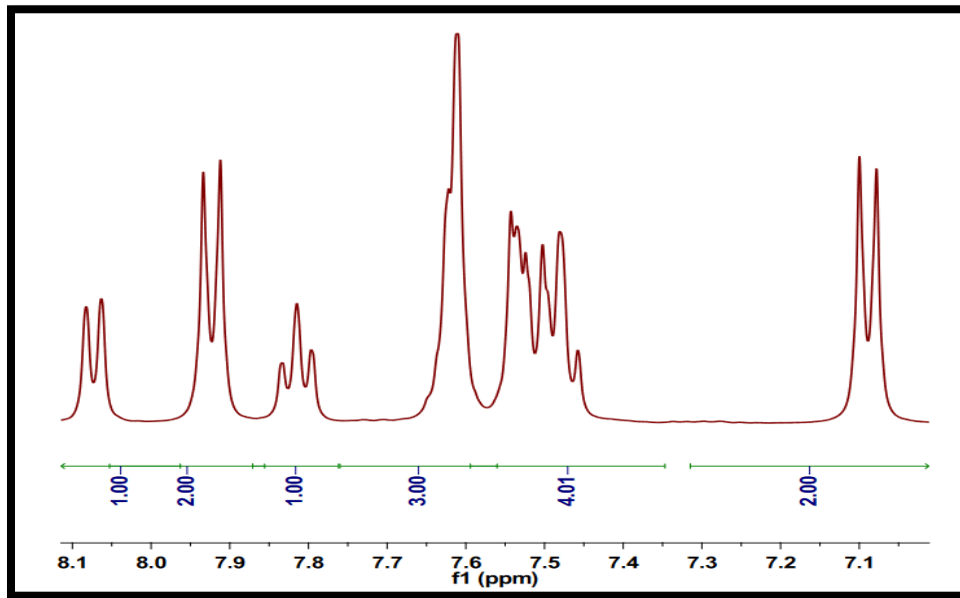


Figure S13: Expanded aromatic region of ¹H NMR spectrum (400 MHz, DMSO-*d*₆) of compound **9c**

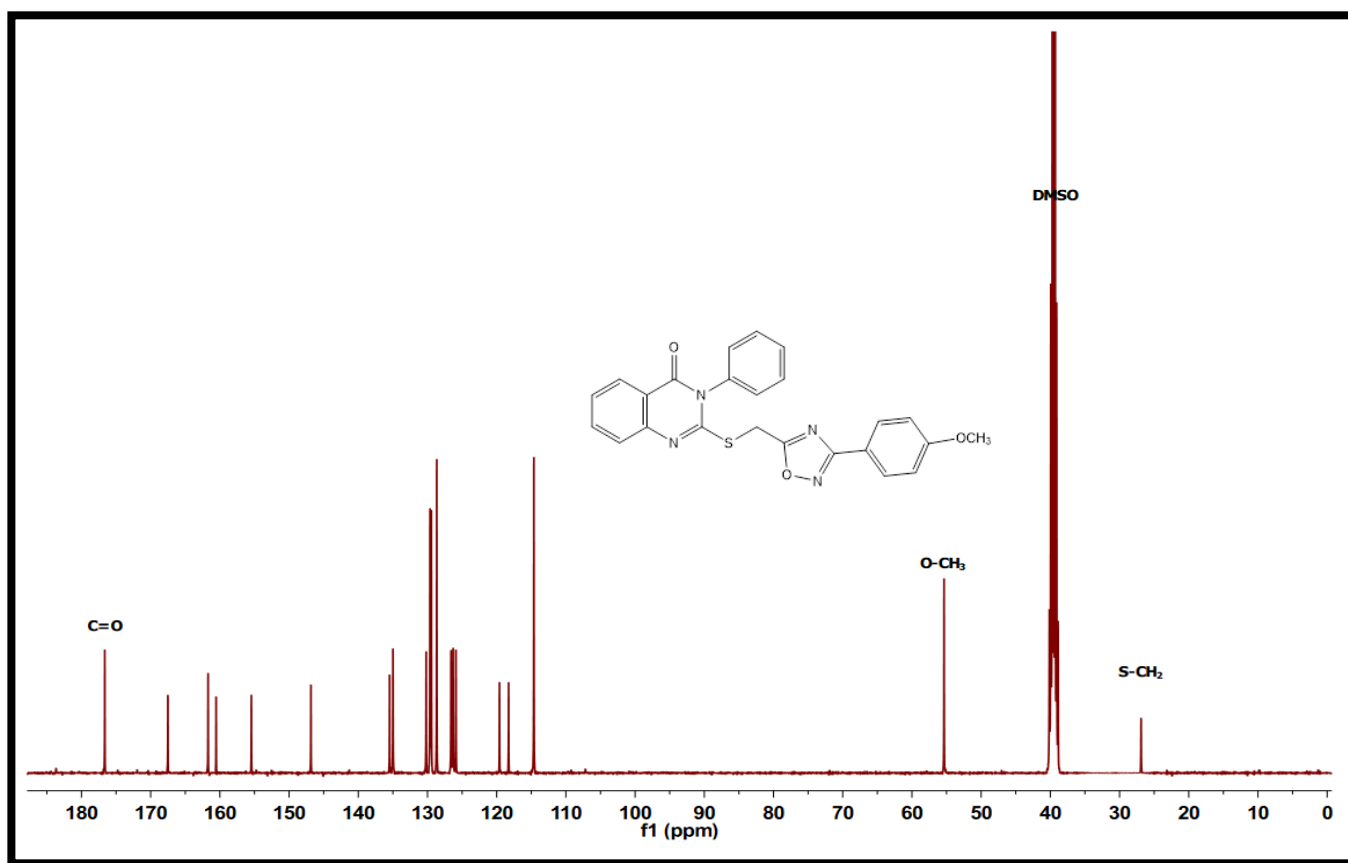


Figure S14: ^{13}C NMR spectrum (100 MHz, $\text{DMSO-}d_6$) of compound **9c**

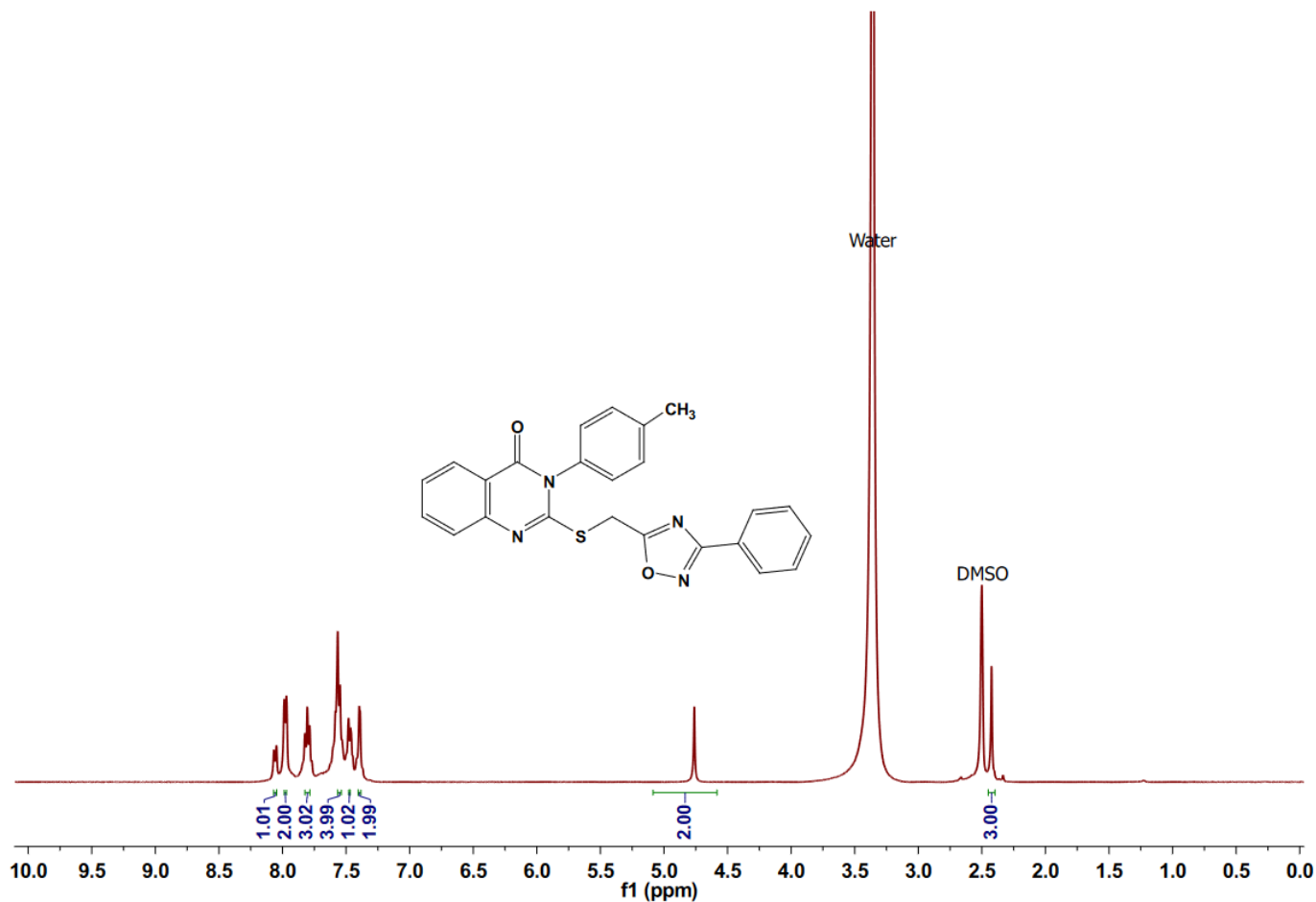


Figure S15: ^1H NMR spectrum (400 MHz, $\text{DMSO-}d_6$) of compound **9d**

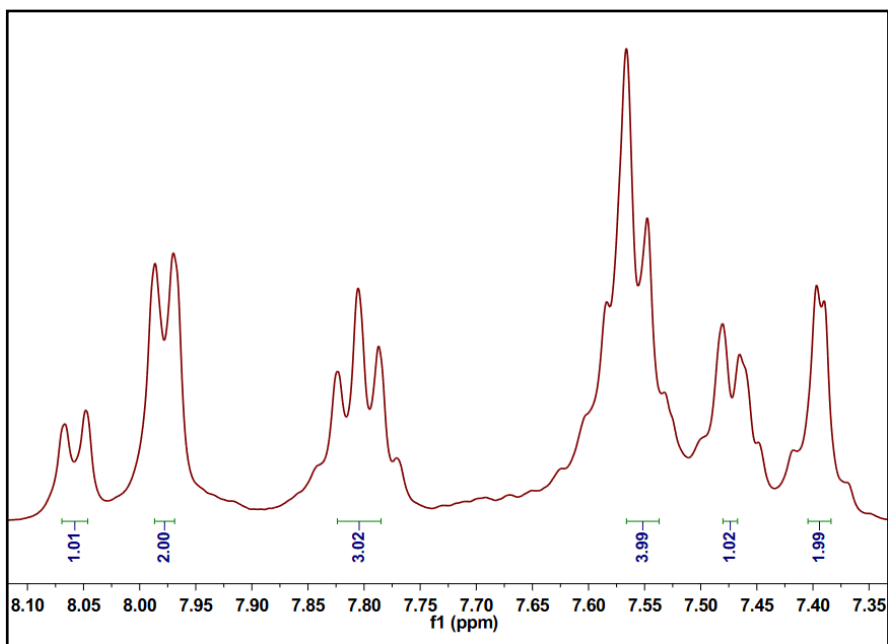


Figure S16: Expanded aromatic region of ^1H NMR spectrum (400 MHz, $\text{DMSO-}d_6$) of compound **9d**

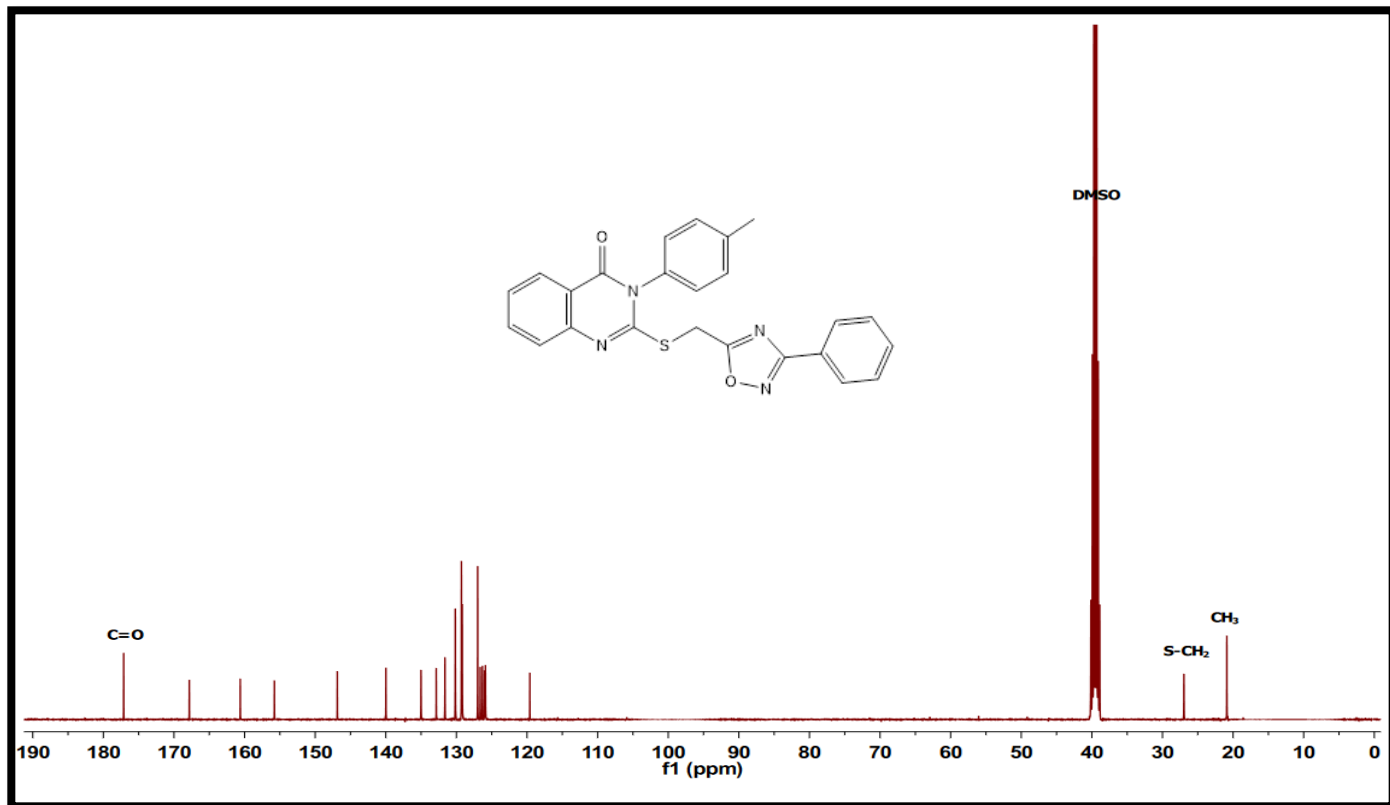


Figure S17: ^{13}C NMR spectrum (100 MHz, $\text{DMSO-}d_6$) of compound **9d**

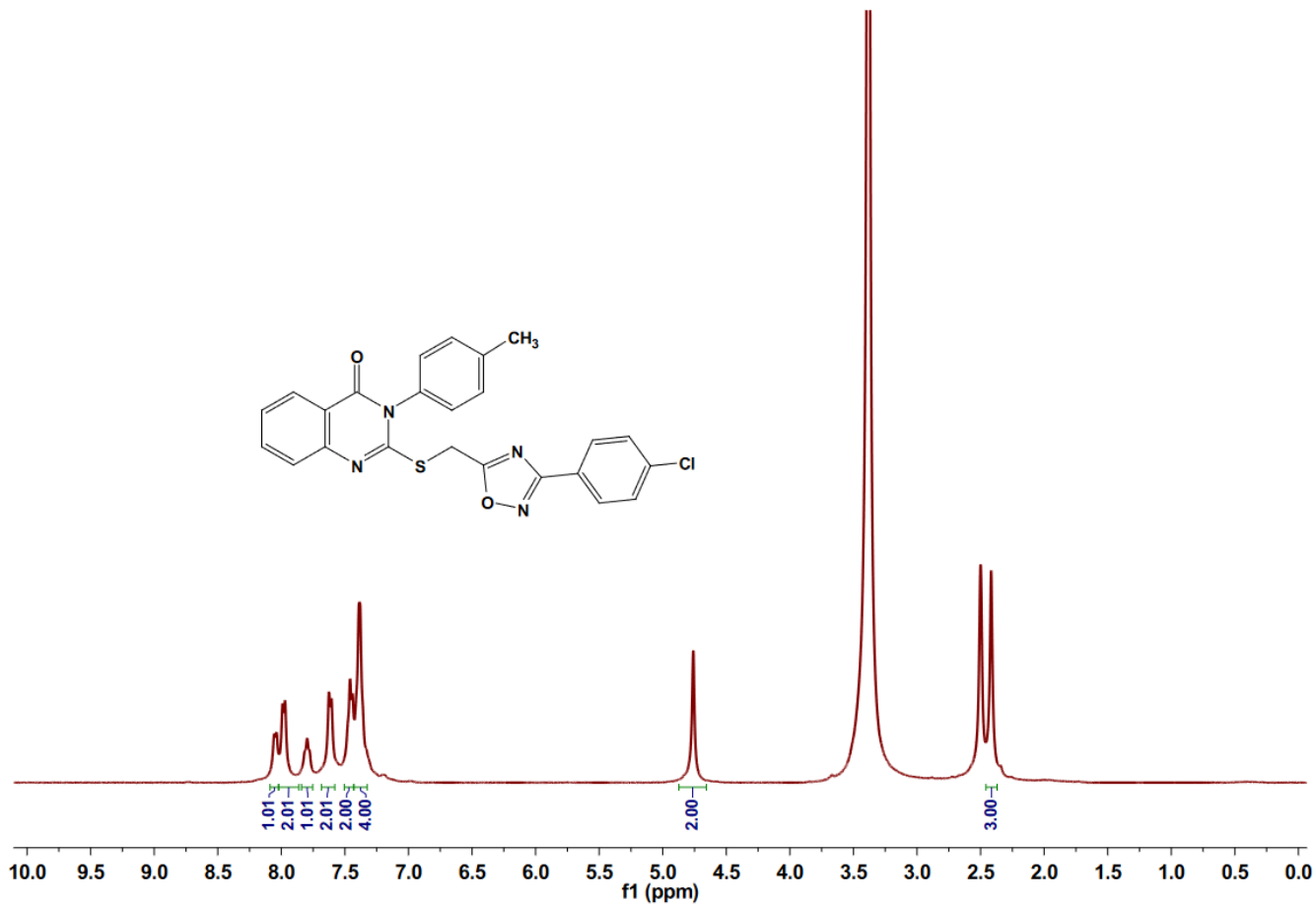


Figure S18: $^1\text{H NMR}$ spectrum (400 MHz, $\text{DMSO-}d_6$) of compound **9e**.

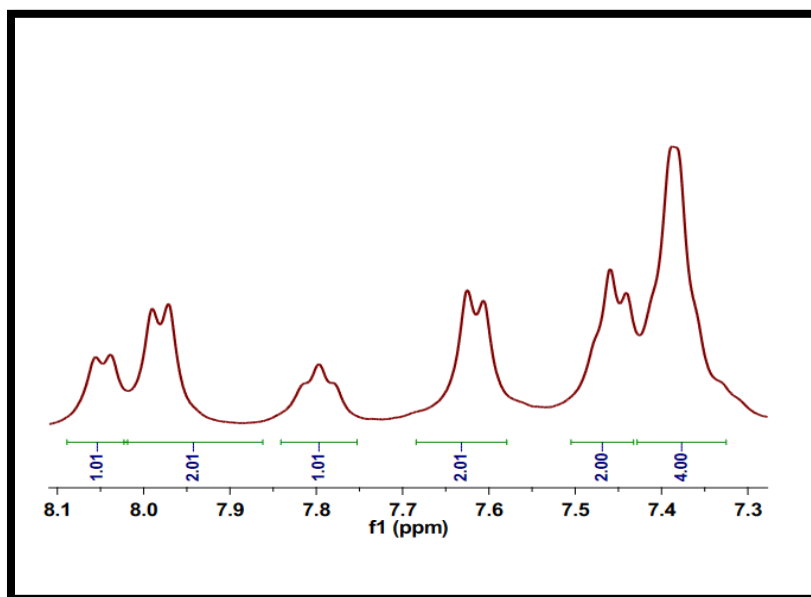


Figure S19: Expanded aromatic region of $^1\text{H NMR}$ spectrum (400 MHz, $\text{DMSO-}d_6$) of compound **9e**

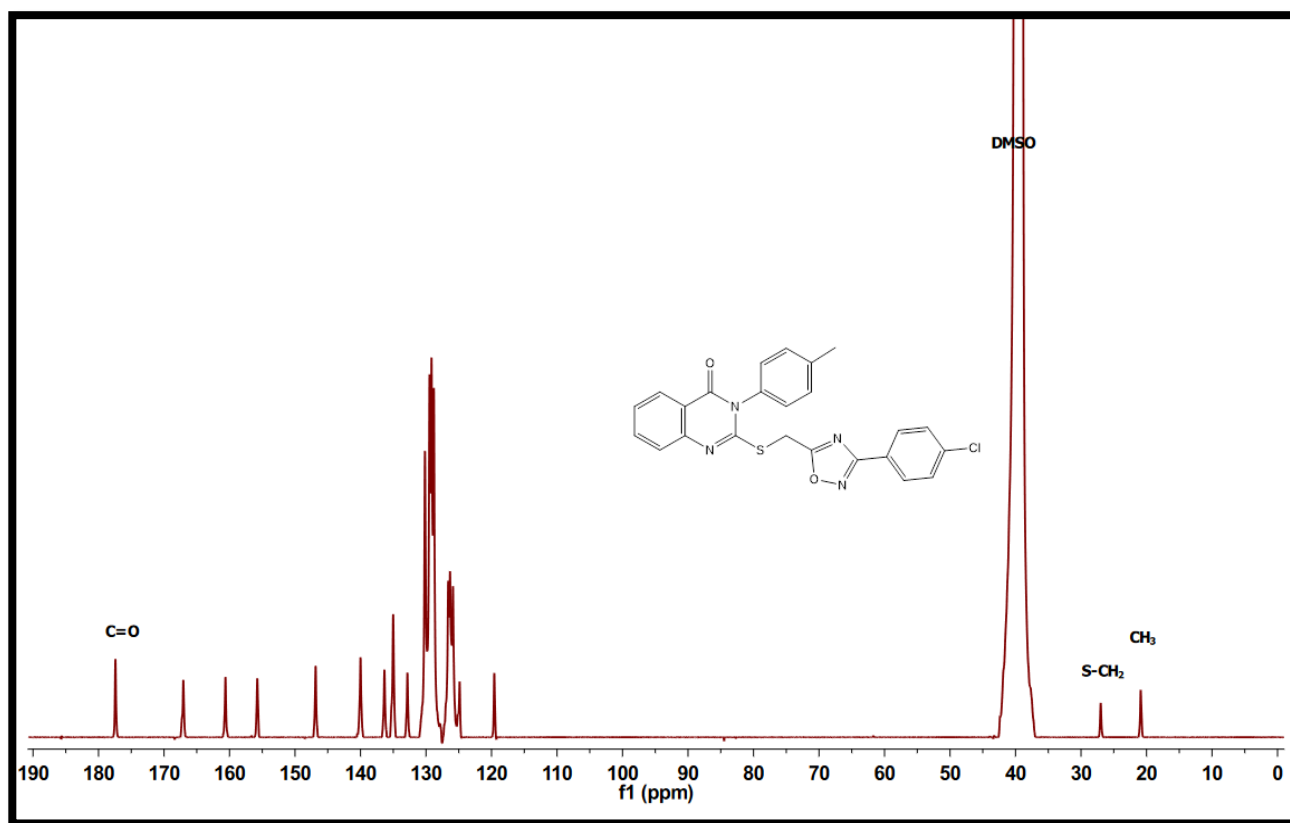


Figure S20: ^{13}C NMR spectrum (100 MHz, $\text{DMSO-}d_6$) of compound **9e**

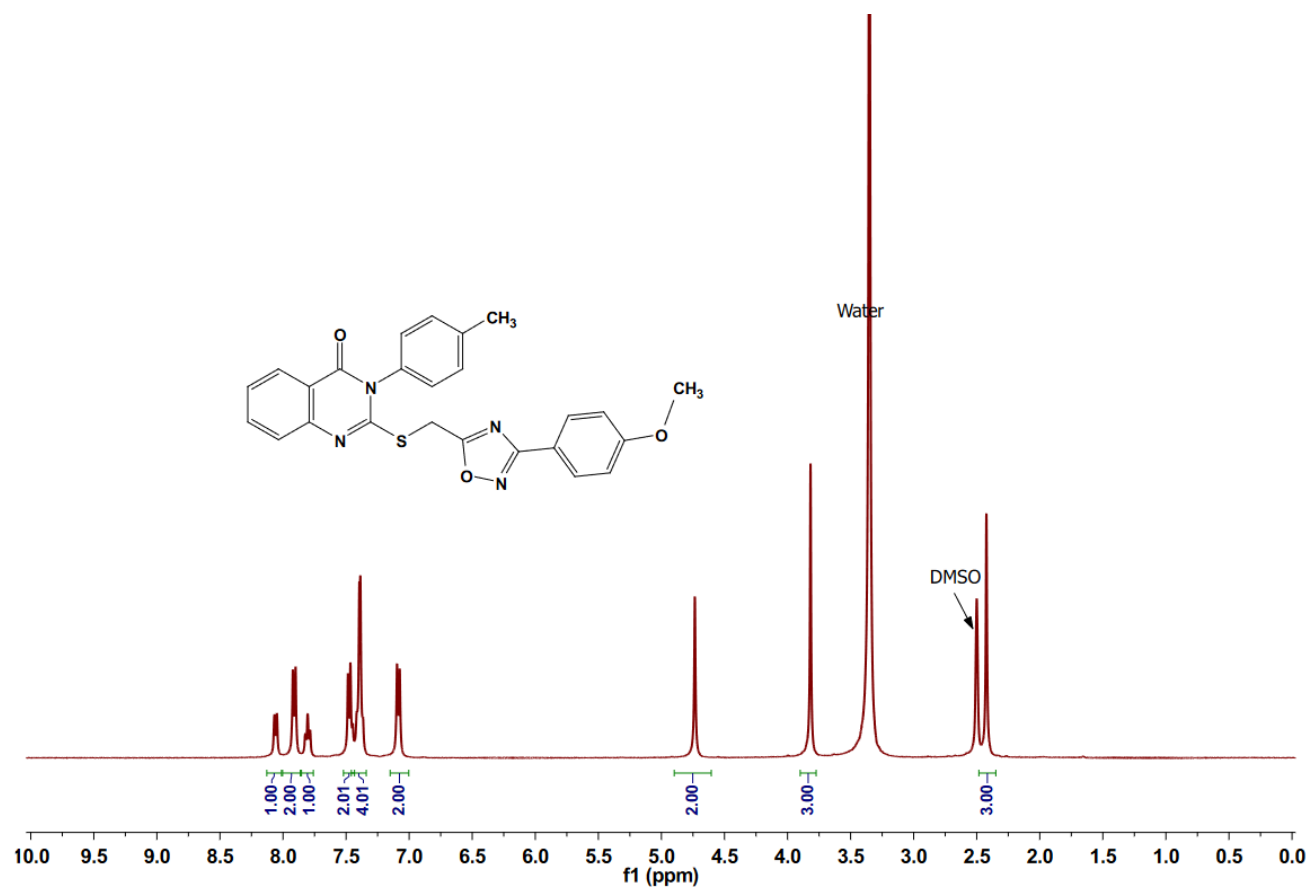


Figure S21: ^1H NMR spectrum (400 MHz, $\text{DMSO-}d_6$) of compound **9f**

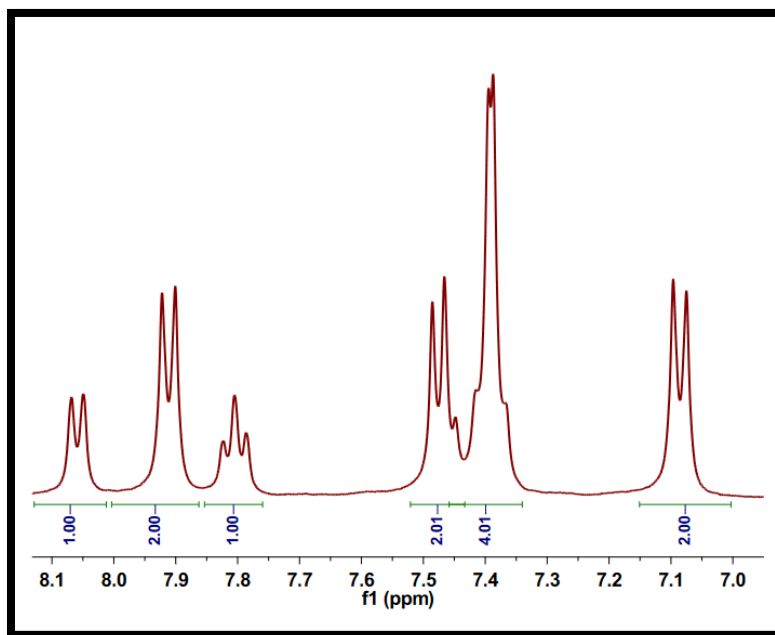


Figure S22: Expanded aromatic region of ^1H NMR spectrum (400 MHz, $\text{DMSO-}d_6$) of compound **9f**

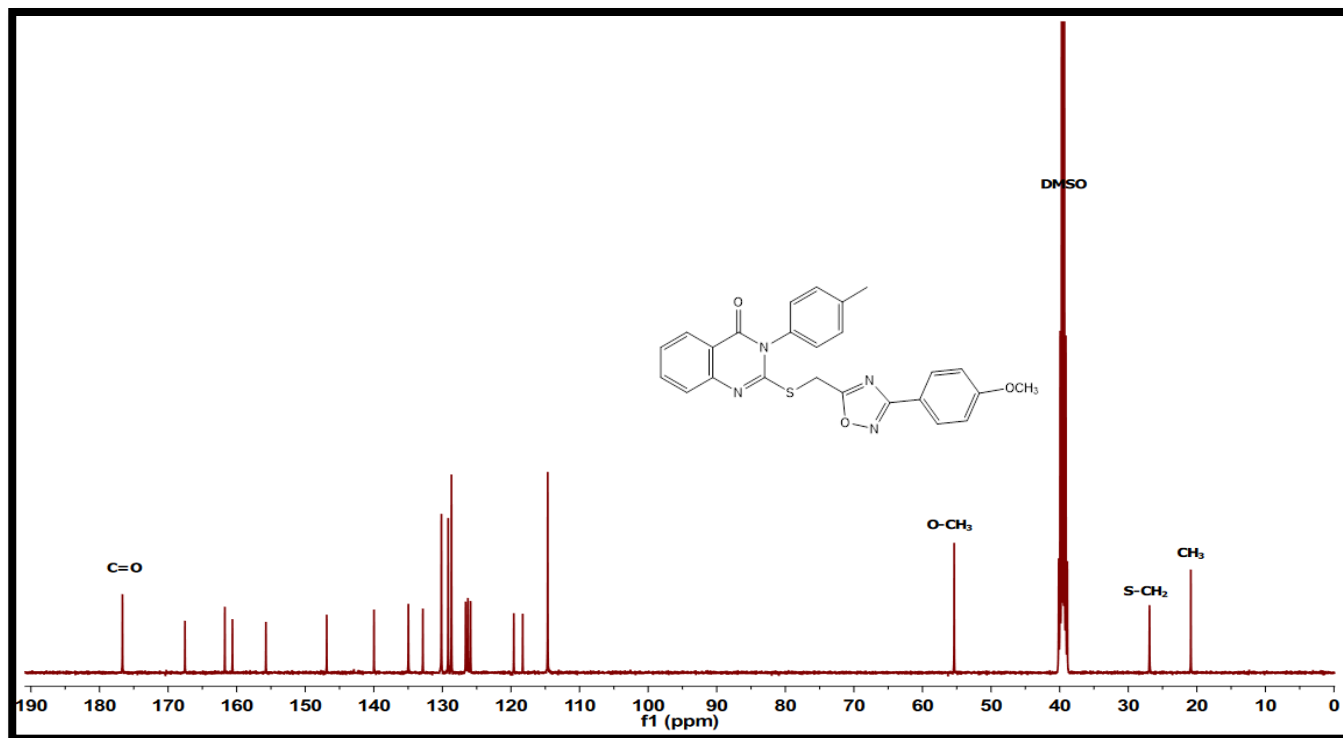


Figure S23: ^{13}C NMR spectrum (100 MHz, $\text{DMSO-}d_6$) of compound **9f**

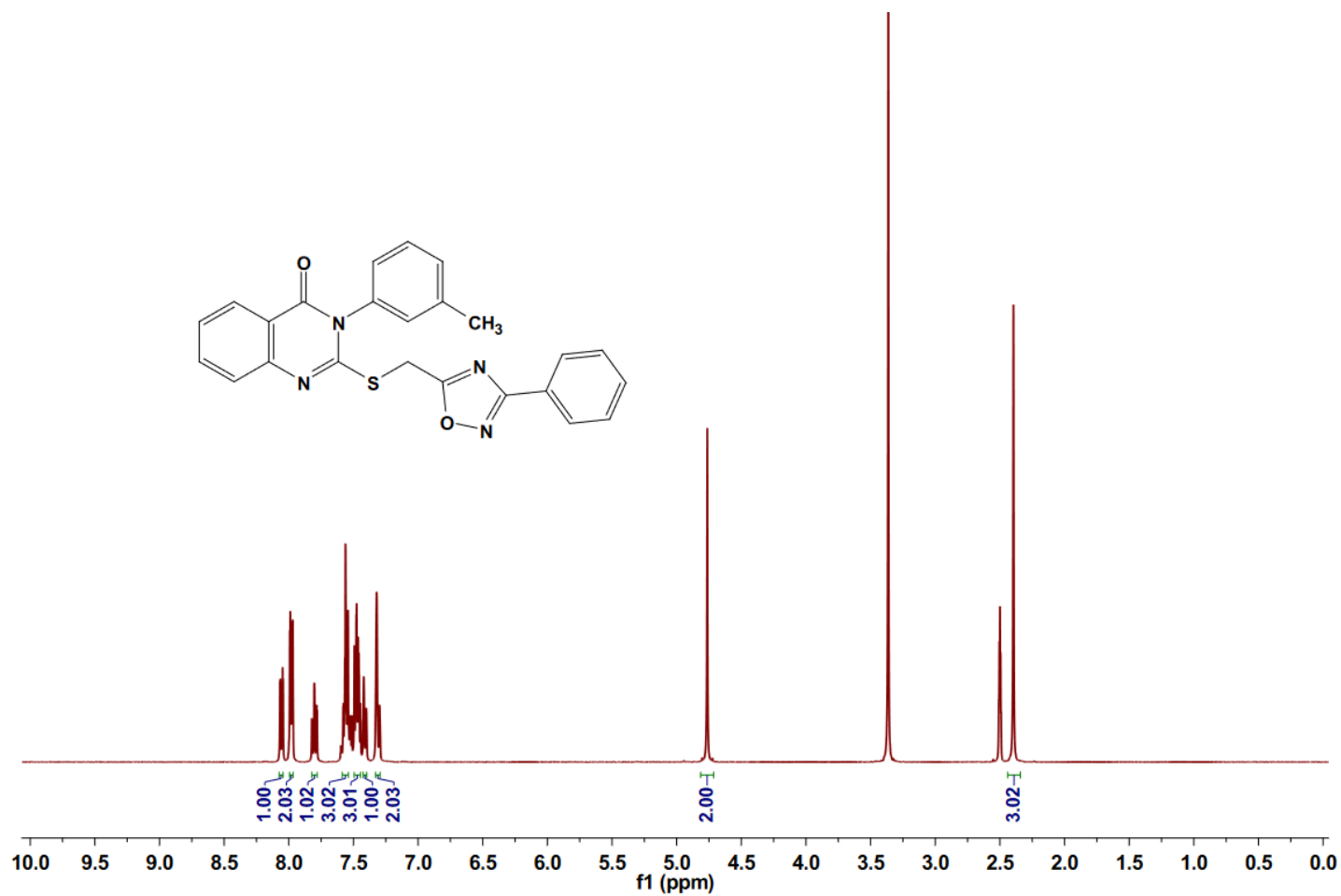


Figure S24: ¹H NMR spectrum (400 MHz, DMSO-*d*₆) of compound **9g**

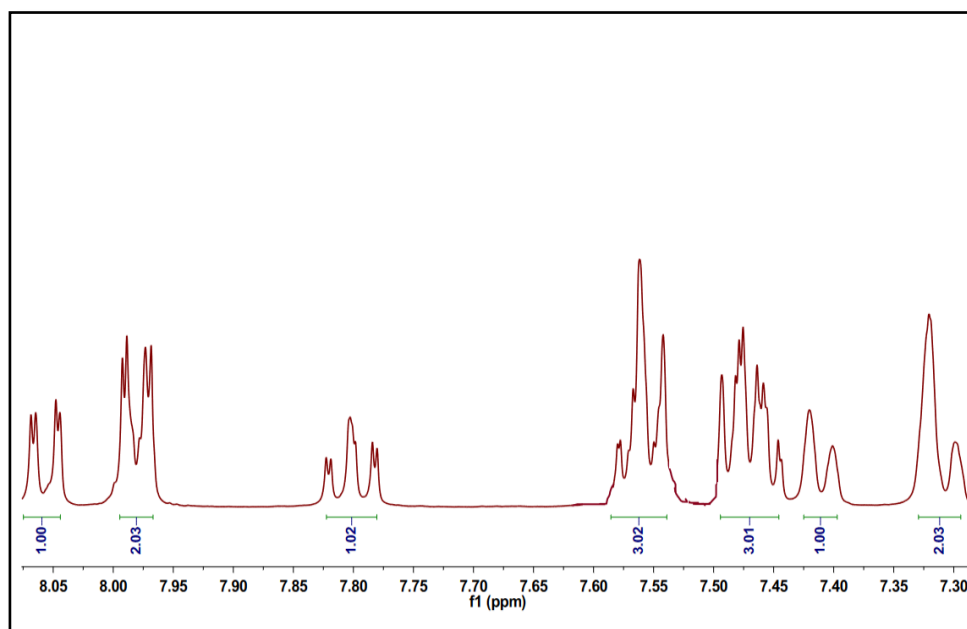


Figure S25: Expanded aromatic region of ¹H NMR spectrum (400 MHz, DMSO-*d*₆) of compound **9g**

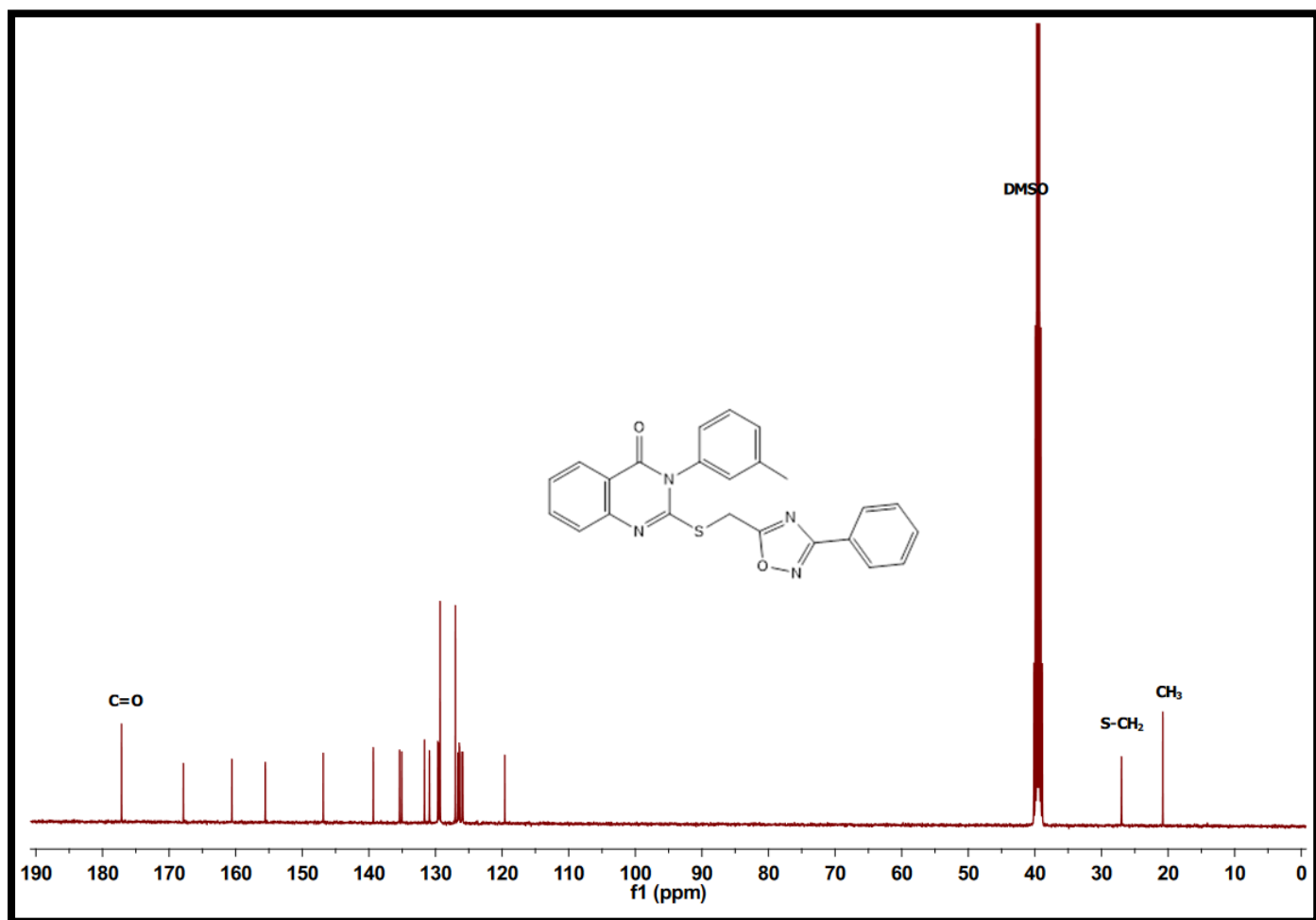


Figure S26: ^{13}C NMR spectrum (100 MHz, $\text{DMSO-}d_6$) of compound **9g**

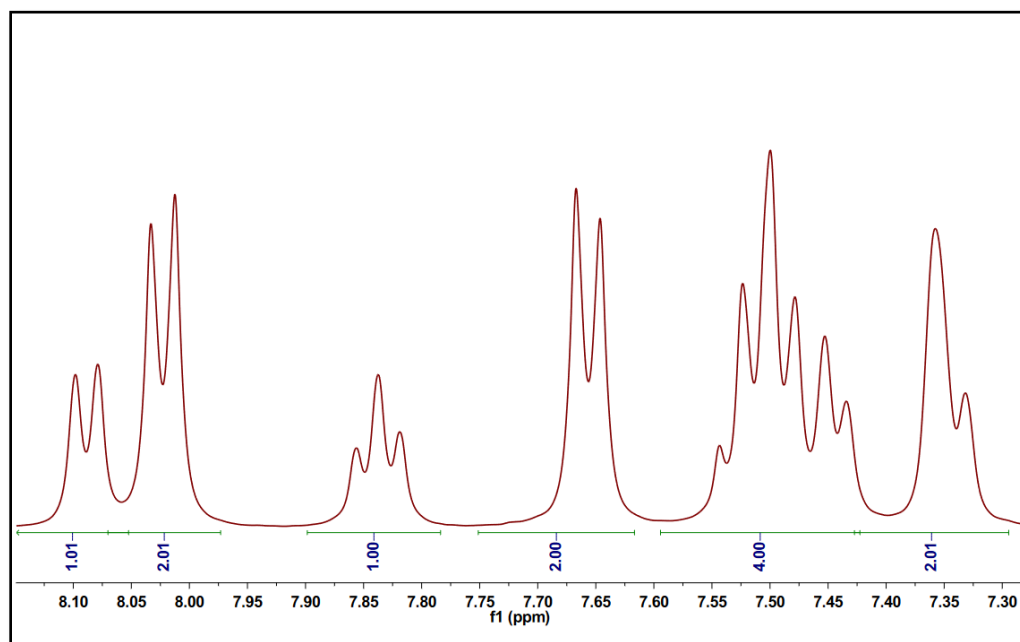
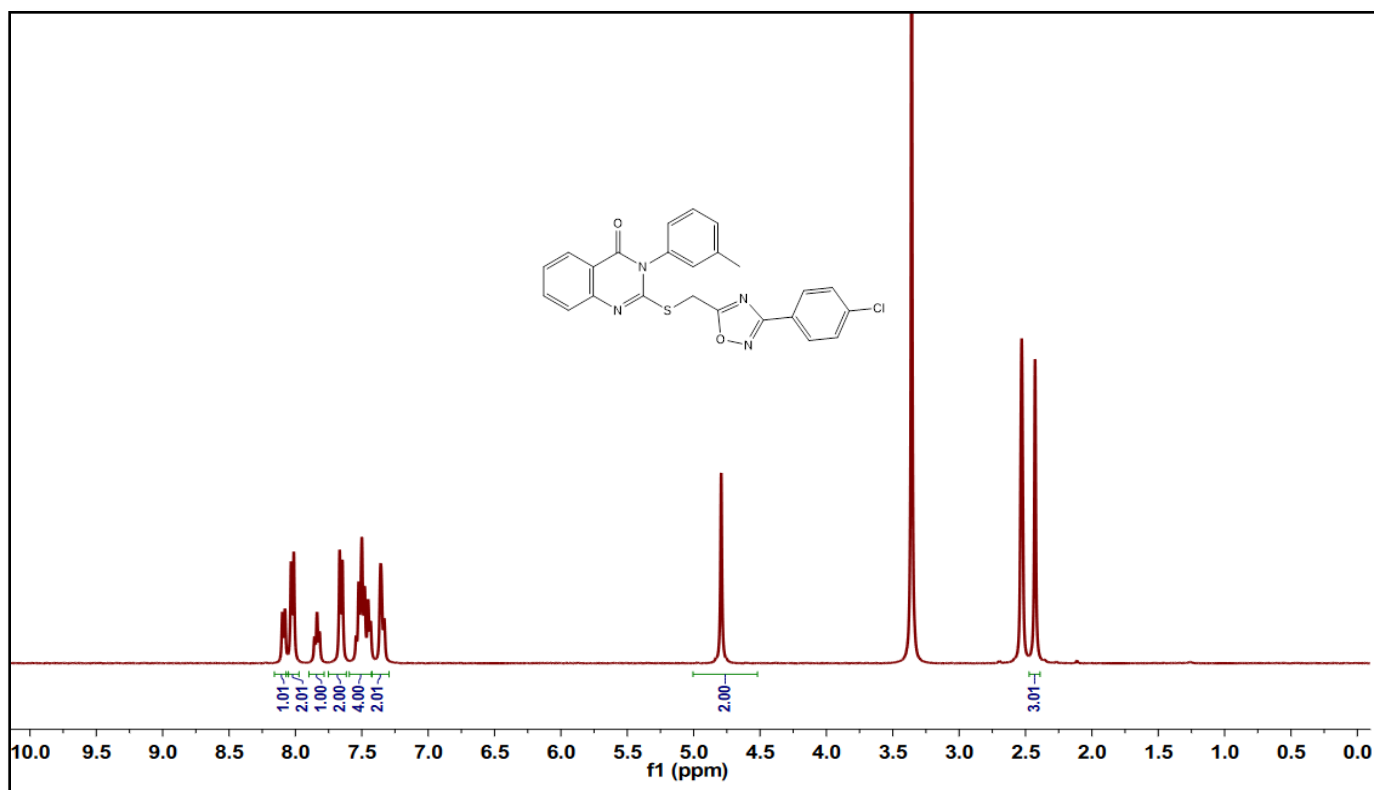


Figure S28: Expanded aromatic region of ^1H NMR spectrum (400 MHz, $\text{DMSO-}d_6$) of compound **9h**

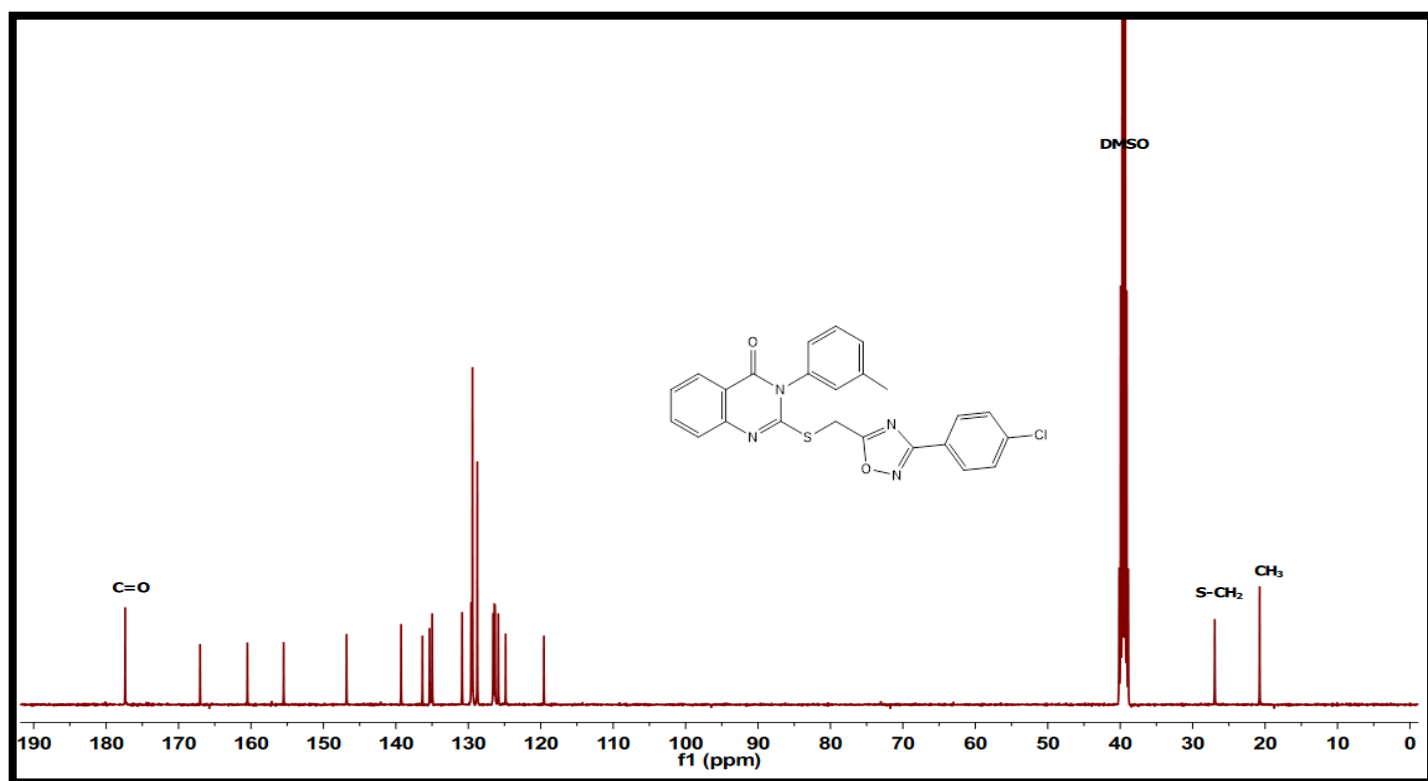


Figure S29: ^{13}C NMR spectrum (100 MHz, $\text{DMSO-}d_6$) of compound **9h**

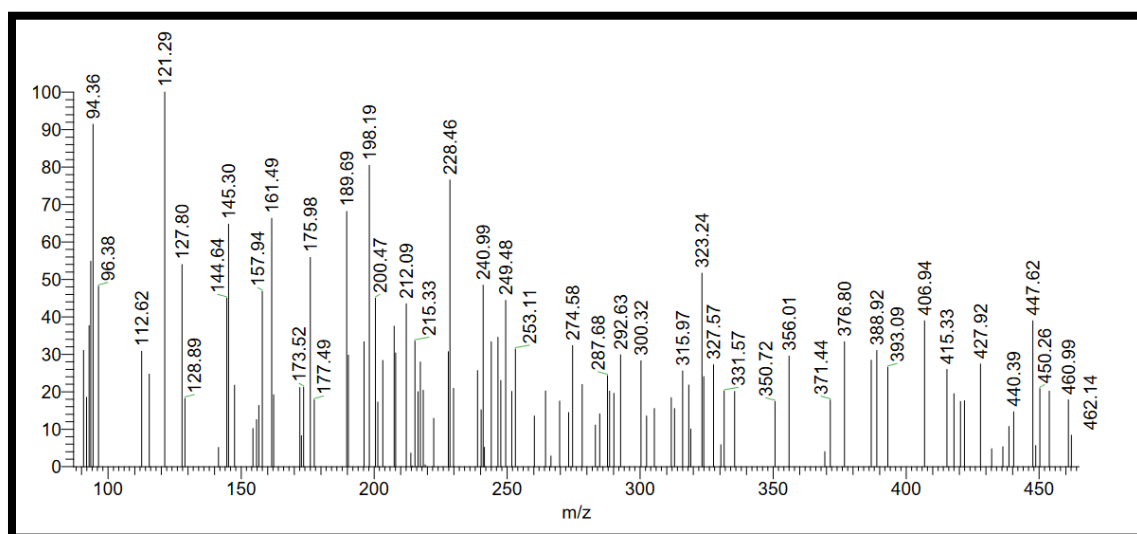


Figure S30: EI-Mass spectrum of compound **9h**

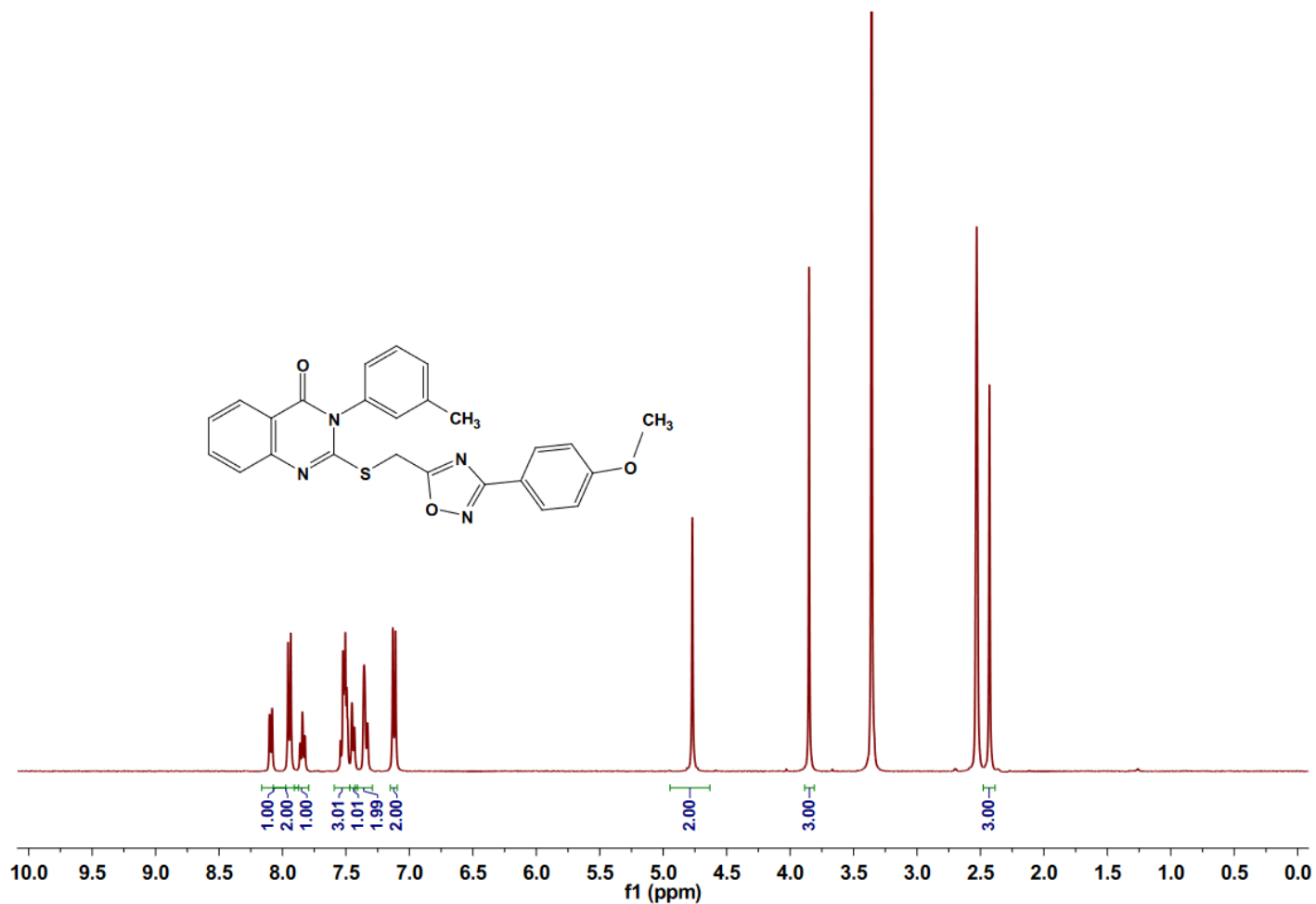


Figure S31: ¹H NMR spectrum (400 MHz, DMSO-*d*₆) of compound **9i**

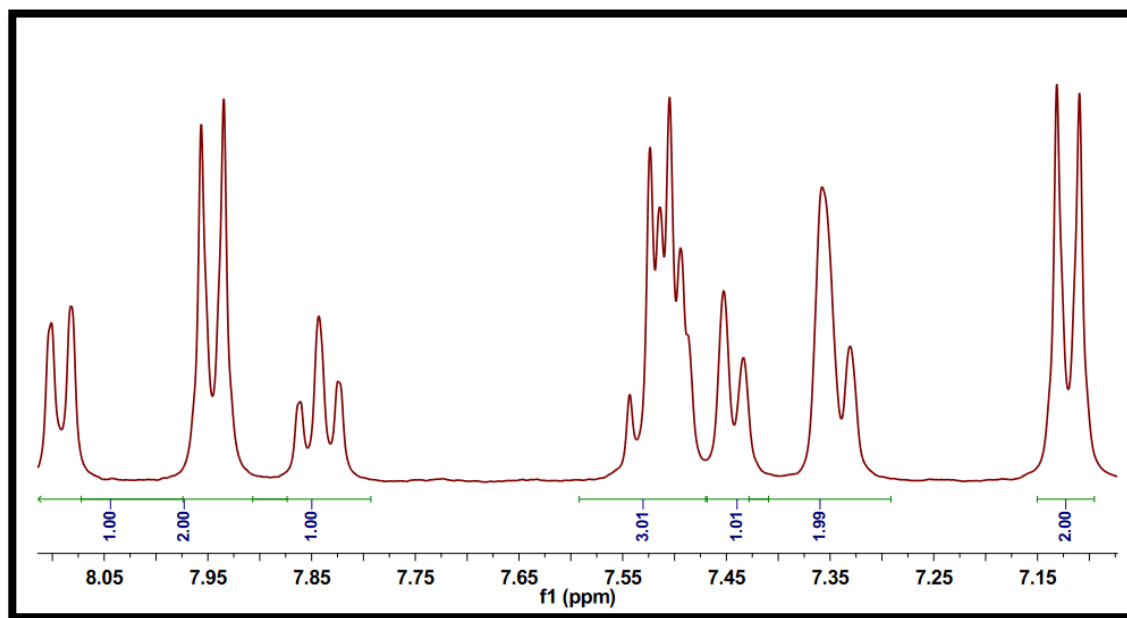


Figure S32: Expanded aromatic region of ¹H NMR spectrum (400 MHz, DMSO-*d*₆) of compound **9i**

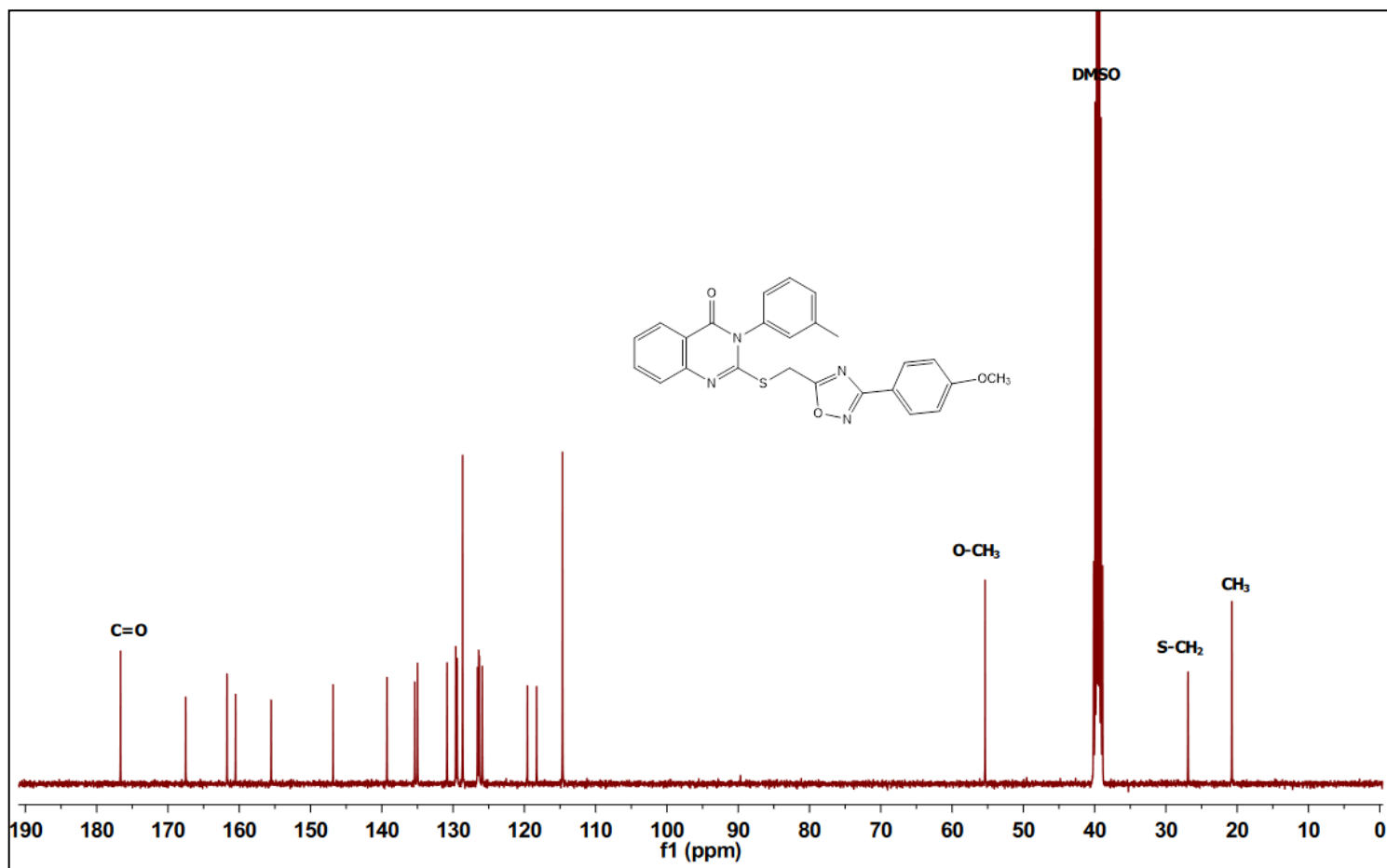


Figure S33: ^{13}C NMR spectrum (100 MHz, $\text{DMSO-}d_6$) of compound **9i**

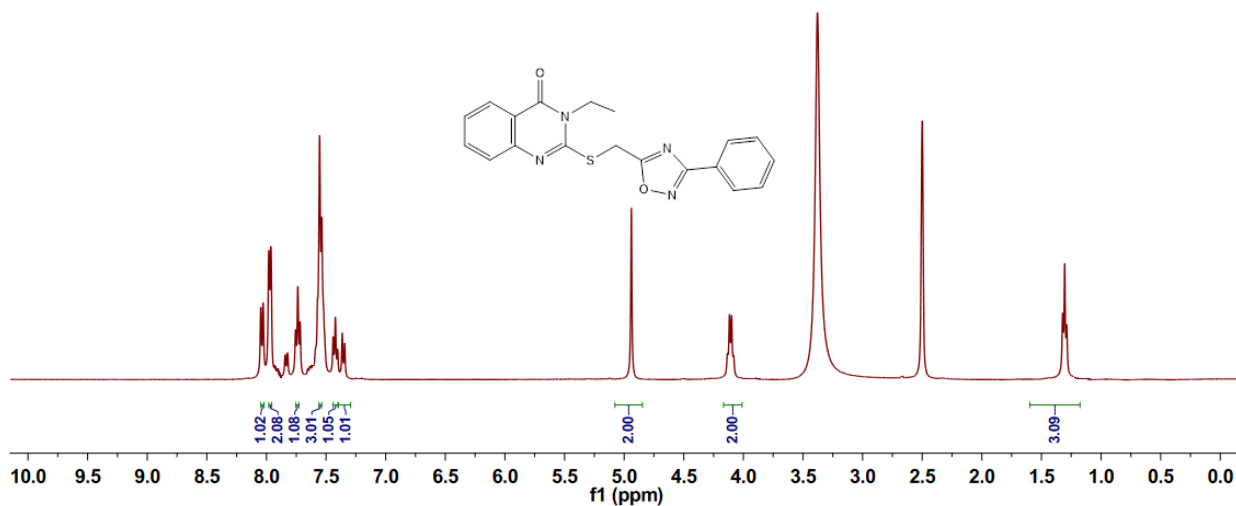


Figure S34: ^1H NMR spectrum (400 MHz, $\text{DMSO-}d_6$) of compound **9j**

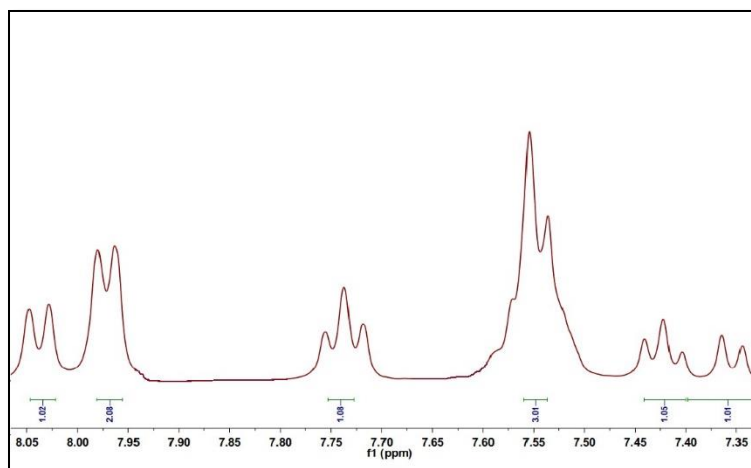


Figure S35: Expanded aromatic region of ^1H NMR spectrum (400 MHz, $\text{DMSO-}d_6$) of compound **9j**

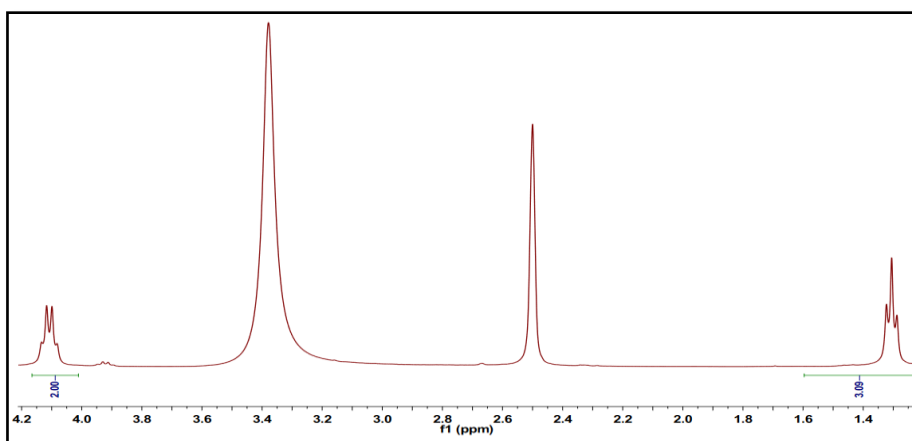


Figure S36: Expanded aliphatic region of ^1H NMR spectrum (400 MHz, $\text{DMSO-}d_6$) of compound **9j**

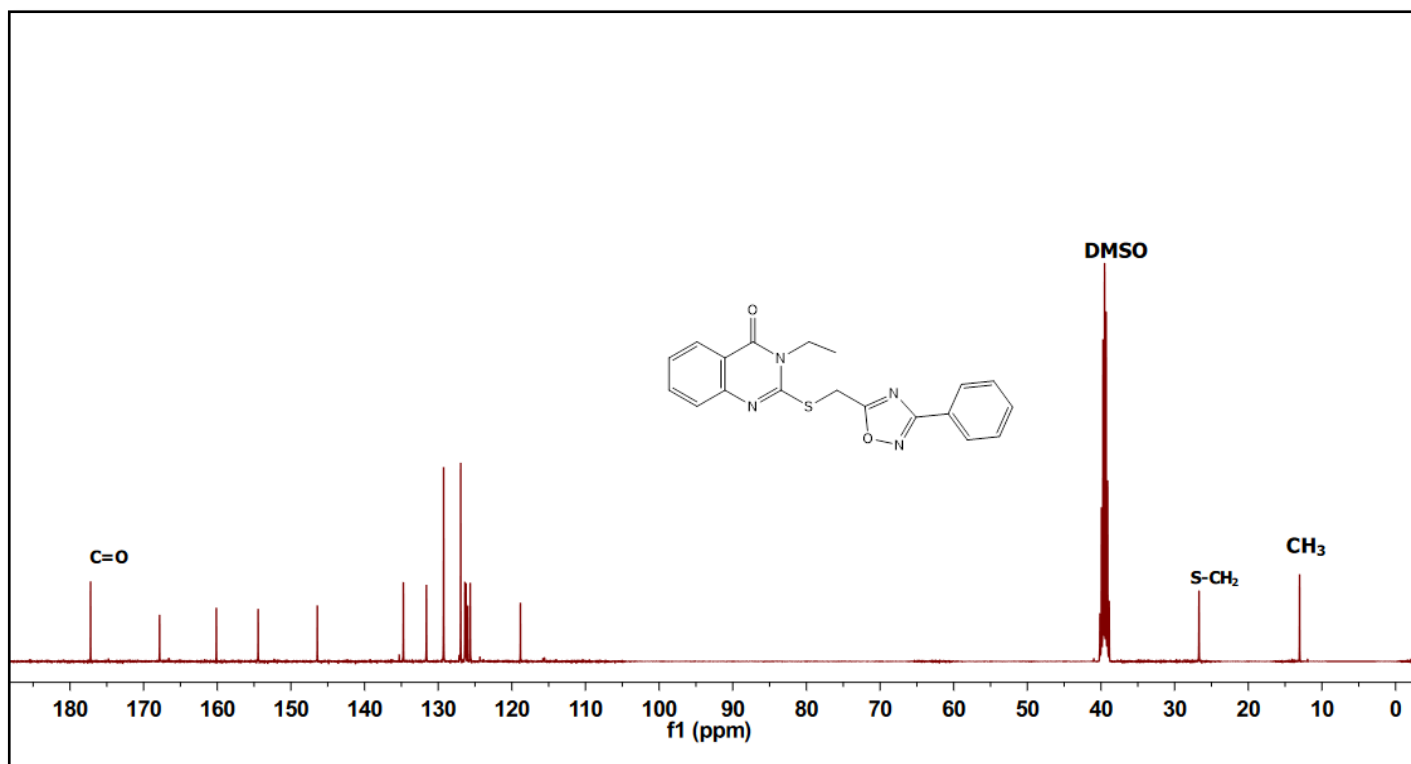


Figure S37: ^{13}C NMR spectrum (100 MHz, $\text{DMSO-}d_6$) of compound **9j**

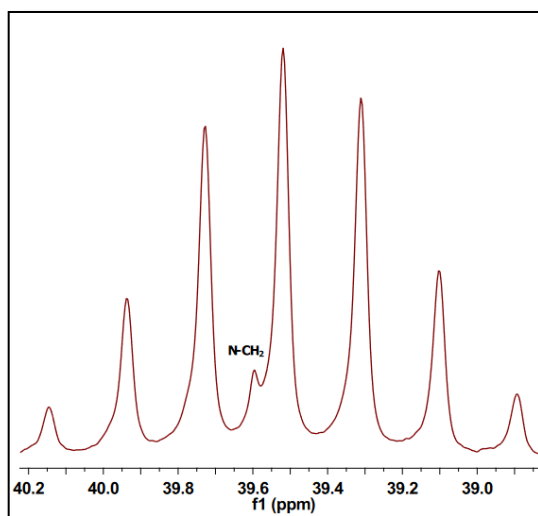


Figure S38: Expanded DMSO region of ^{13}C NMR spectrum (100 MHz, $\text{DMSO-}d_6$) of compound **9j**

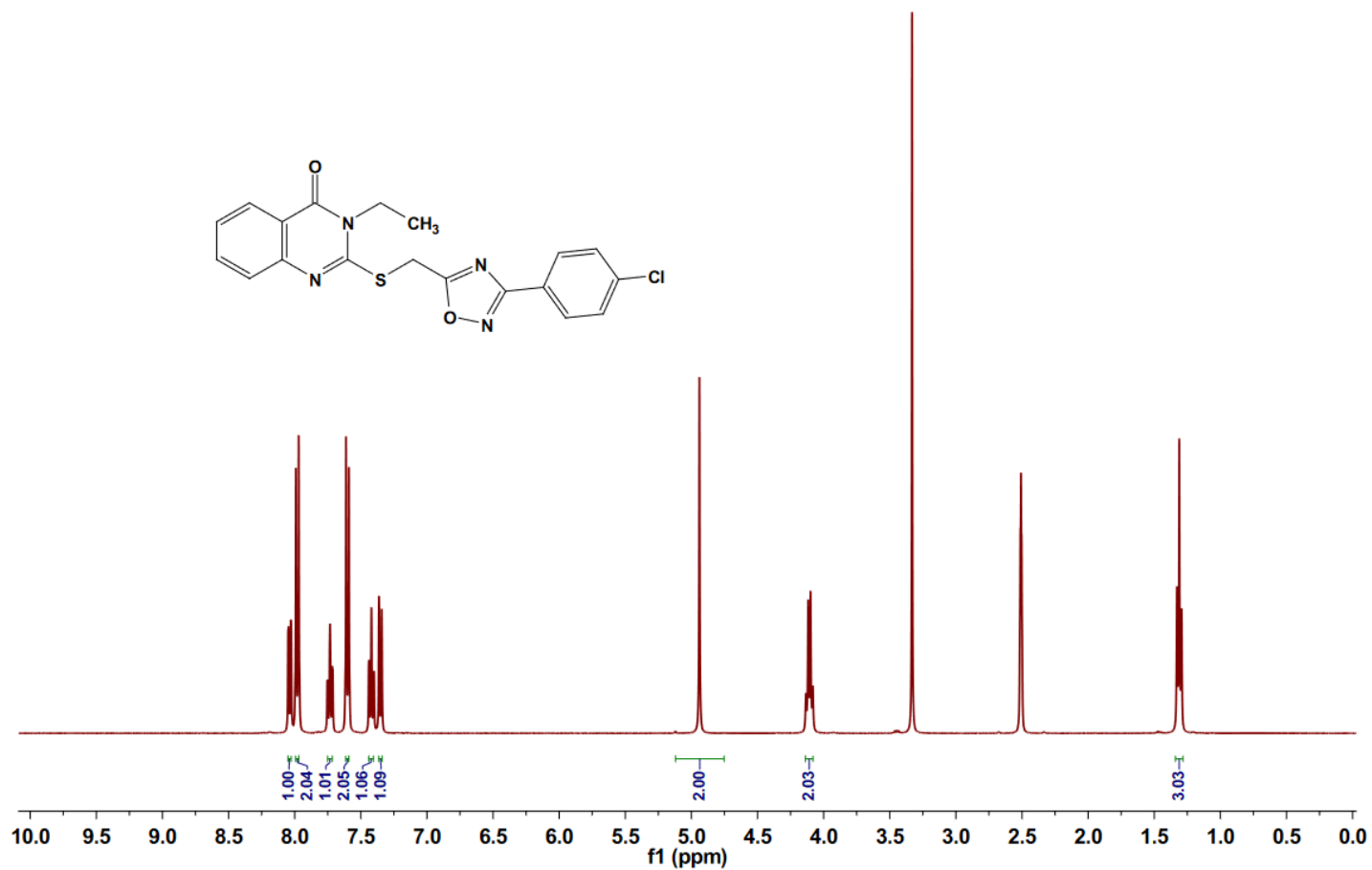


Figure S39: ¹H NMR spectrum (400 MHz, DMSO-*d*₆) of compound **9k**

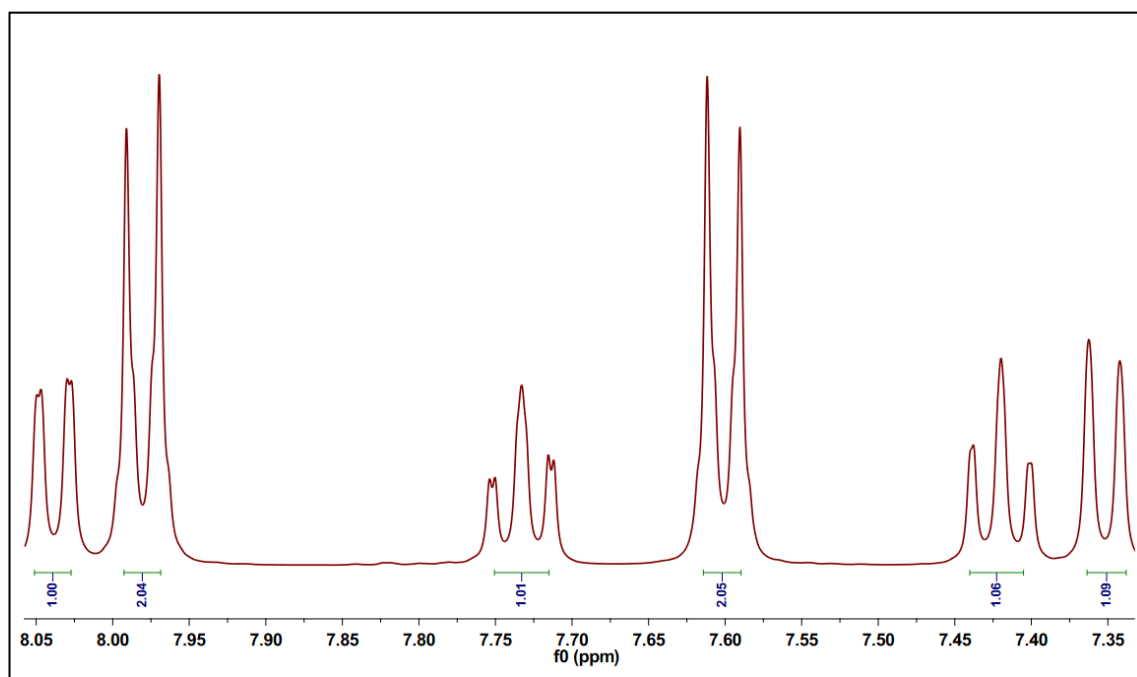


Figure S40: Expanded aromatic region of ¹H NMR spectrum (400 MHz, DMSO-*d*₆) of compound **9k**

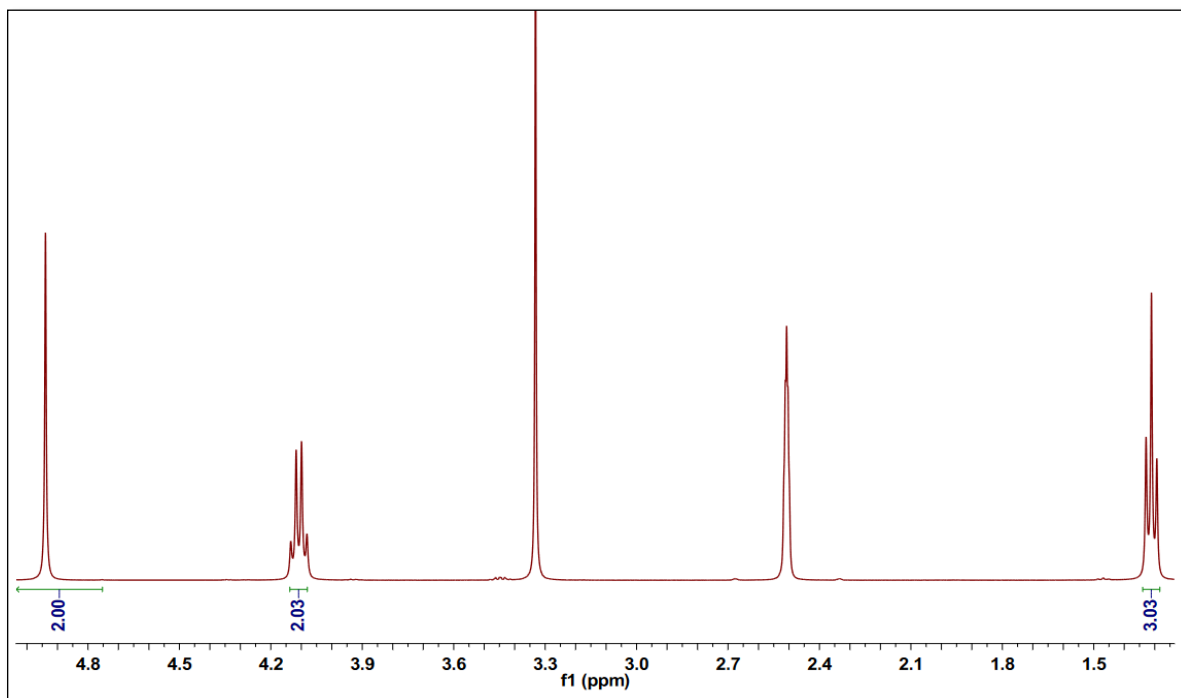


Figure S41: Expanded aliphatic region of ^1H NMR spectrum (400 MHz, $\text{DMSO-}d_6$) of compound **9k**

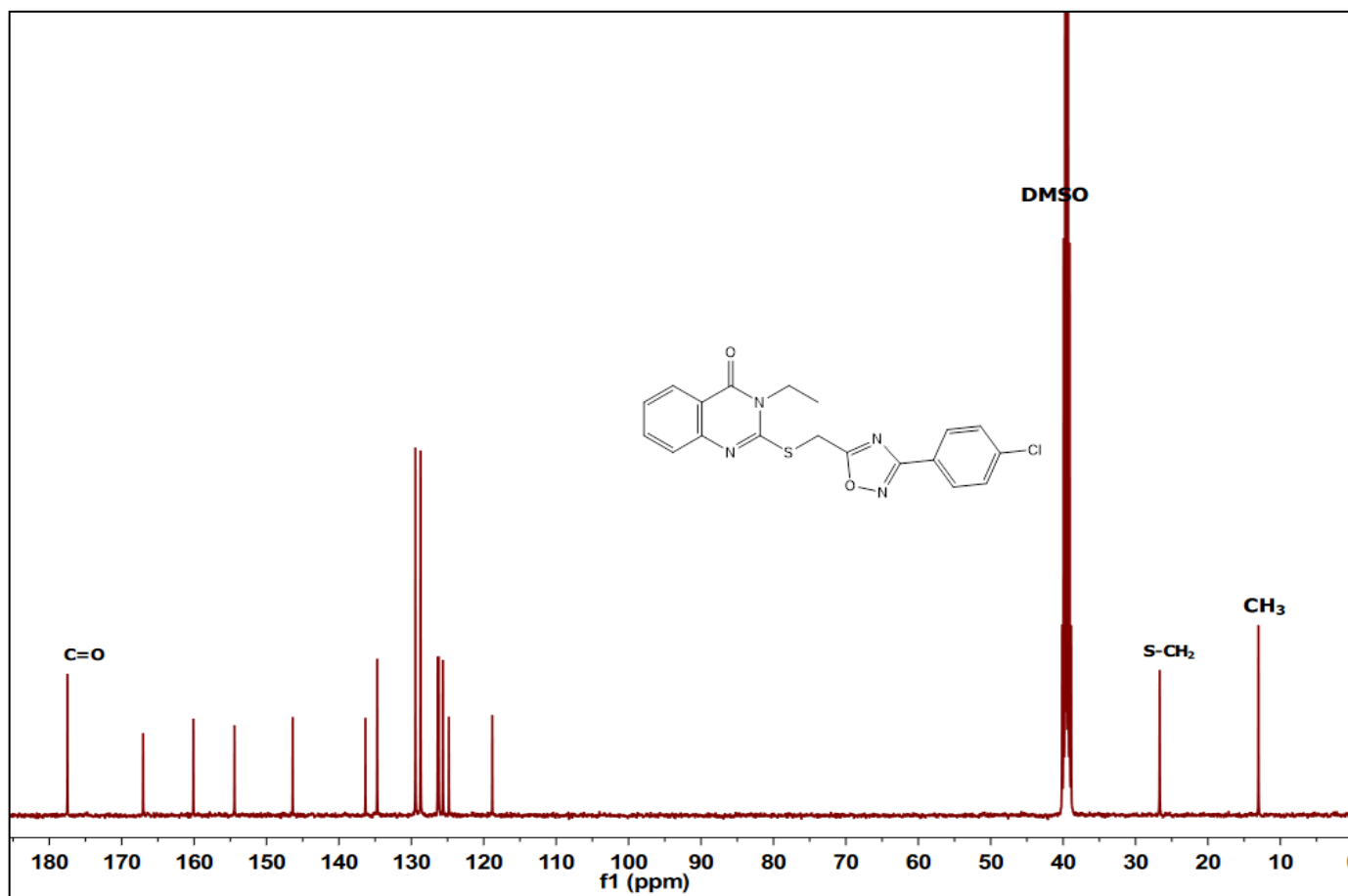


Figure S42: ^{13}C NMR spectrum (100 MHz, $\text{DMSO-}d_6$) of compound **9k**

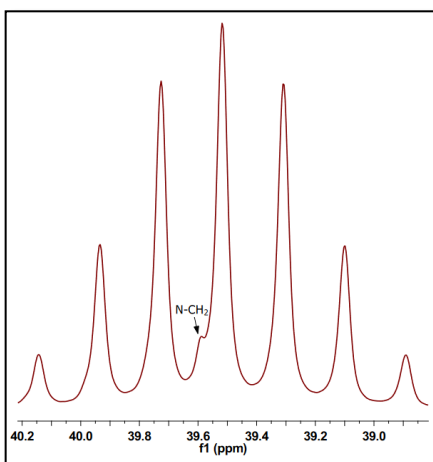


Figure S43: Expanded DMSO region of ^{13}C NMR spectrum (100 MHz, $\text{DMSO-}d_6$) of compound **9k**

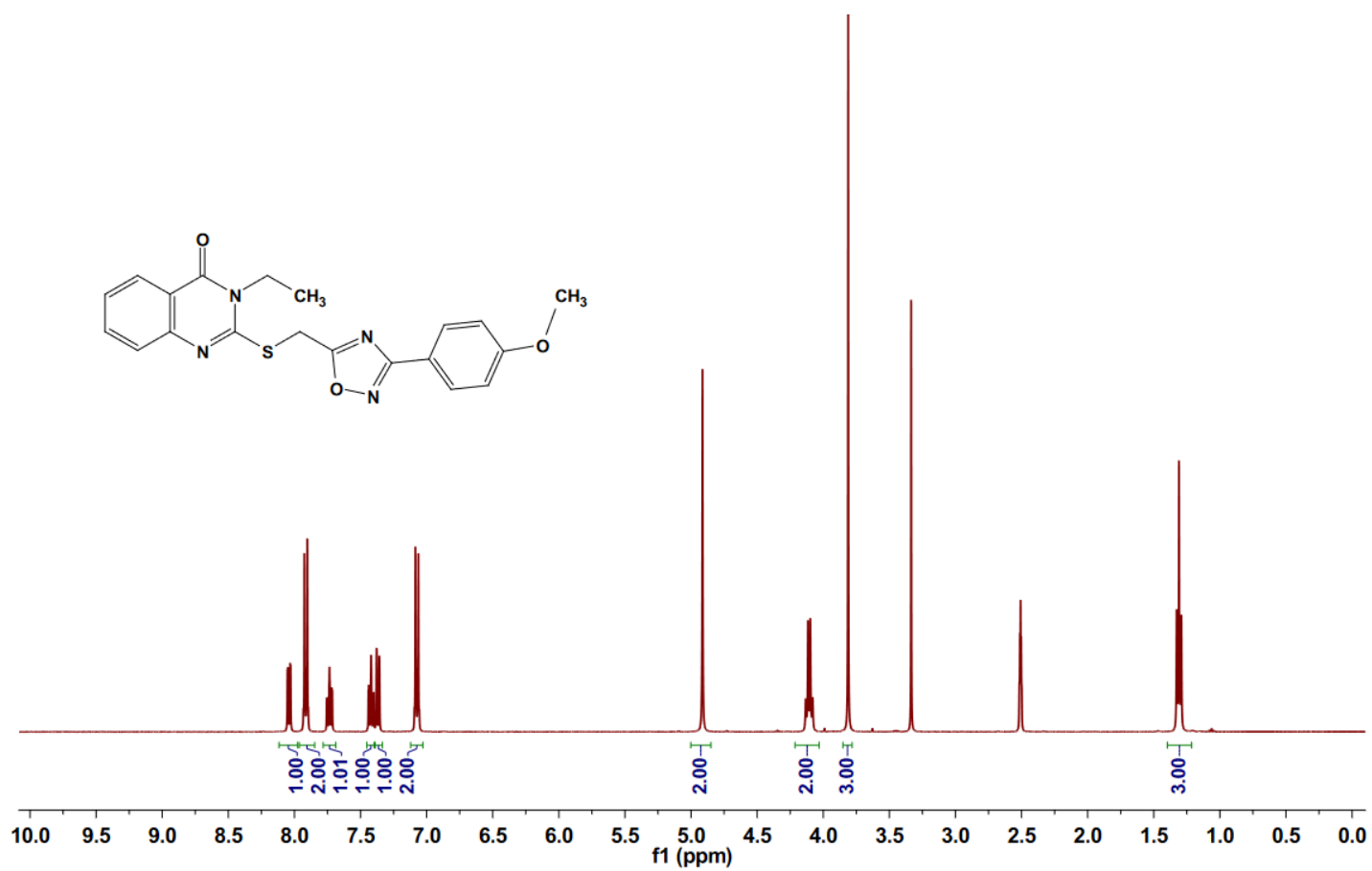


Figure S44: ^1H NMR spectrum (400 MHz, $\text{DMSO-}d_6$) of compound **9l**

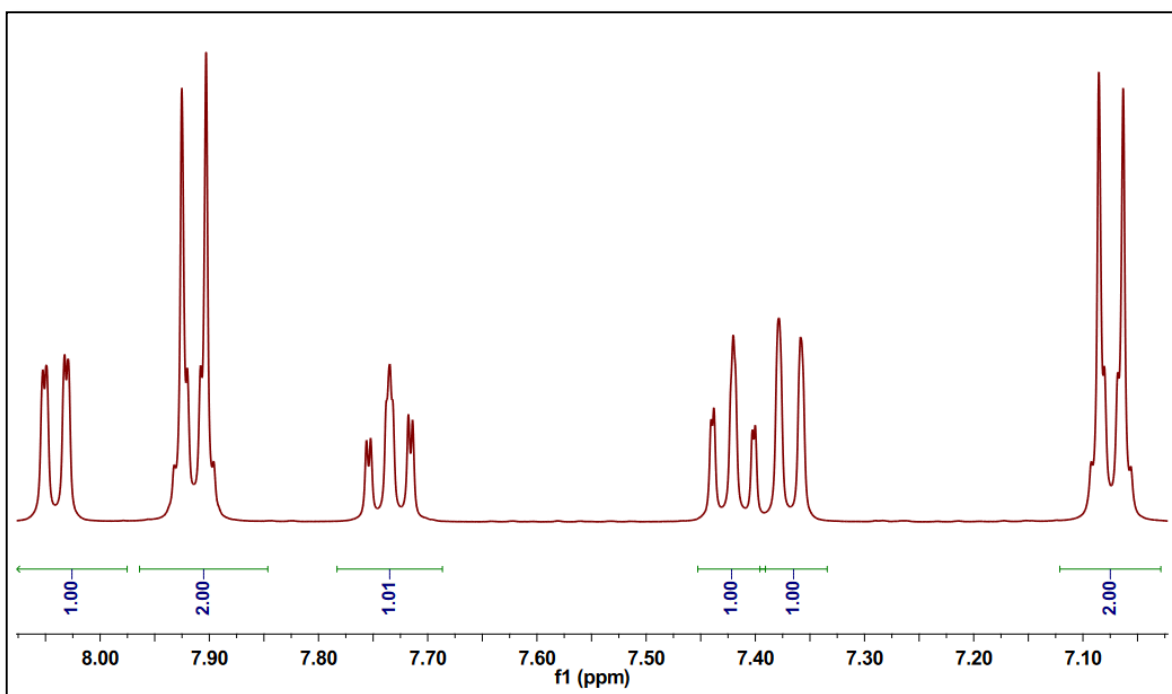


Figure S45: Expanded aromatic region of ^1H NMR spectrum (400 MHz, $\text{DMSO}-d_6$) of compound **91**

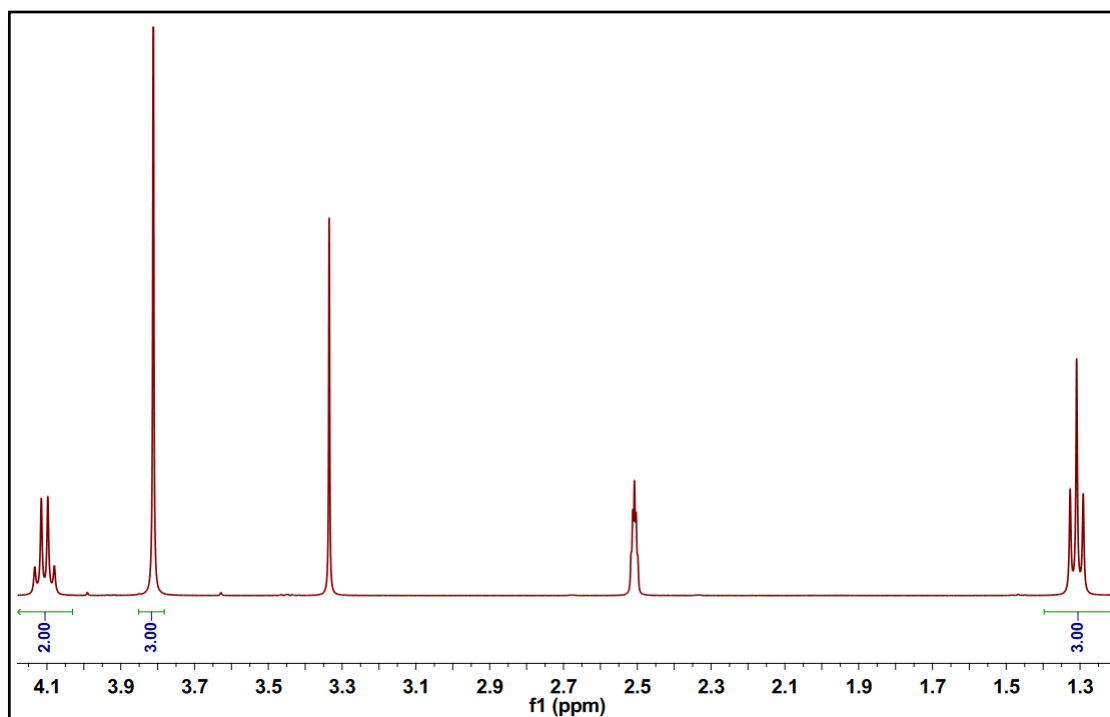


Figure S46: Expanded aliphatic region of ^1H NMR spectrum (400 MHz, $\text{DMSO}-d_6$) of compound **91**

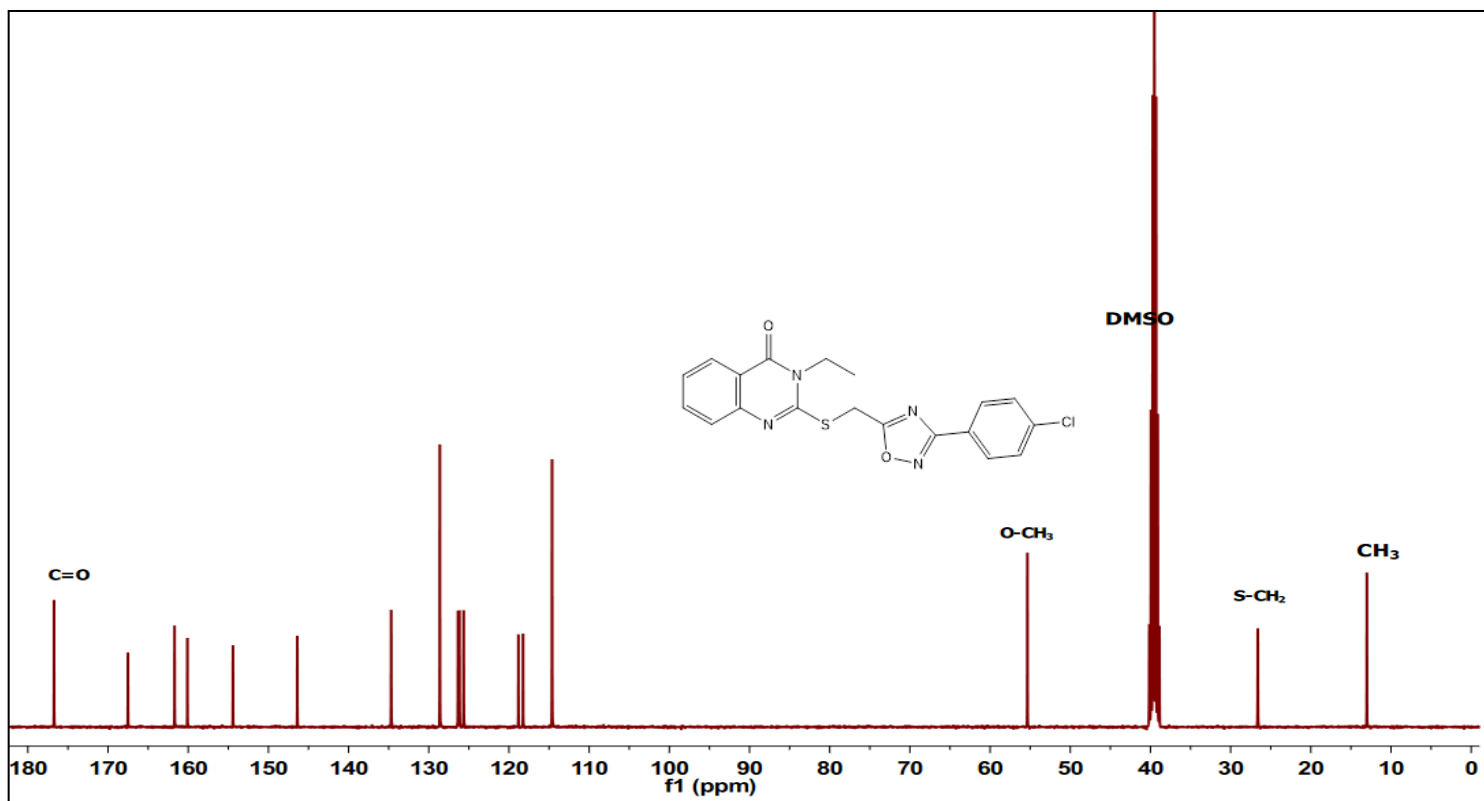


Figure S47: ^{13}C NMR spectrum (100 MHz, $\text{DMSO-}d_6$) of compound **91**

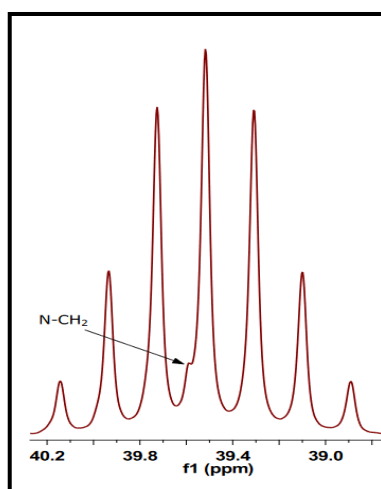


Figure S48: Expanded DMSO region of ^{13}C NMR spectrum (100 MHz, $\text{DMSO-}d_6$) of compound **91**

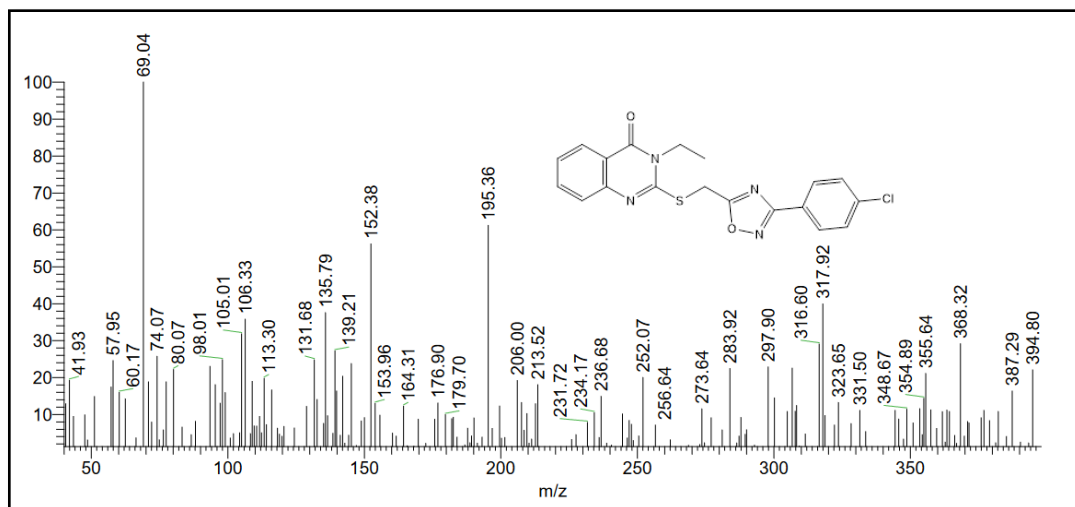


Figure S49: EI-Mass spectrum of compound 9l

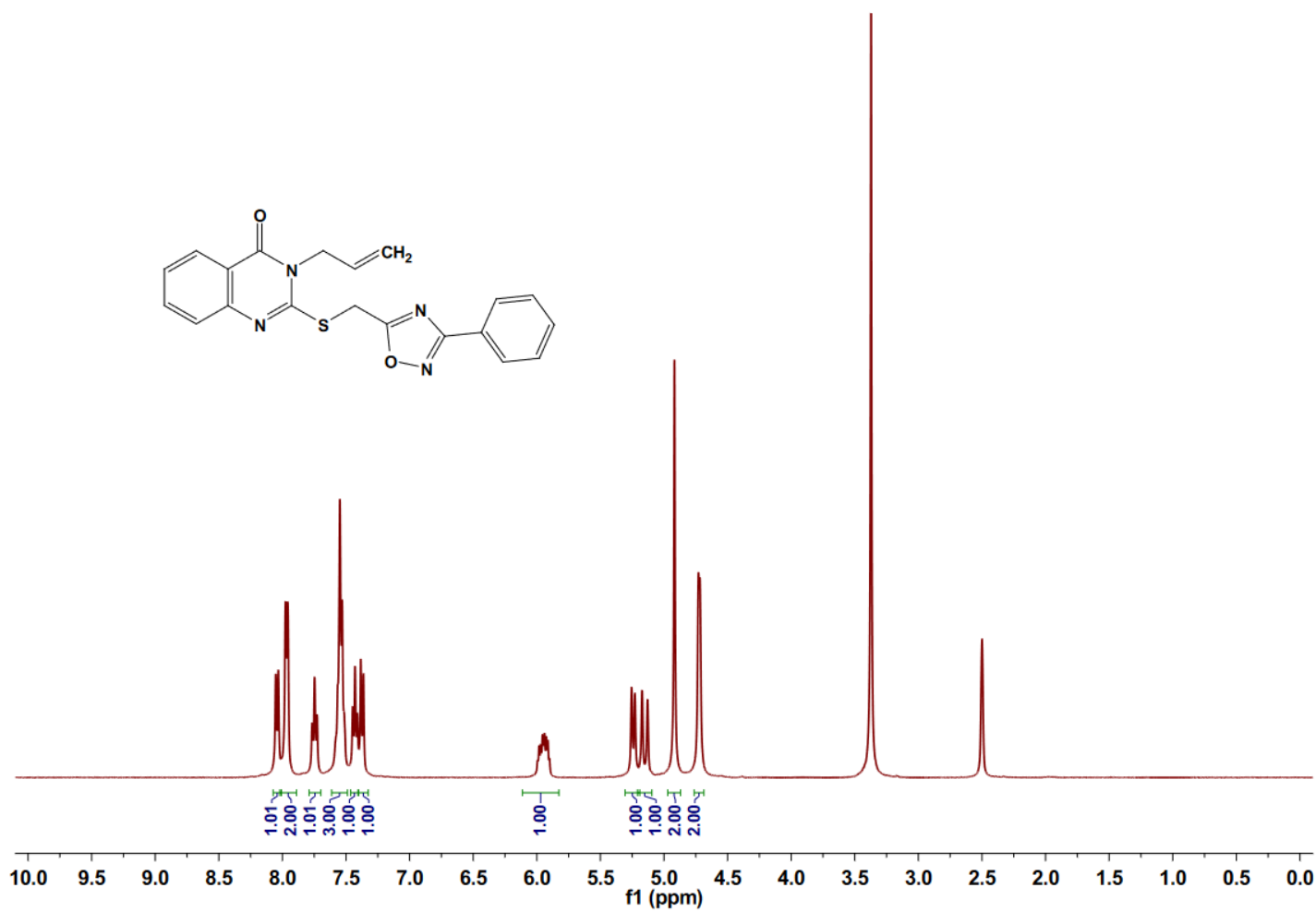


Figure S50: ¹H NMR spectrum (400 MHz, DMSO-*d*₆) of compound 9m

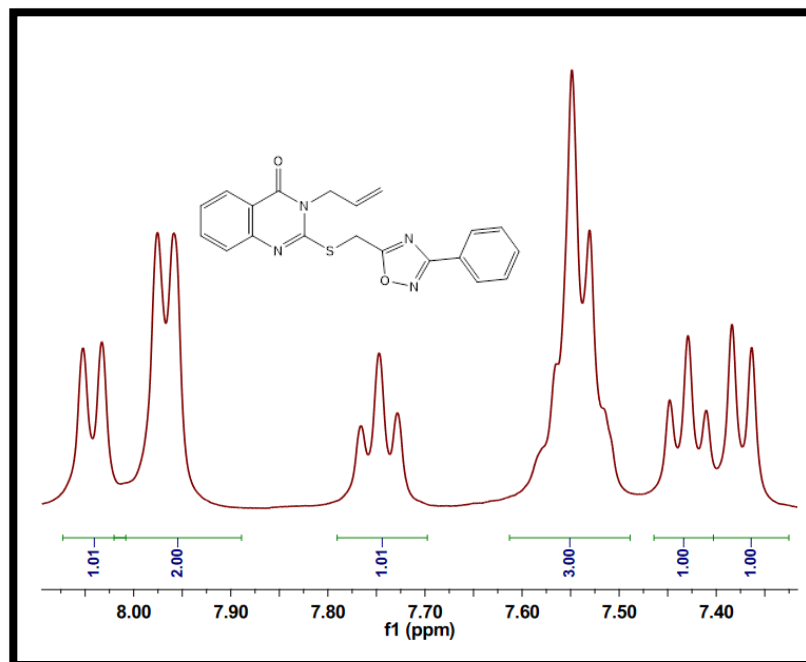


Figure S51: Expanded aromatic region of ¹H NMR spectrum (400 MHz, DMSO-*d*₆) of compound **9m**

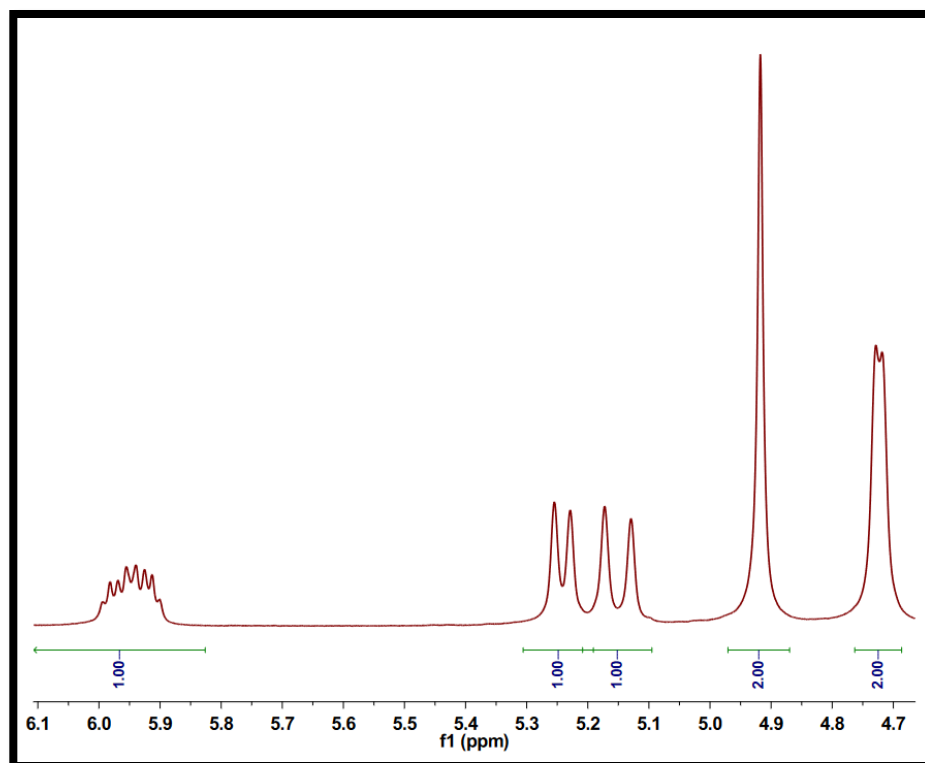


Figure S52: Expanded aliphatic and olefinic regions of ¹H NMR spectrum (400 MHz, DMSO-*d*₆) of compound **9m**

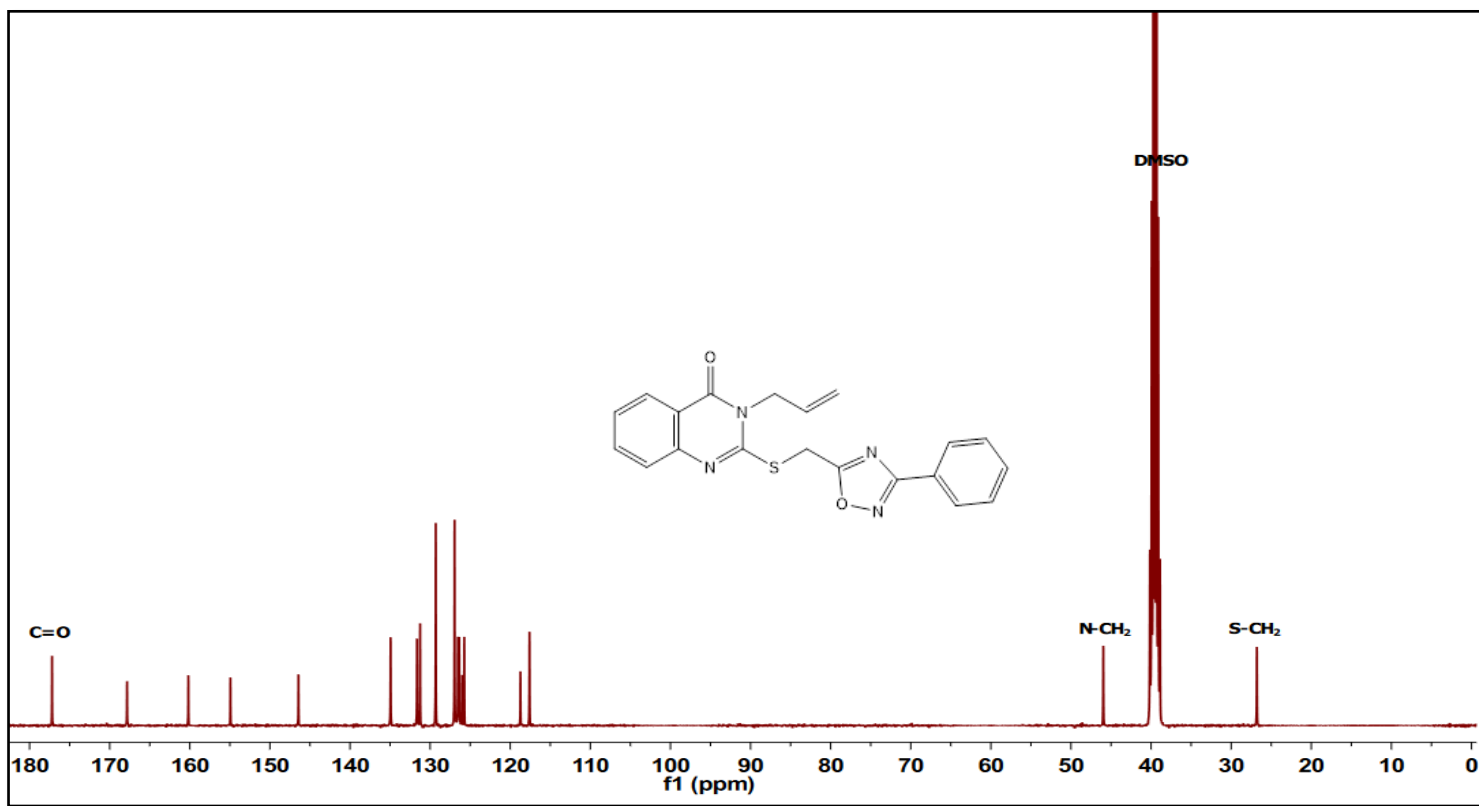


Figure S53: ^{13}C NMR spectrum (100 MHz, $\text{DMSO-}d_6$) of compound **9m**

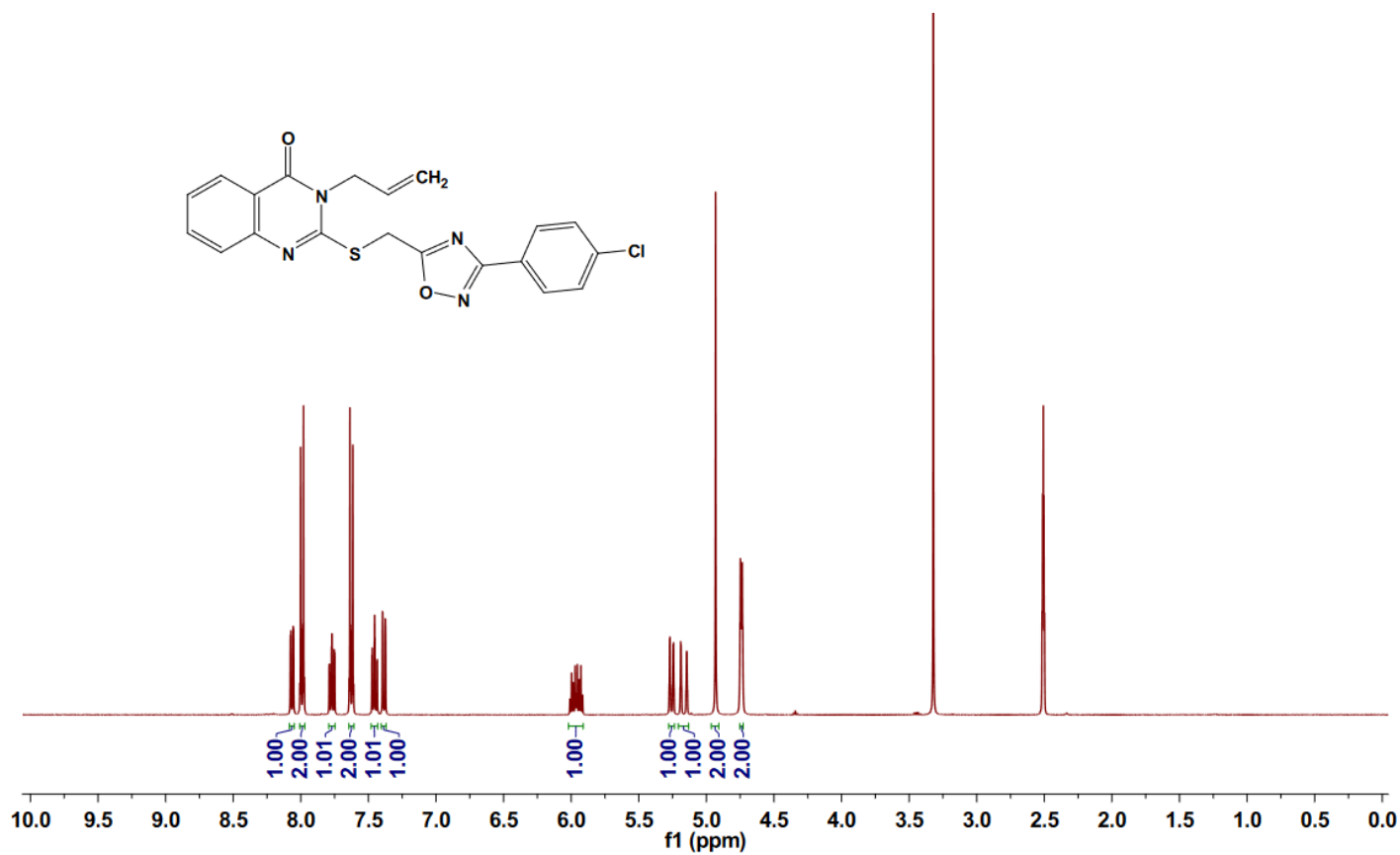


Figure S54: ¹H NMR spectrum (400 MHz, DMSO-*d*₆) of compound **9n**

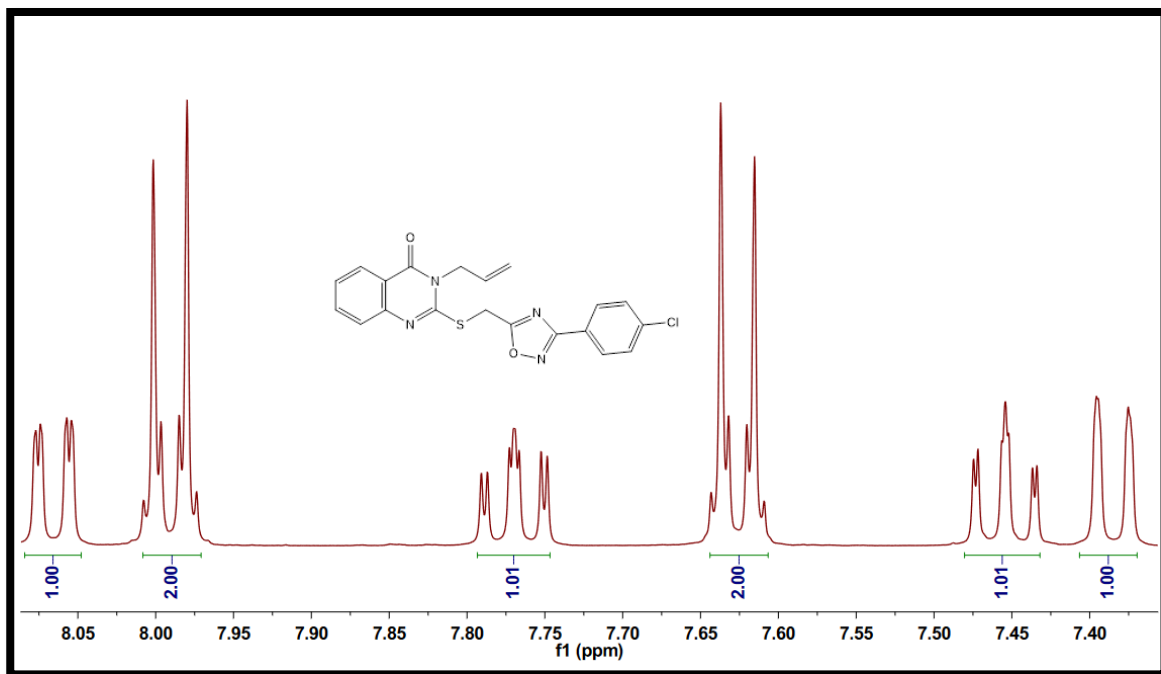


Figure S55: Expanded aromatic region of ^1H NMR spectrum (400 MHz, $\text{DMSO-}d_6$) of compound **9n**

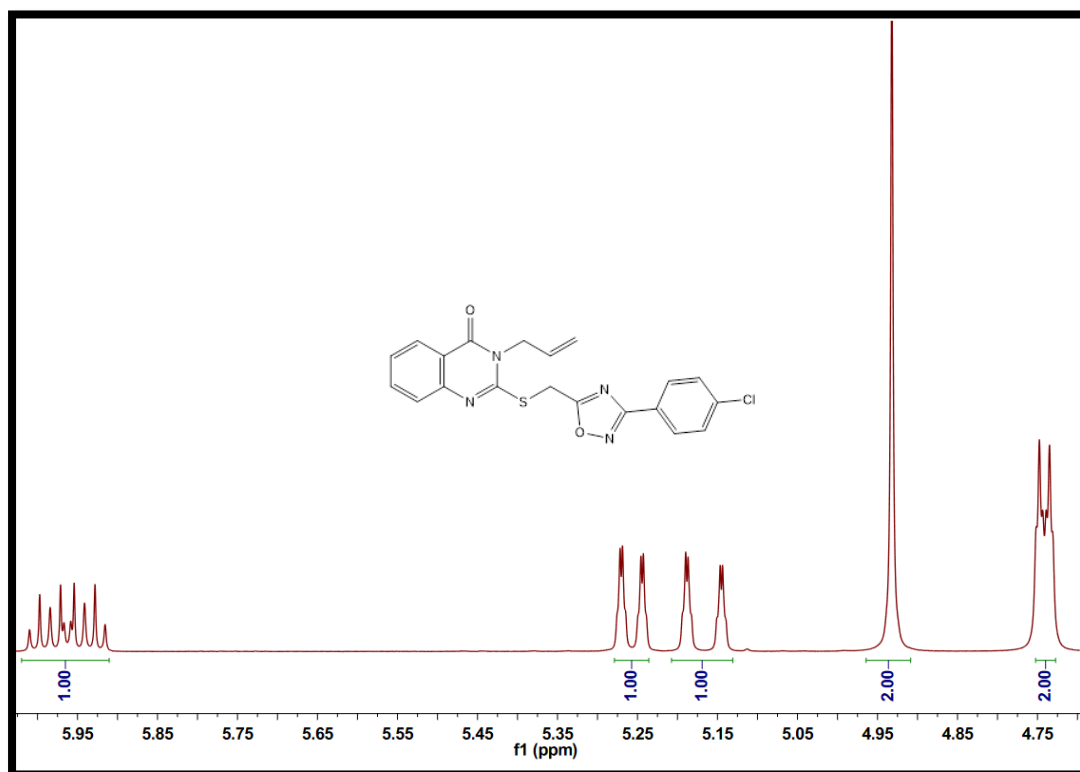


Figure S56: Expanded aliphatic and olefinic regions of ^1H NMR spectrum (400 MHz, $\text{DMSO-}d_6$) of compound **9n**

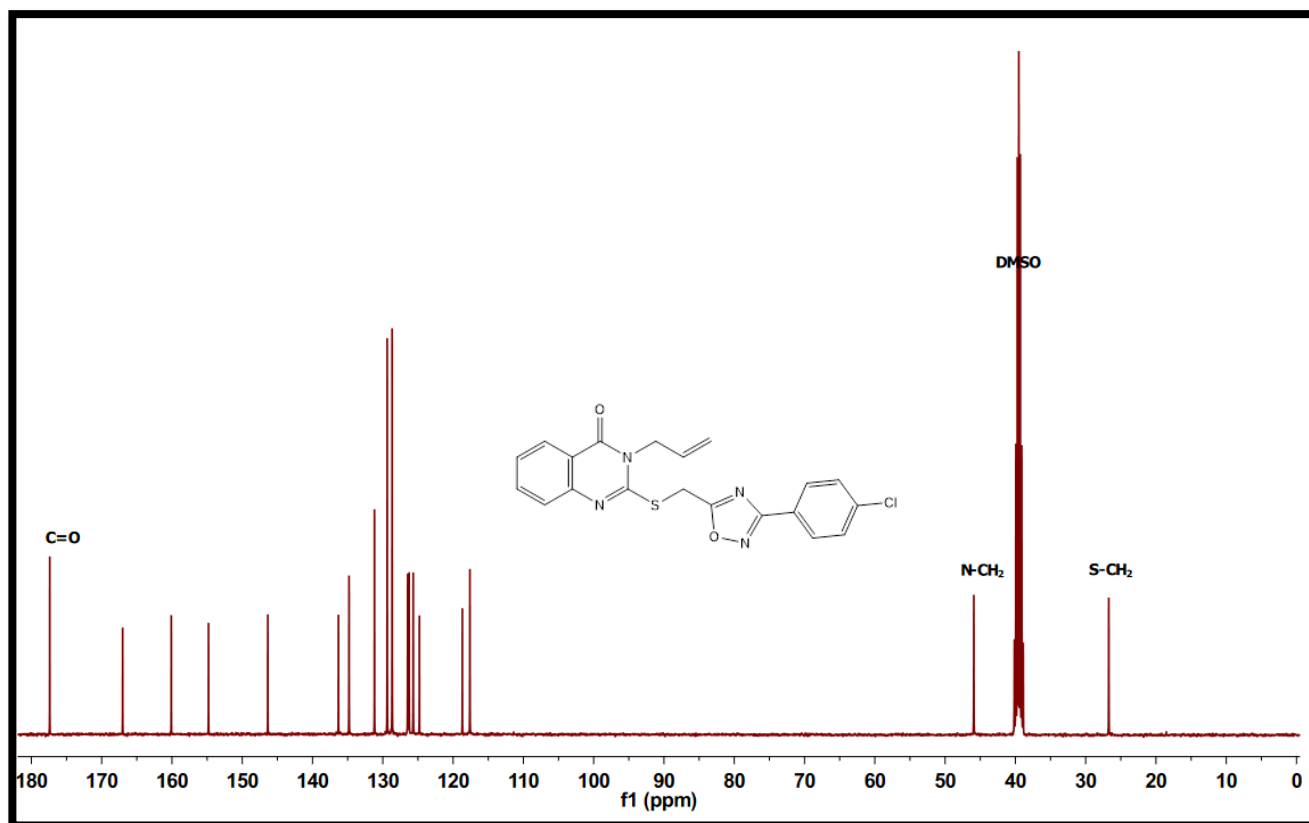


Figure S57: ^{13}C NMR spectrum (100 MHz, $\text{DMSO-}d_6$) of compound 9n

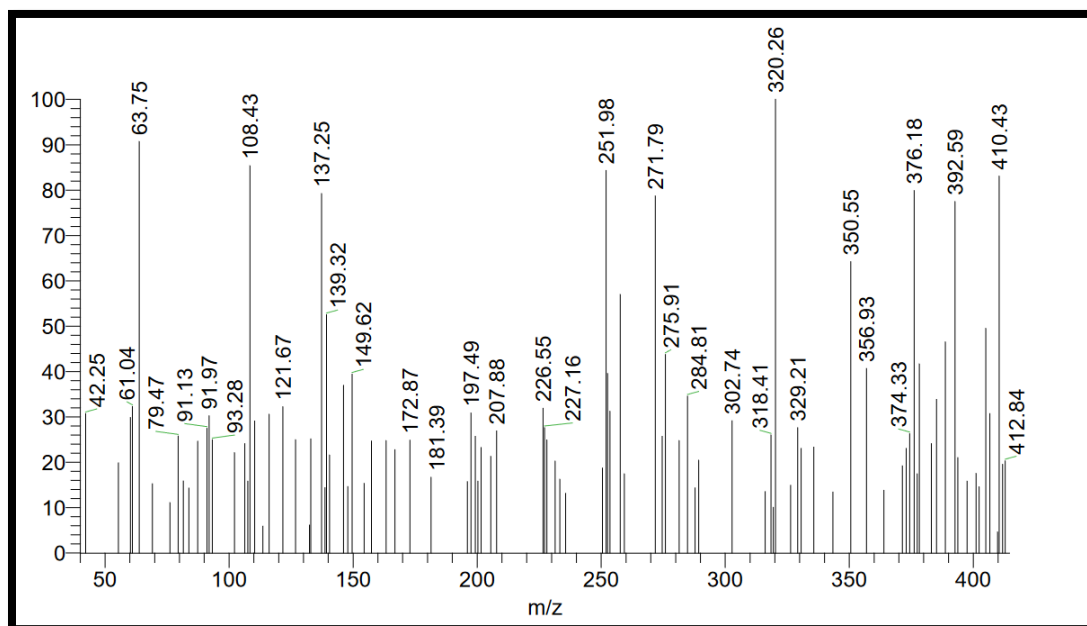


Figure S58: EI-Mass spectrum of compound 9n

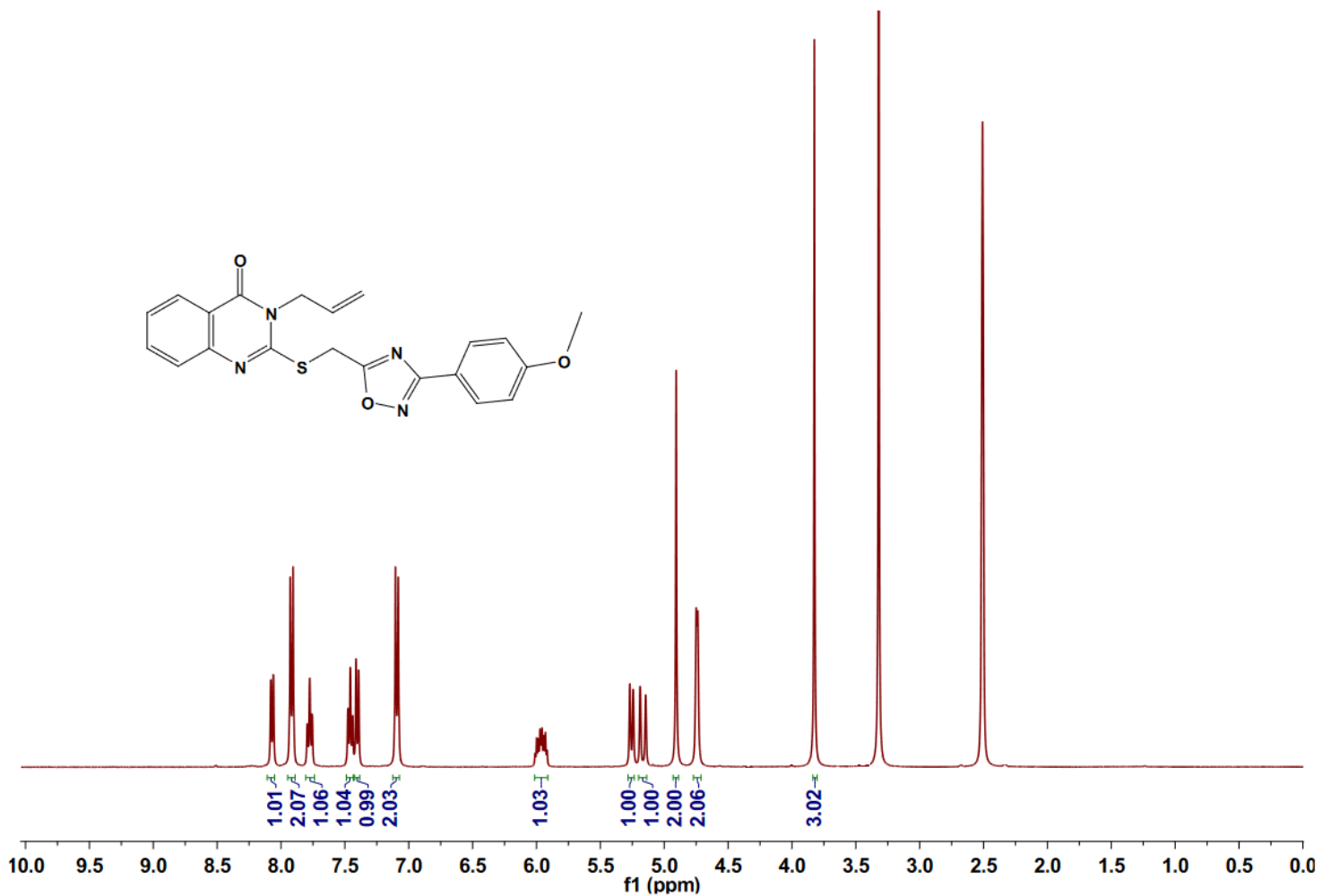


Figure S59: ¹H NMR spectrum (400 MHz, DMSO-*d*₆) of compound **9o**

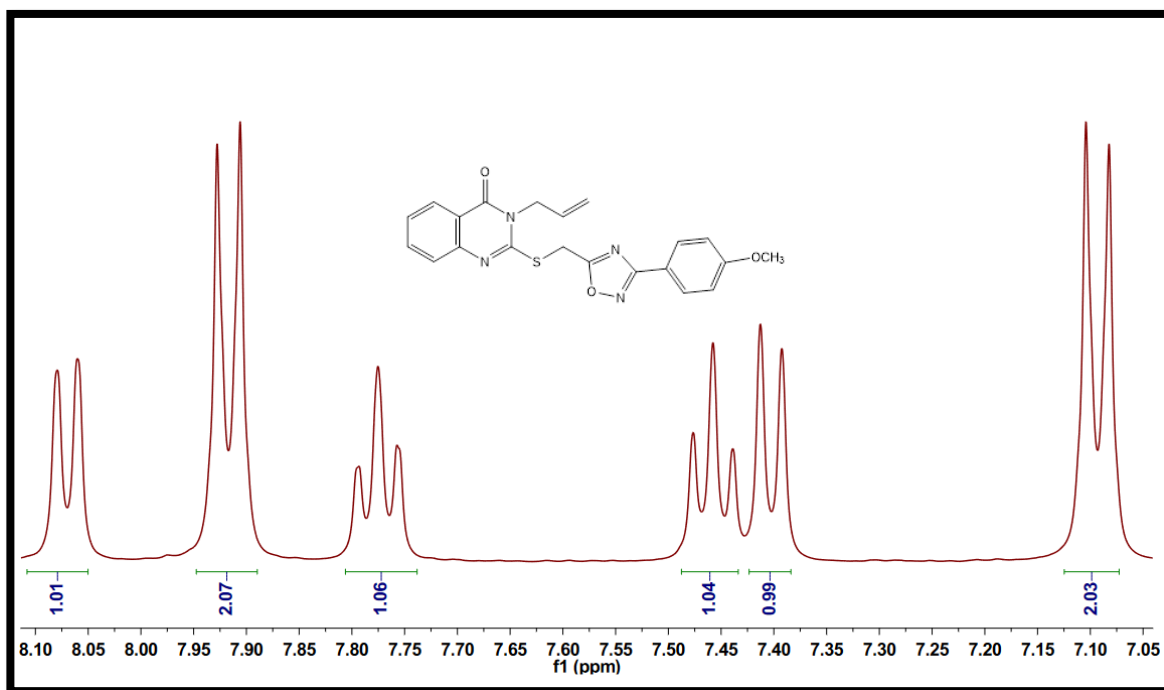


Figure S60: Expanded aromatic region of ^1H NMR spectrum (400 MHz, $\text{DMSO-}d_6$) of compound **9o**

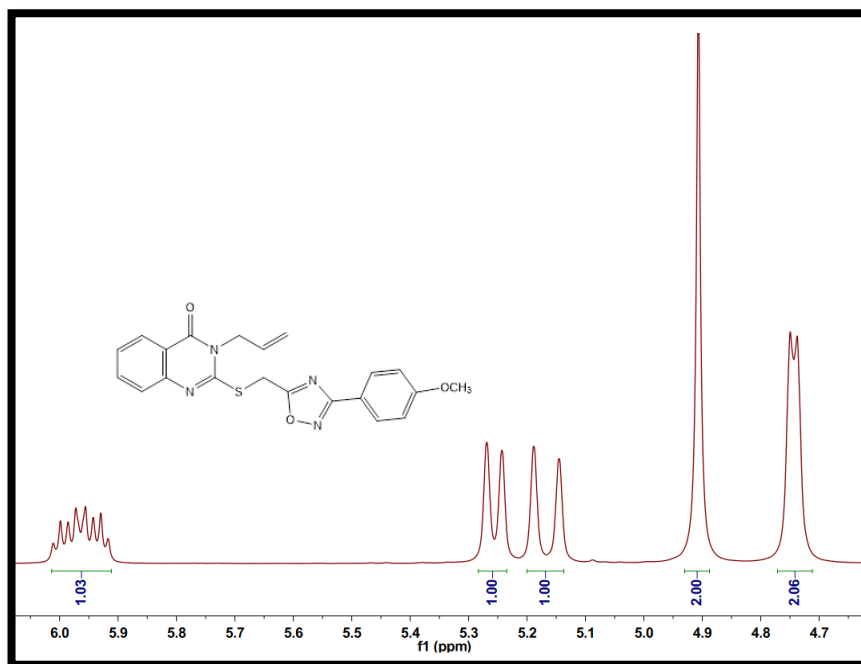


Figure S61: Expanded aliphatic and olefinic regions of ^1H NMR spectrum (400 MHz, $\text{DMSO-}d_6$) of compound **9o**

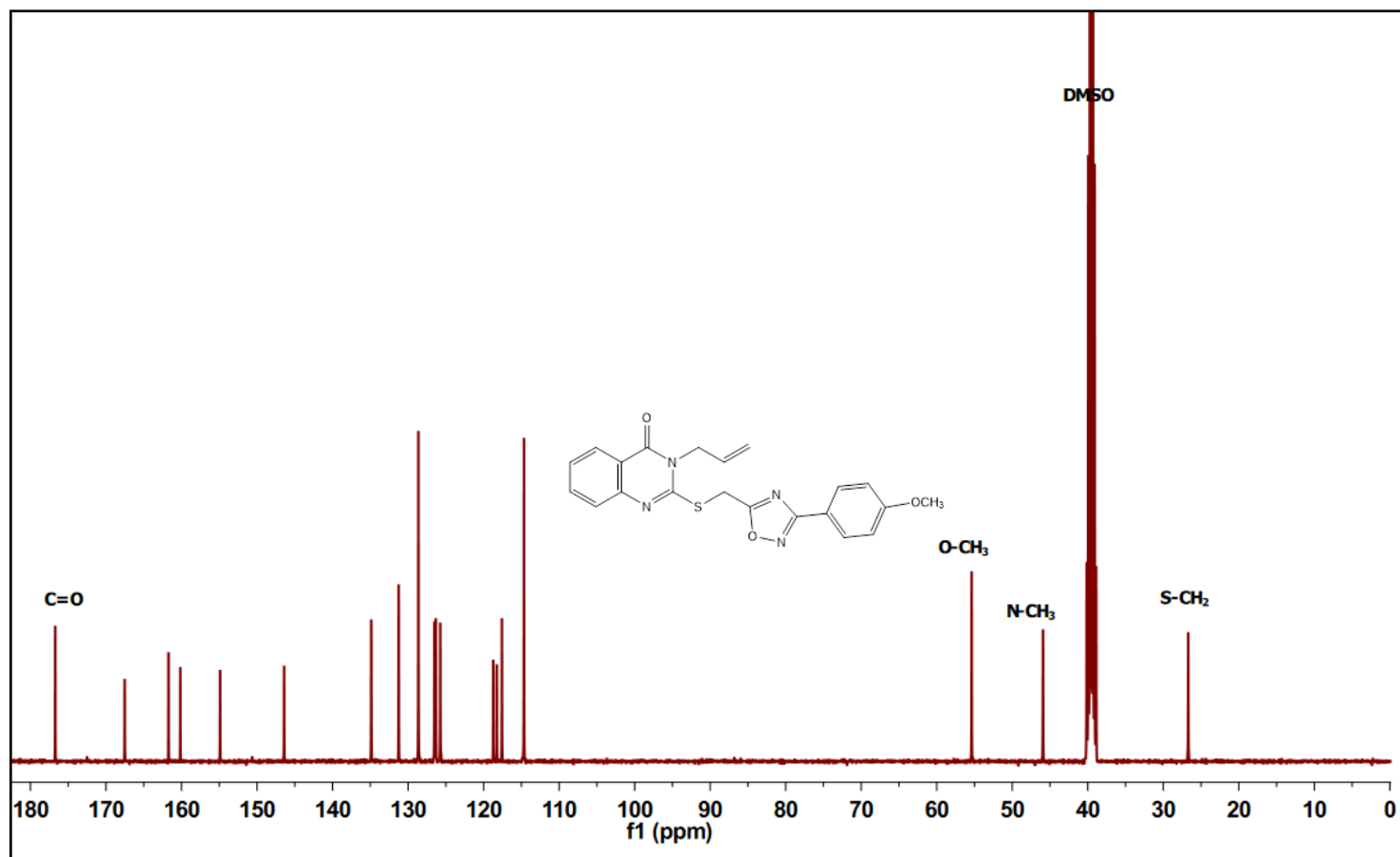


Figure S62: ^{13}C NMR spectrum (100 MHz, $\text{DMSO-}d_6$) of compound **9o**

Al-Azhar University The Regional Center for Mycology and Biotechnology



Requester Data:

Name: Dr. Amira Mahmoud

Authority: Assuit University

Sample Data:

Fifteen samples had been submitted for elemental analysis.

Analysis Report:

Sample Code	C%	H%	N%	S%
AM001p	61.97	3.50	12.71	7.28
AM002m	62.39	3.85	12.40	6.89
AM003A	58.70	3.73	13.91	7.94
AM004E	57.49	3.86	14.27	8.12
AM005P	64.91	4.27	12.89	7.23
AM006m	65.62	4.61	12.49	7.14
AM007A	62.29	4.53	14.02	7.81
AM008E	61.13	4.74	14.37	8.20
AM009	62.37	3.80	12.42	6.89
AM010	65.62	4.61	12.41	6.98
AM011	66.81	3.85	13.82	7.85
AM012	67.36	4.09	13.41	7.60
AM013	64.05	4.42	15.17	8.64
AM014	62.89	4.51	15.62	8.71
AM015	67.34	4.43	13.40	7.68

INVESTIGATOR

M. A.

DIRECTOR

H. Saad

Old code	New code
AMoo1P	9b
AM002m	9h
AM003A	9n
AM004E	9k
AM005P	9c
AM006m	9i
AM007A	9o
AM008E	9l
AM009	9e
AM010	9f
AM011	9a
AM012	9g
AM013	9m
AM014	9j
AM015	9d

Al-Azhar University Campus - Nasr City, Cairo, Egypt.

Tel: 0202 22620373

Fax : 0202 22620373

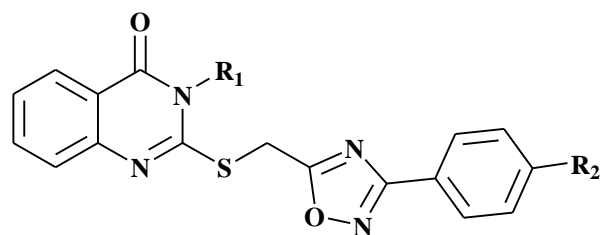
E-mail: remb@azhar.edu.eg

Website: <http://www.azhar.edu.eg.htm> * http://www.azhar.edu.eg/pages/fungi_center.htm

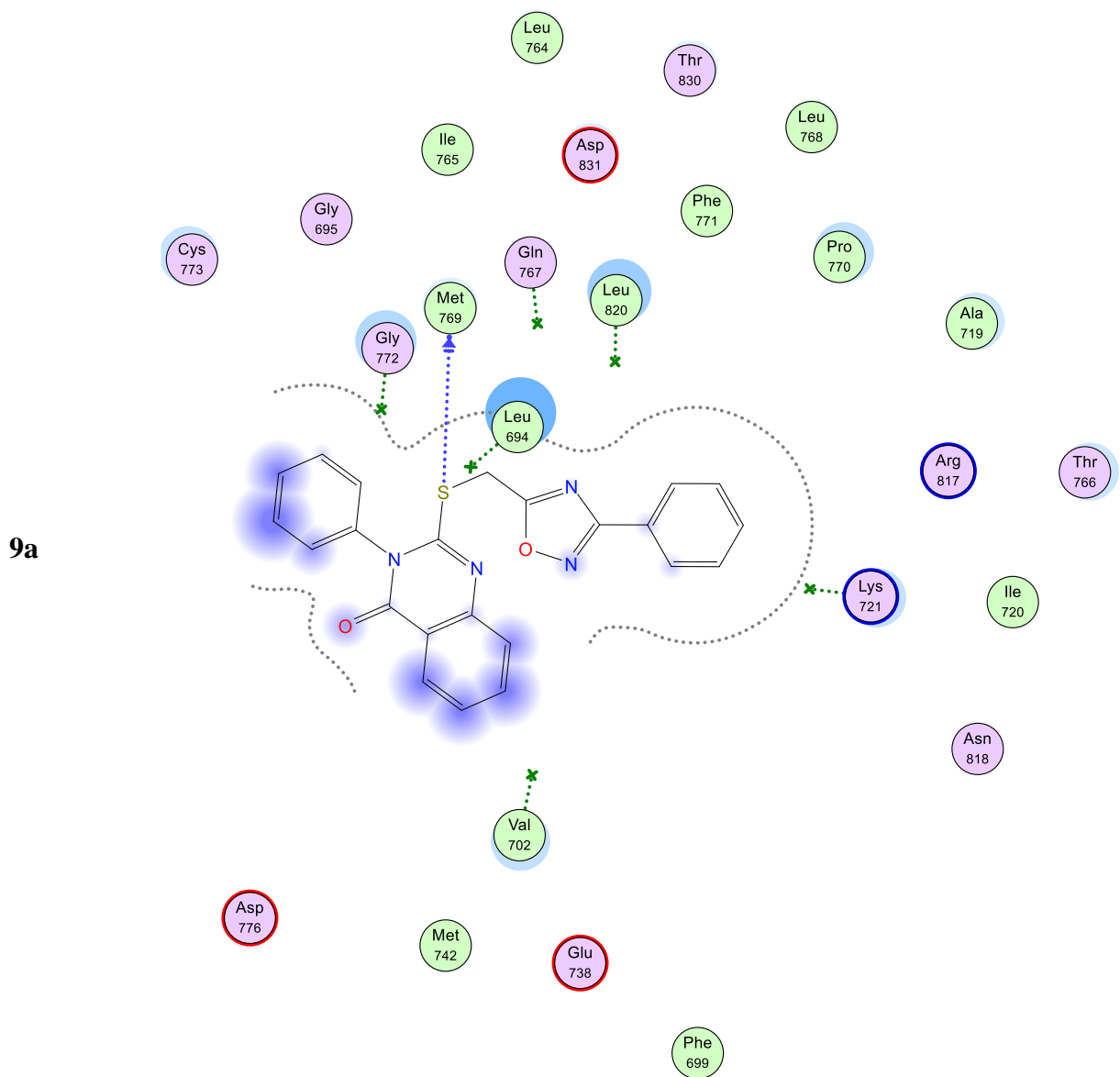
Facebook : RCMBAZHAR

P.O. box mail : 11751 Nasr City Cairo, Egypt.

Oxadiazoles Docking Poses Within EGFR, EGFR^{T790M}, & BRAF^{V600E} Active Sites

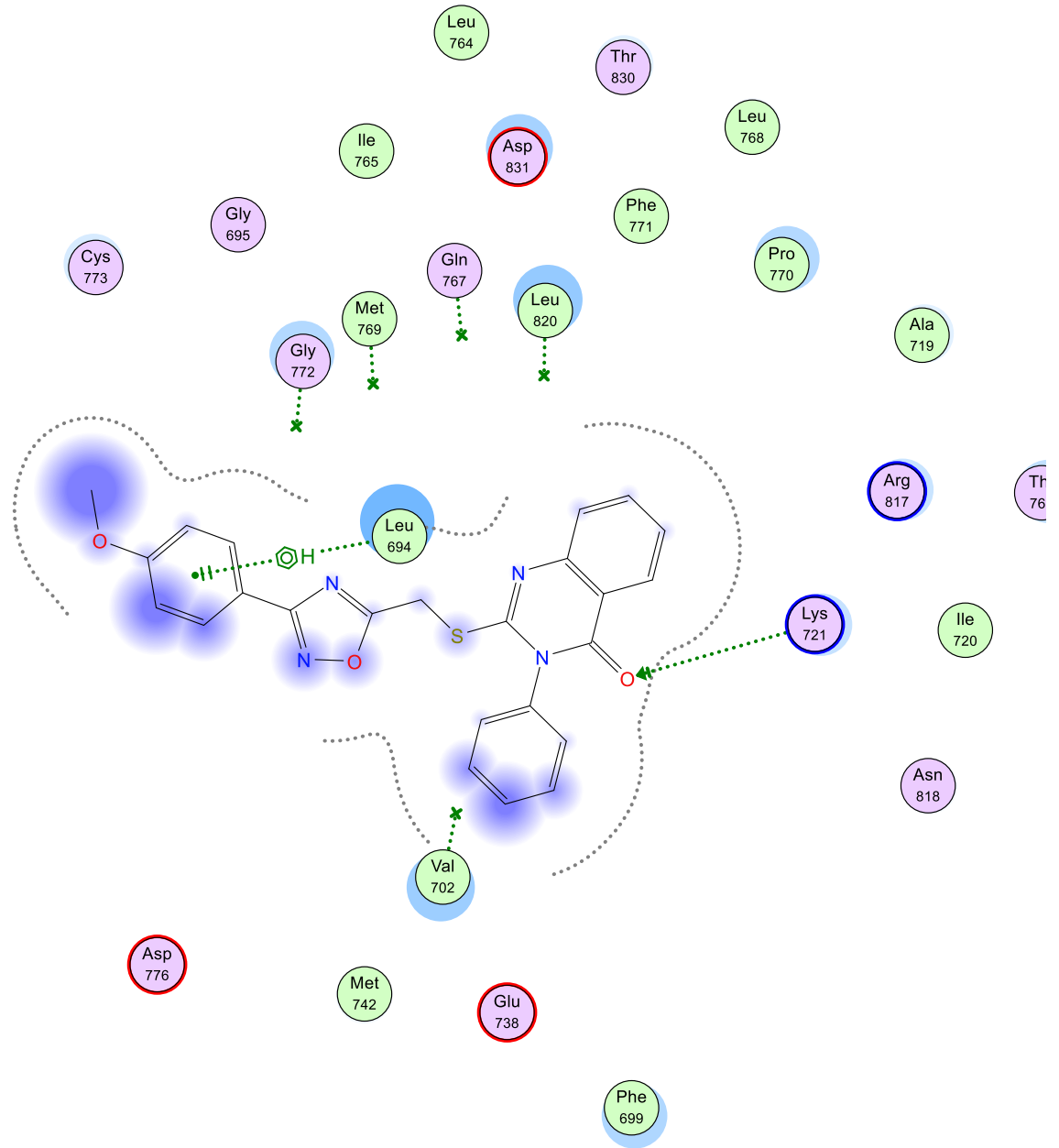


(9a-o)

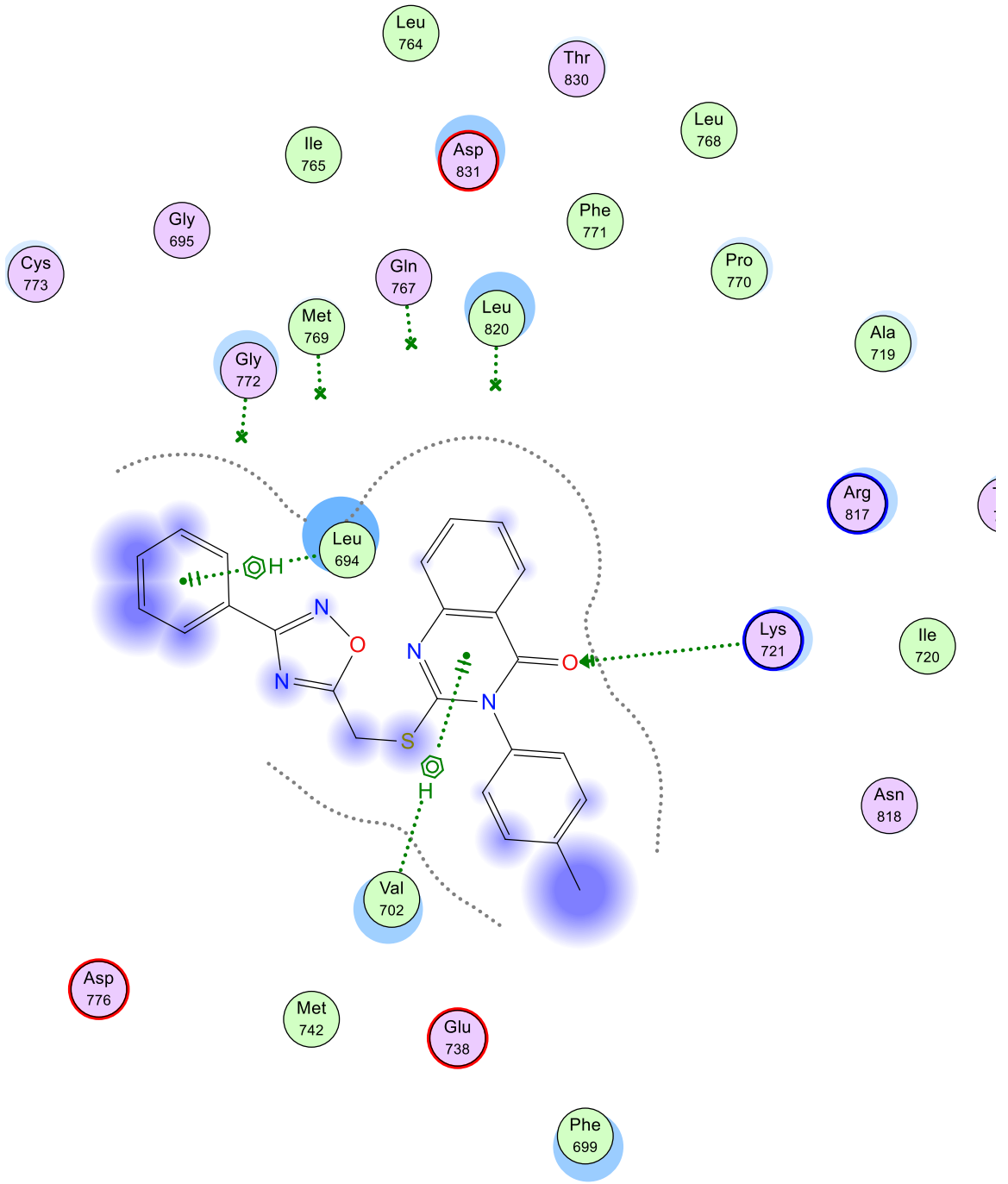


9a

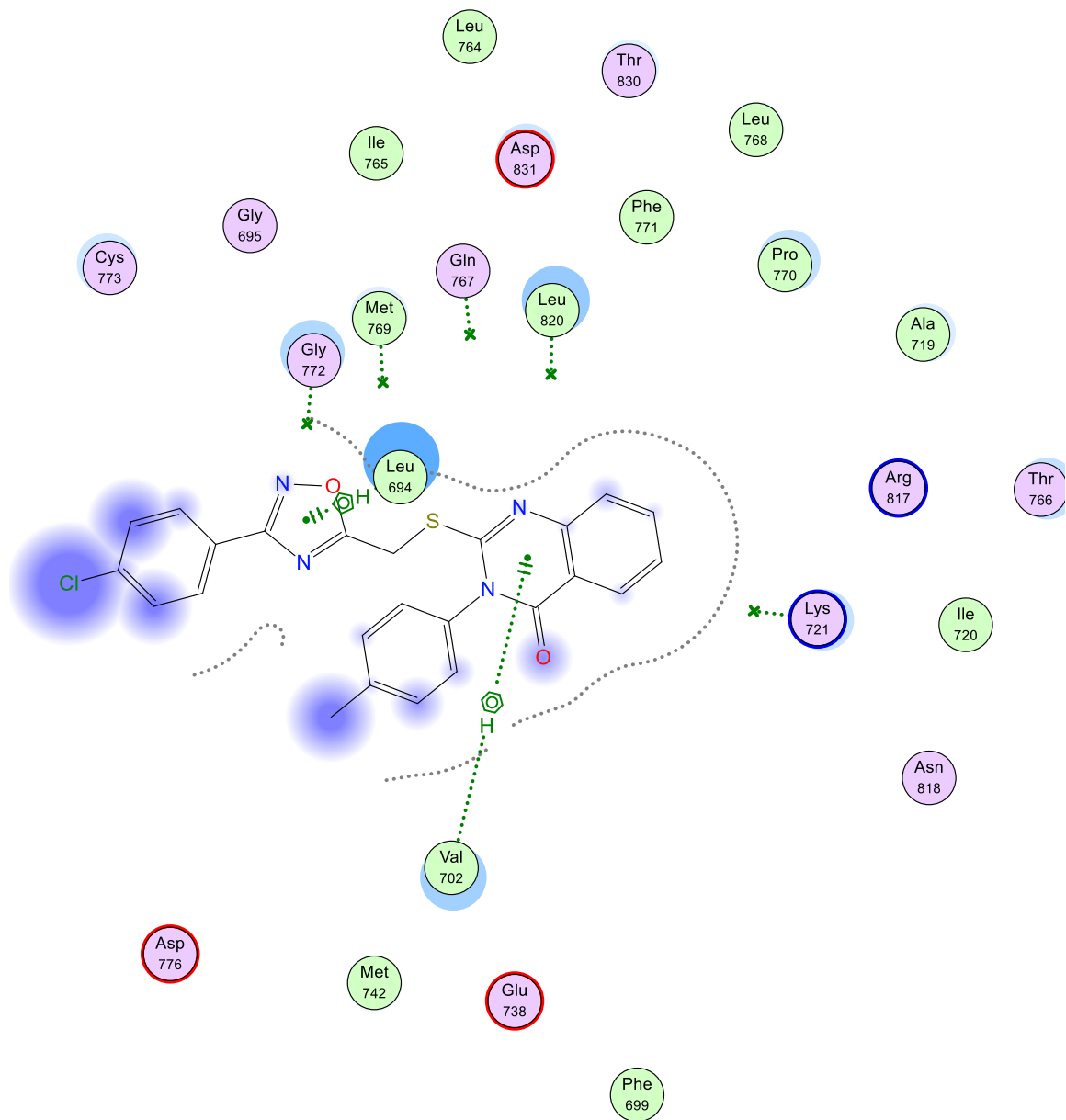
9c



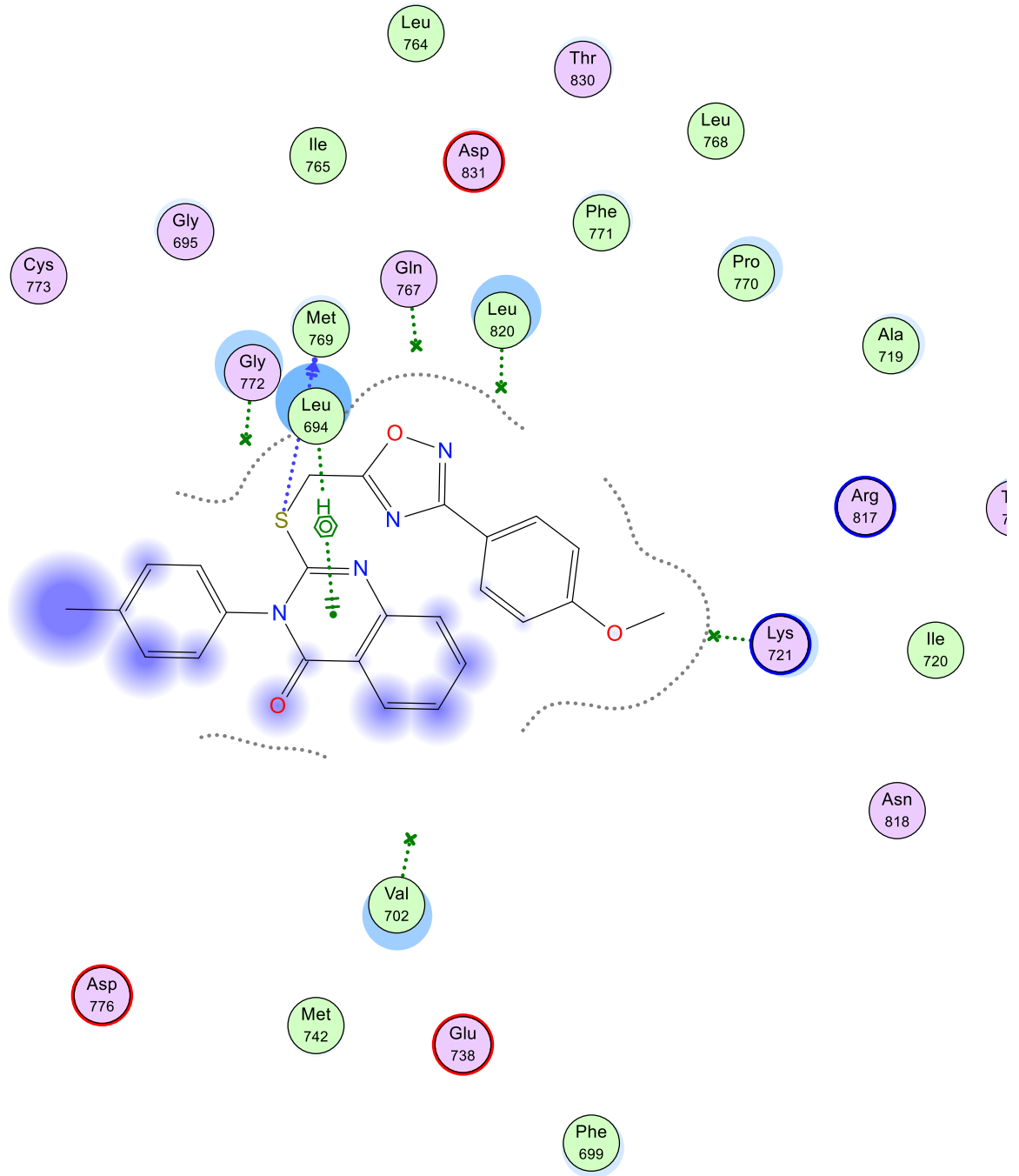
9d



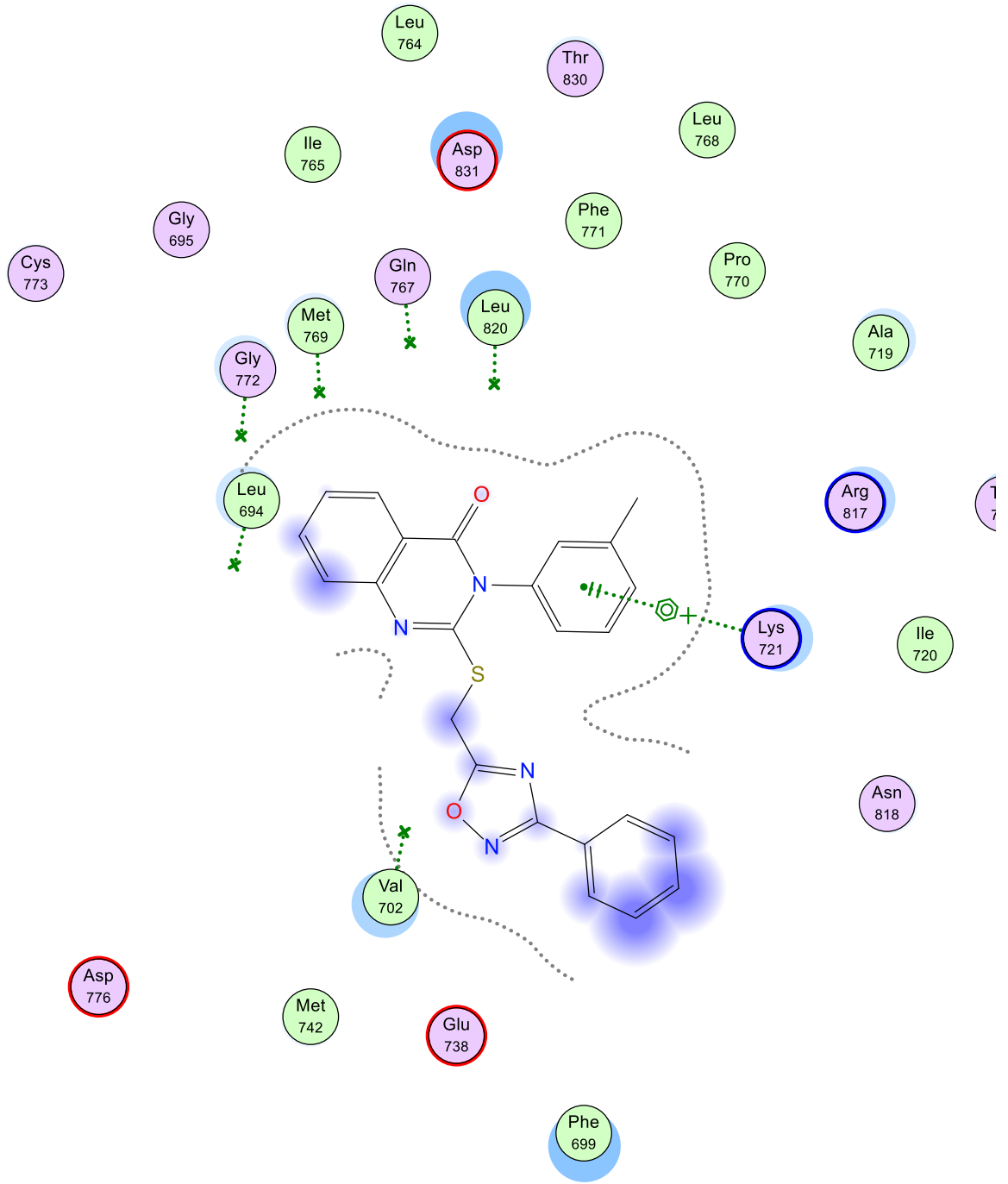
9e



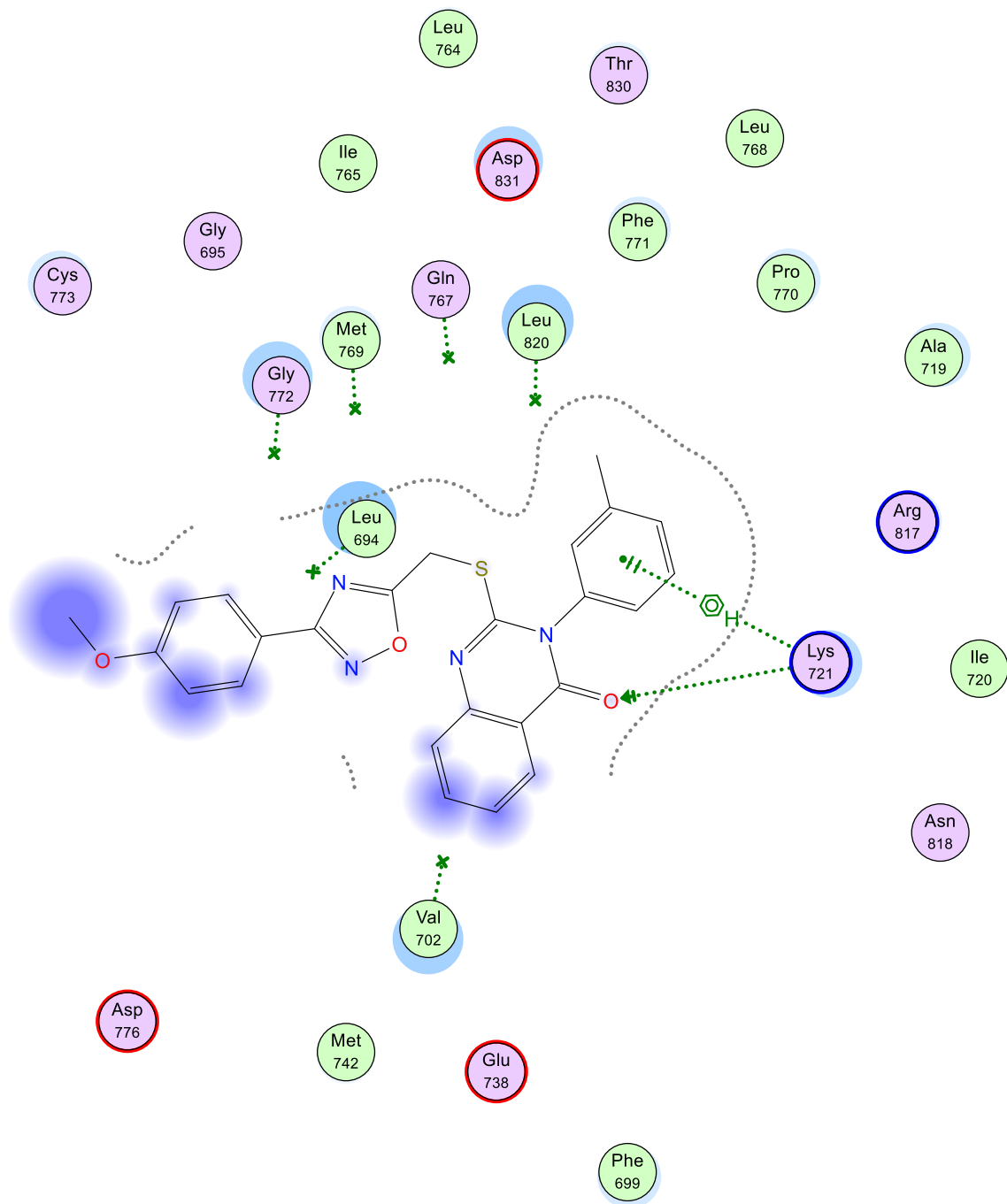
9f



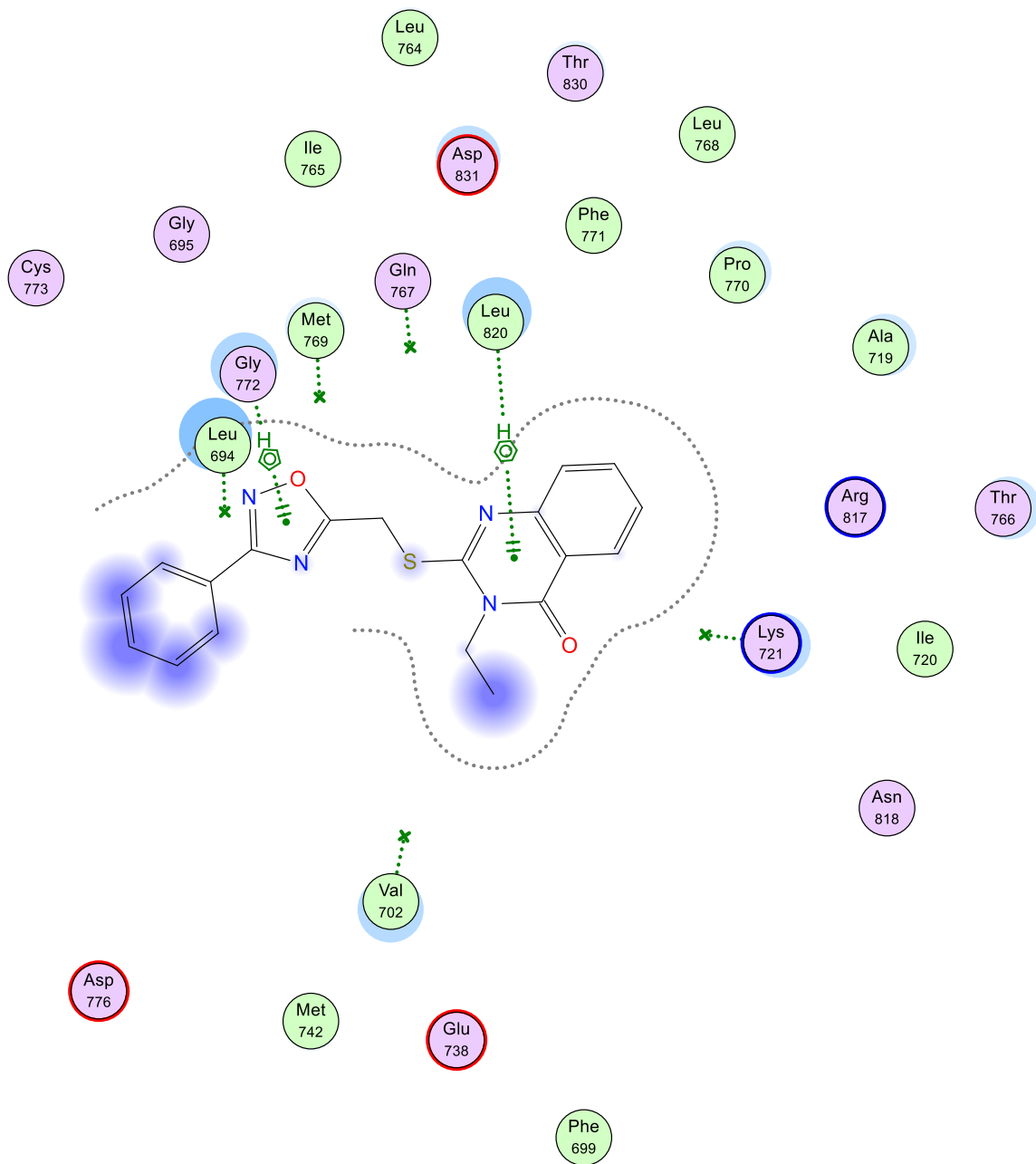
9g



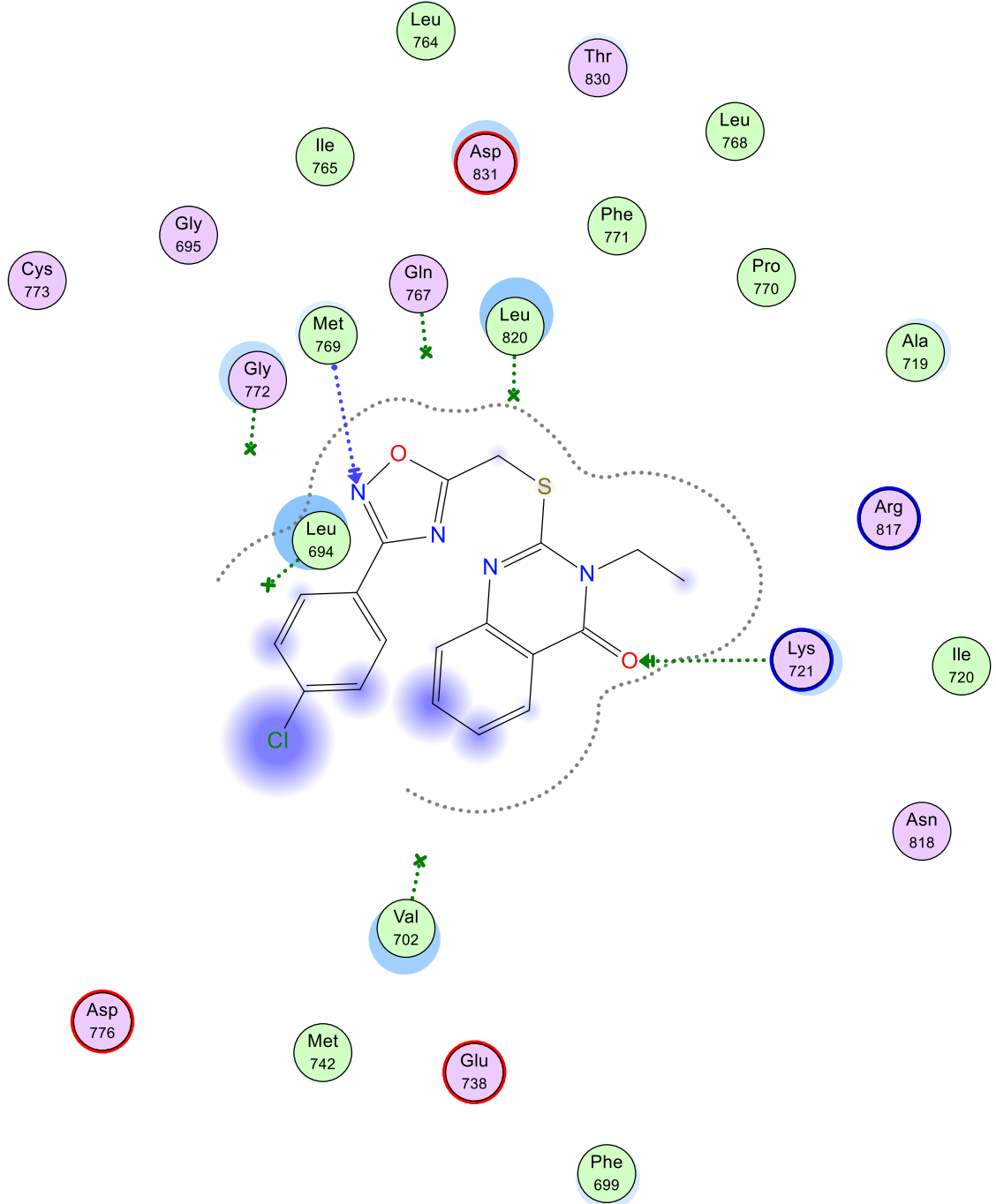
9i



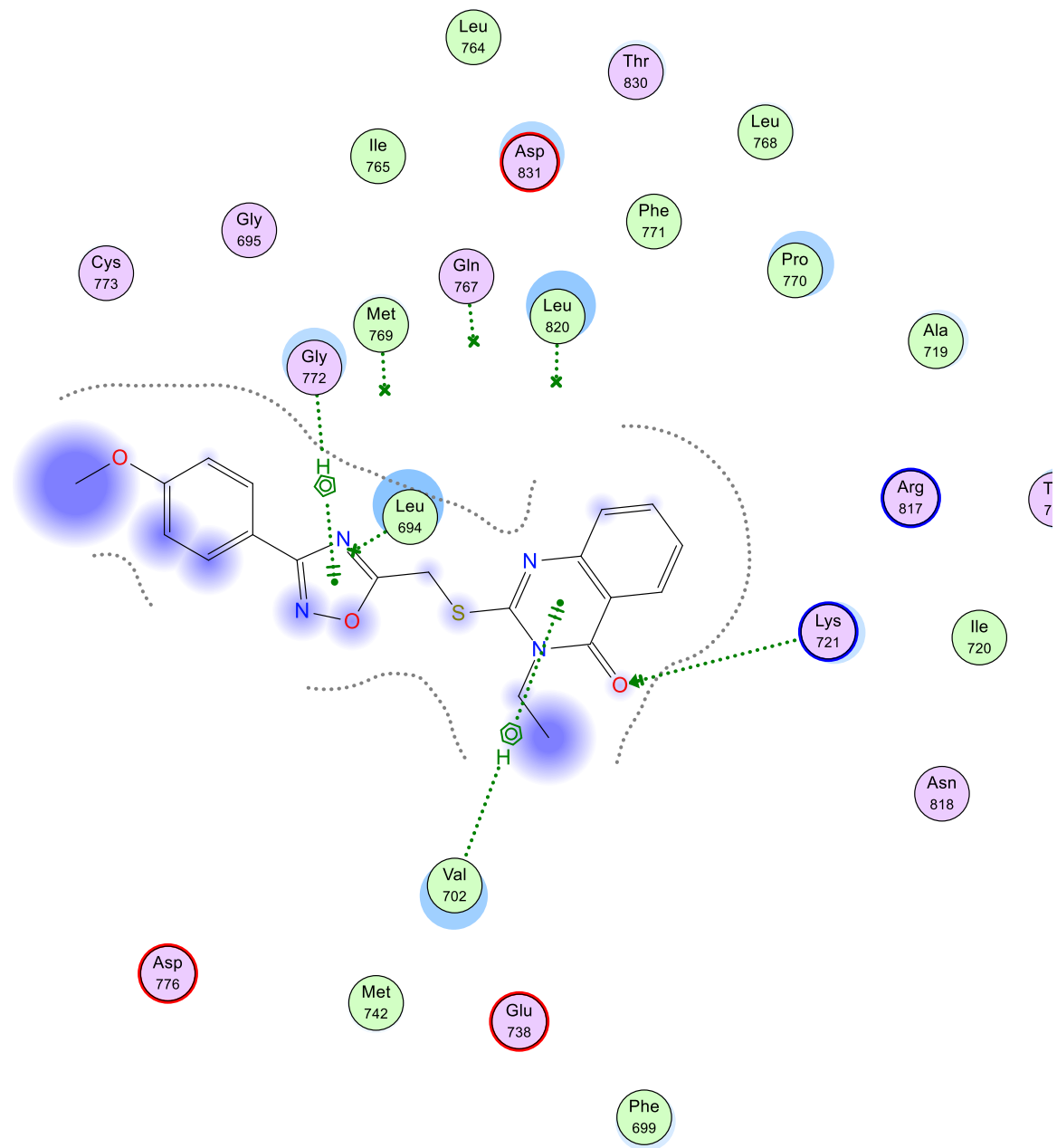
9j



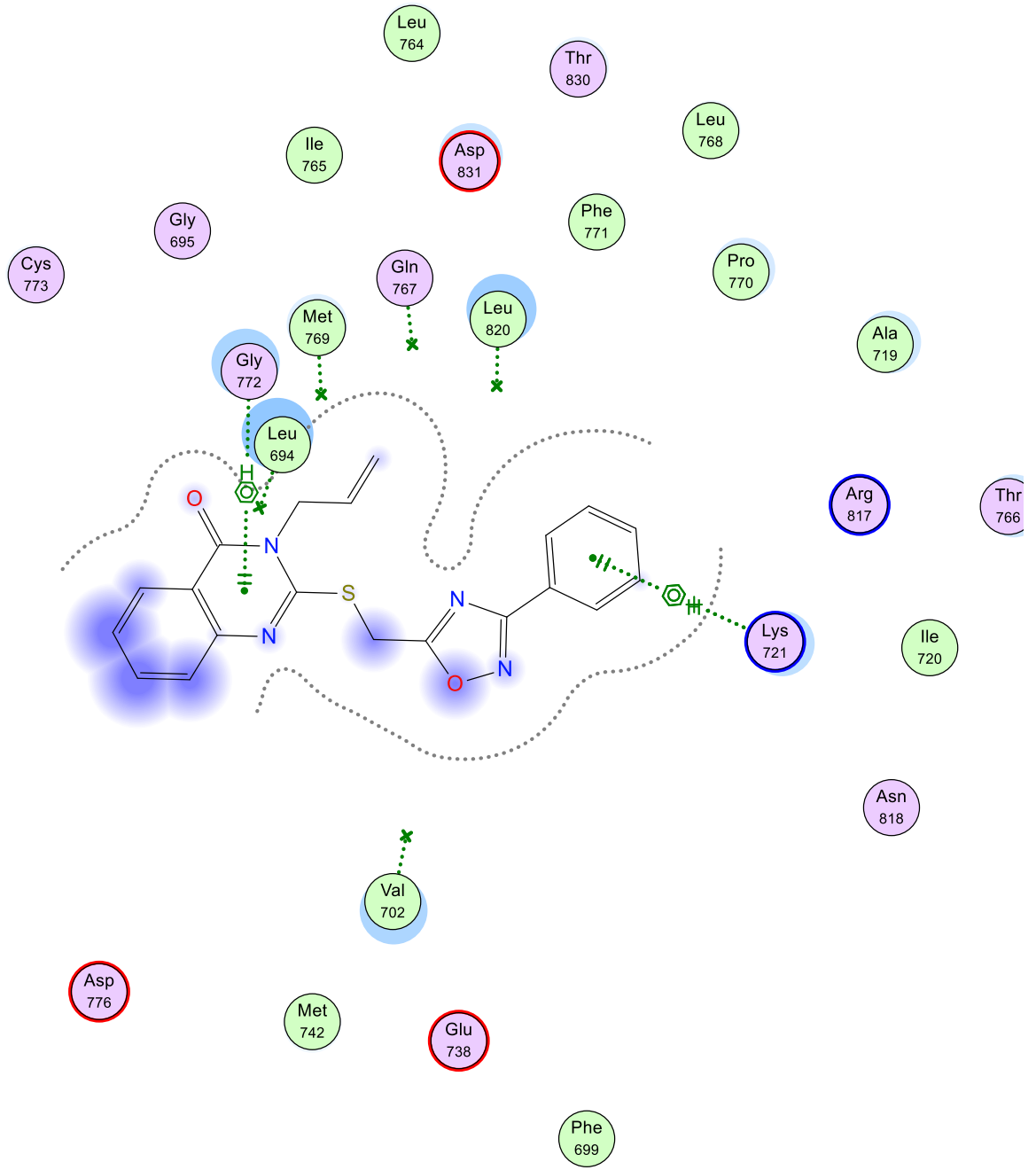
9k



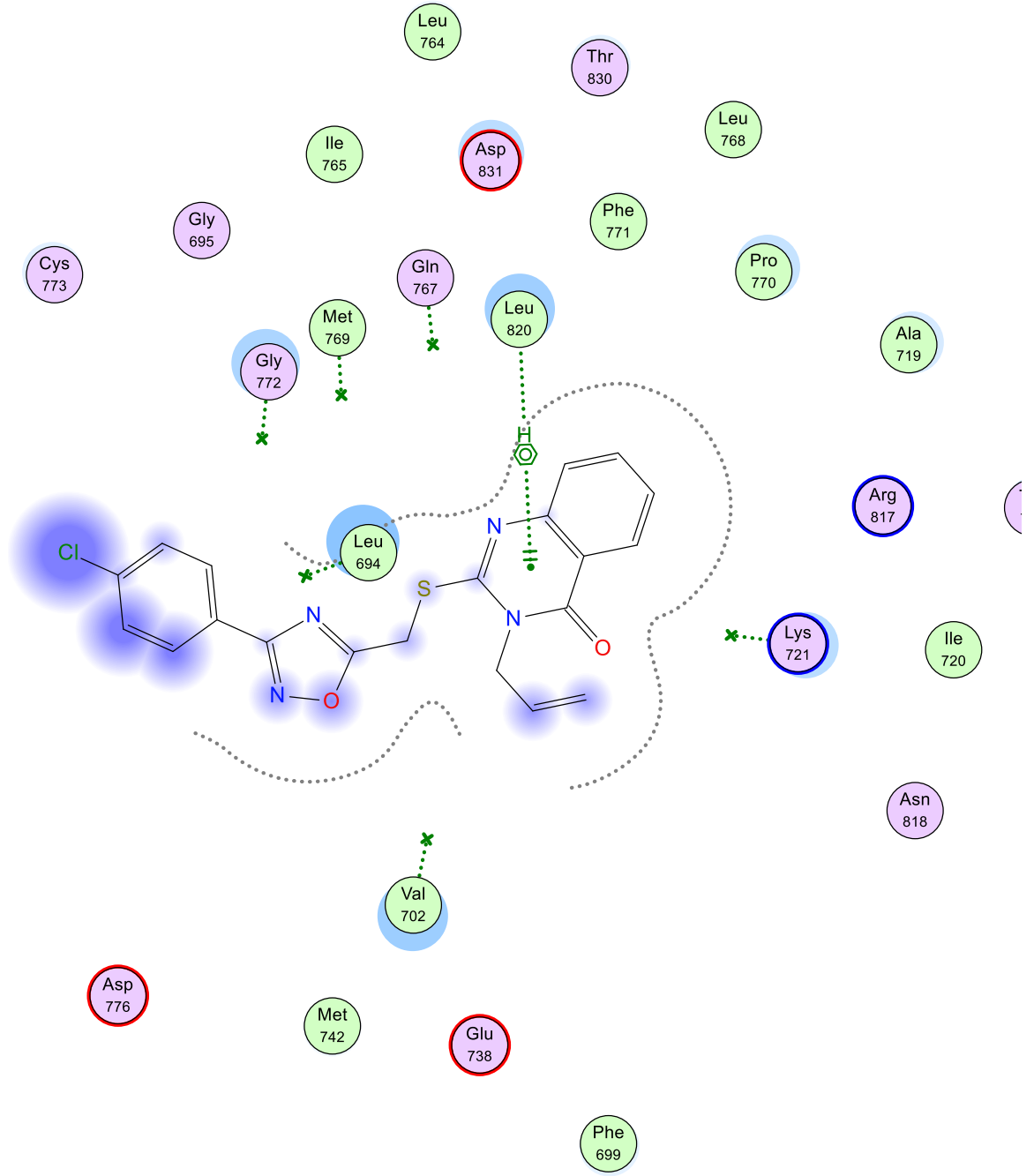
91



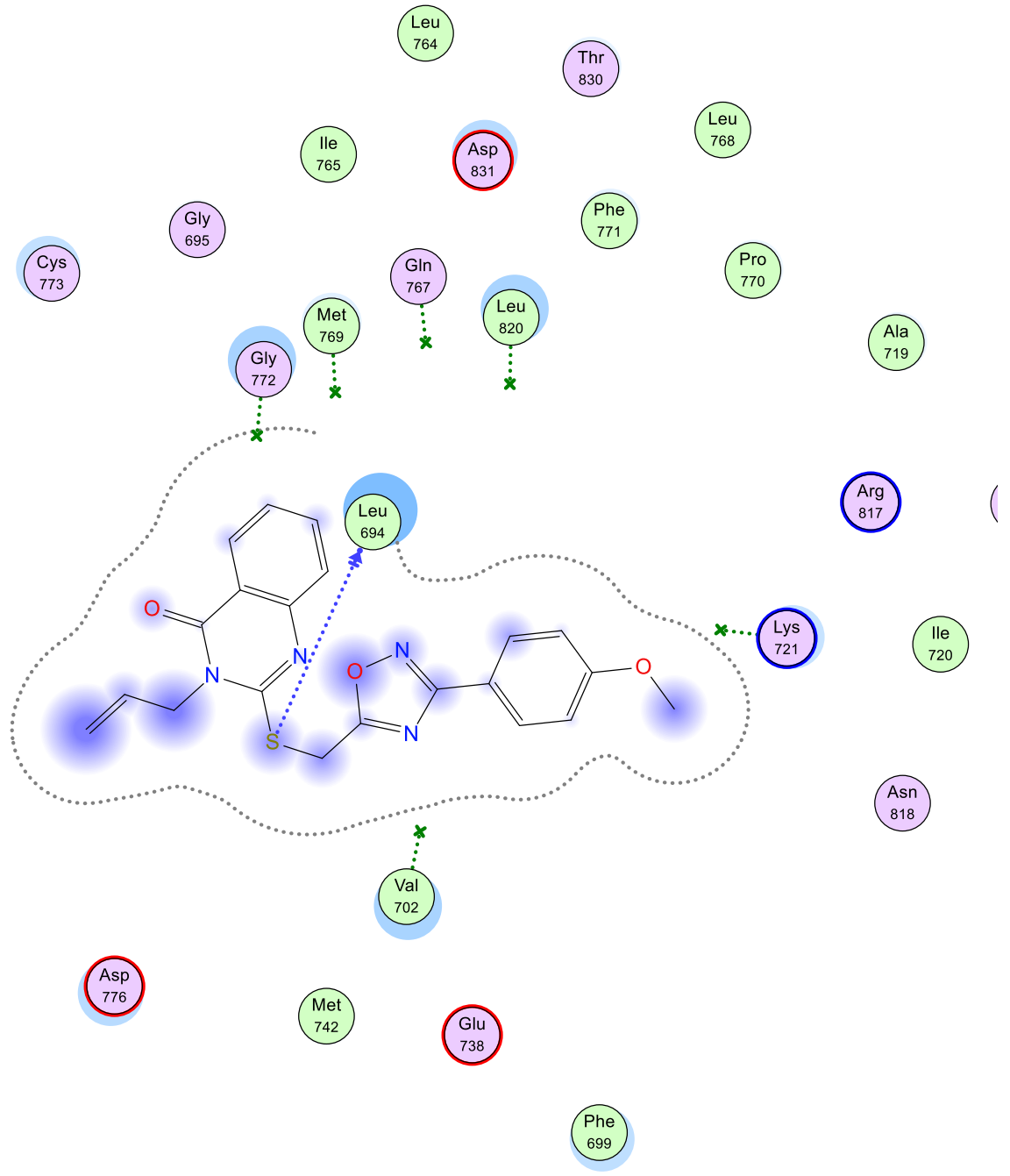
9m



9n



90



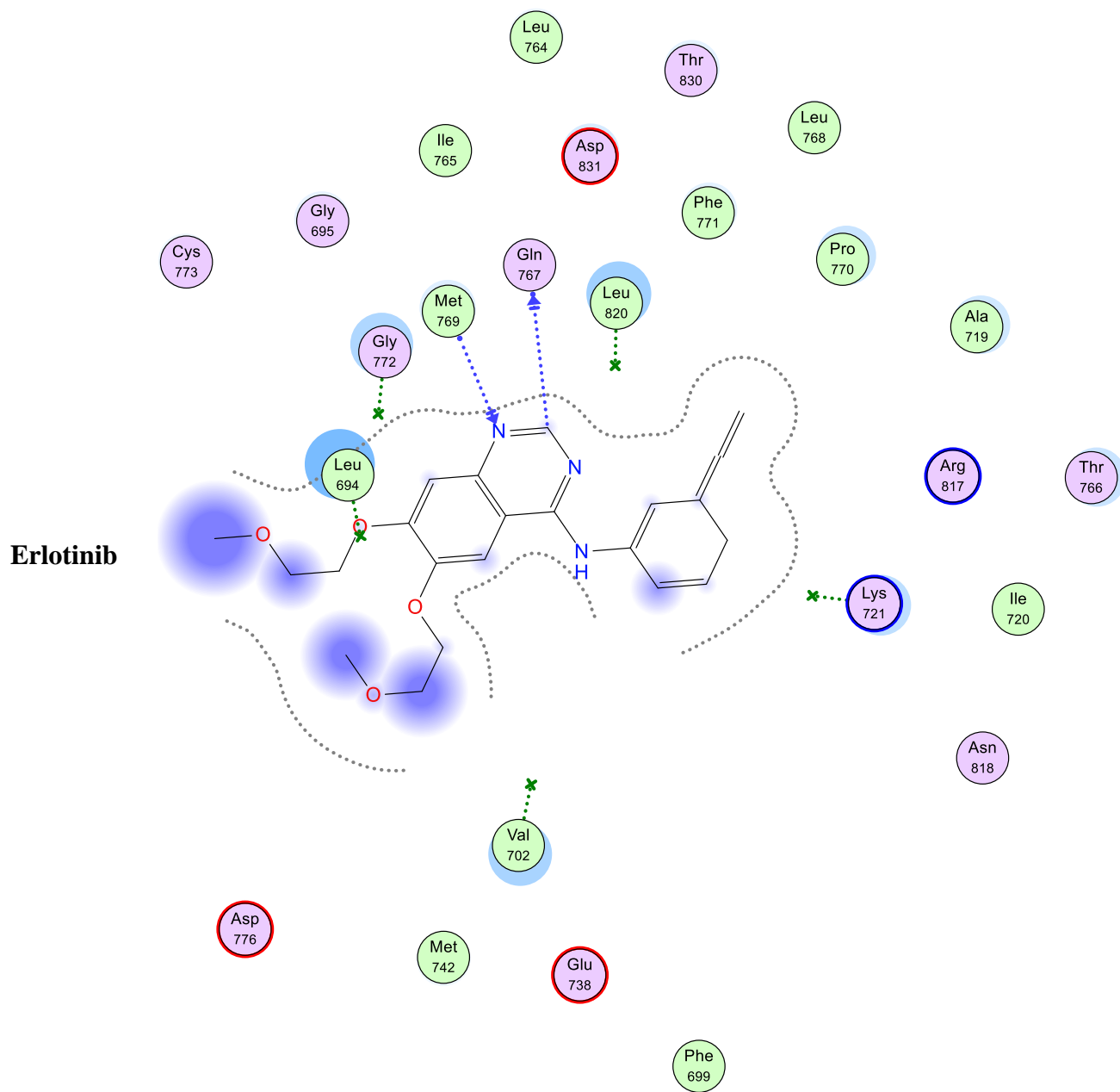
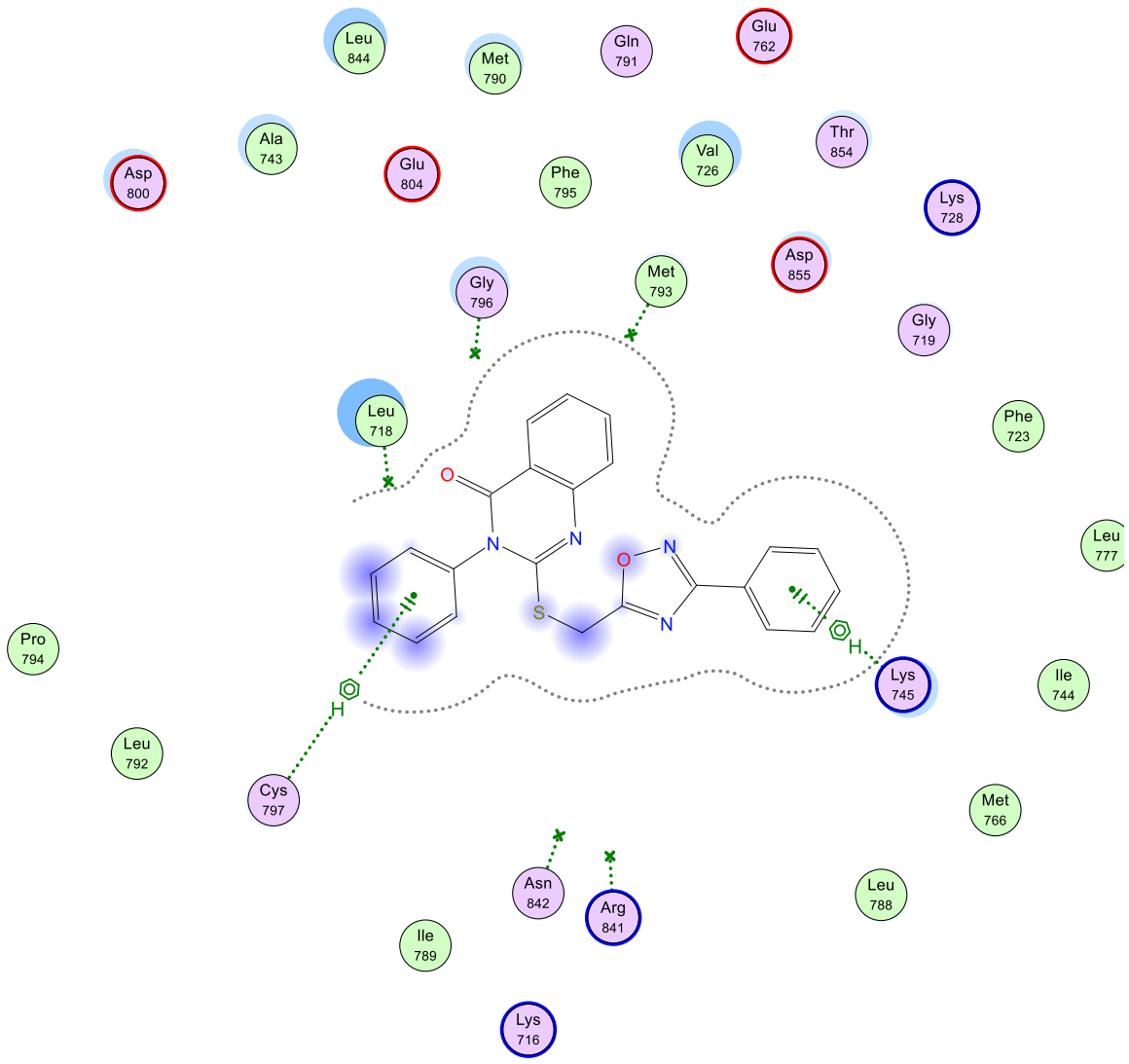
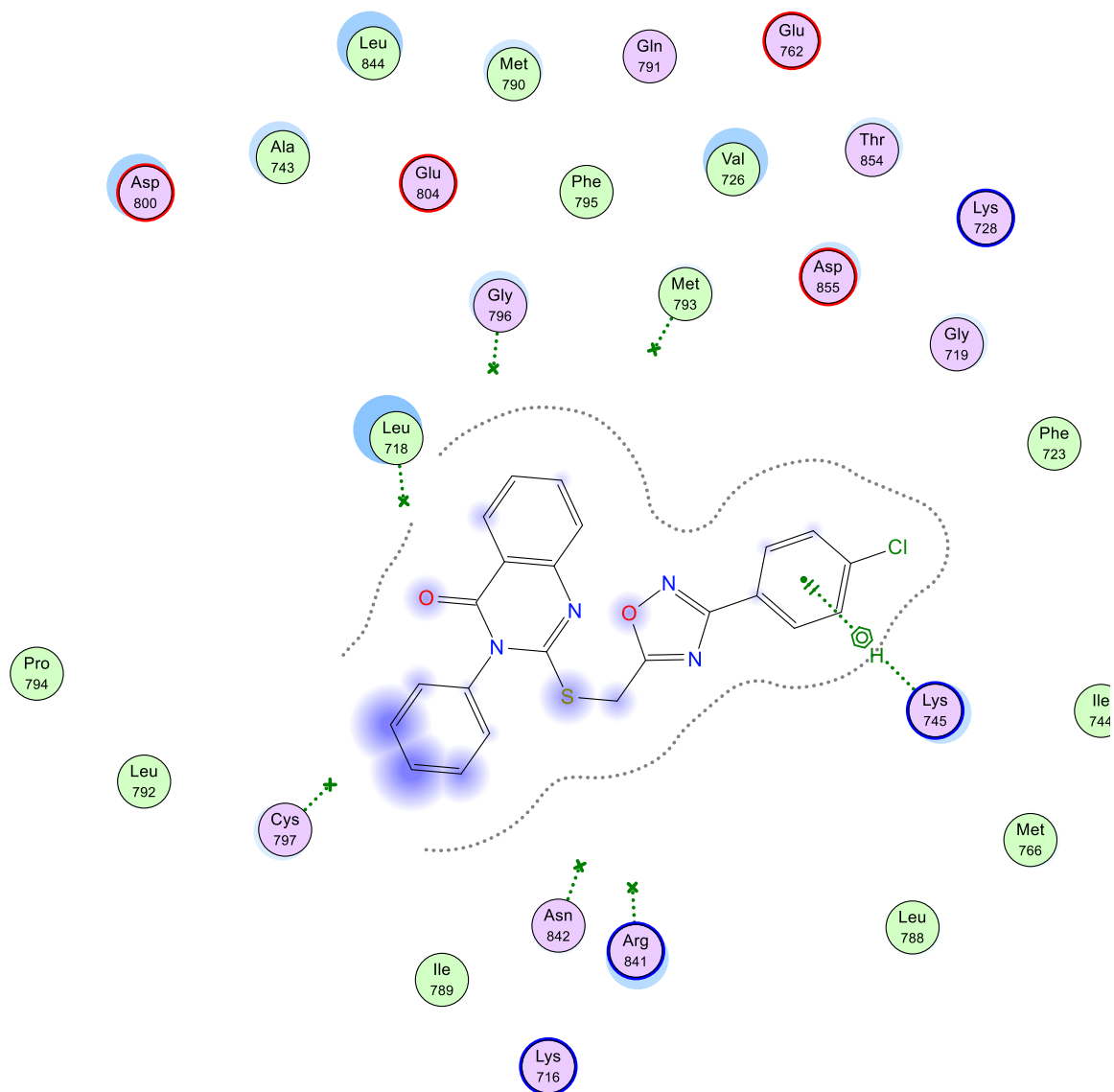


Fig. S.I. ????? Docking poses of derivatives (9a-o) within EGFR (PDB ID: 1M17) active site showing H-bonding and H-Pi interactions with key amino acid residues (Met 769, Glu 767, Lys 721, Leu 684, Val 702).

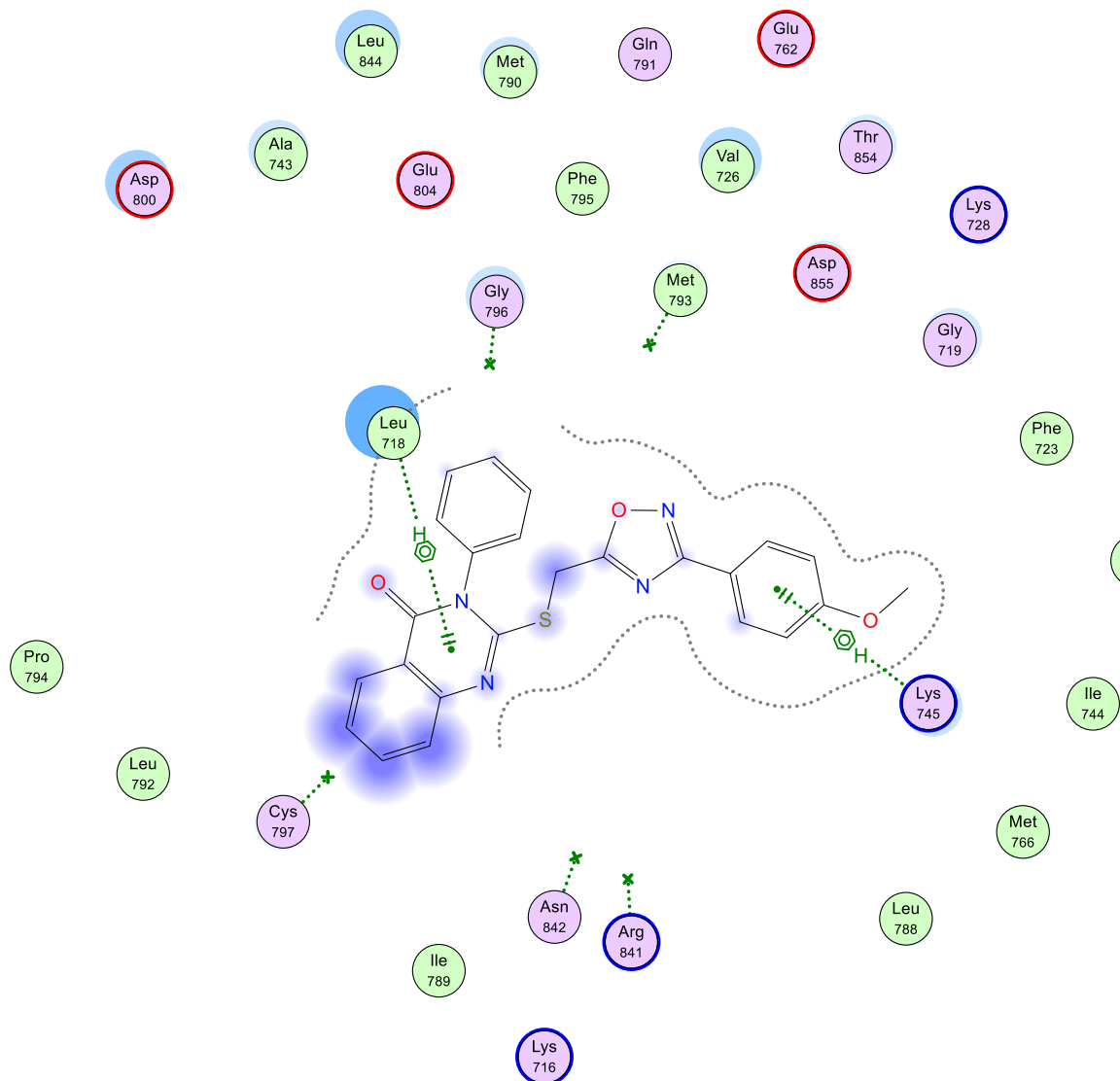
9a



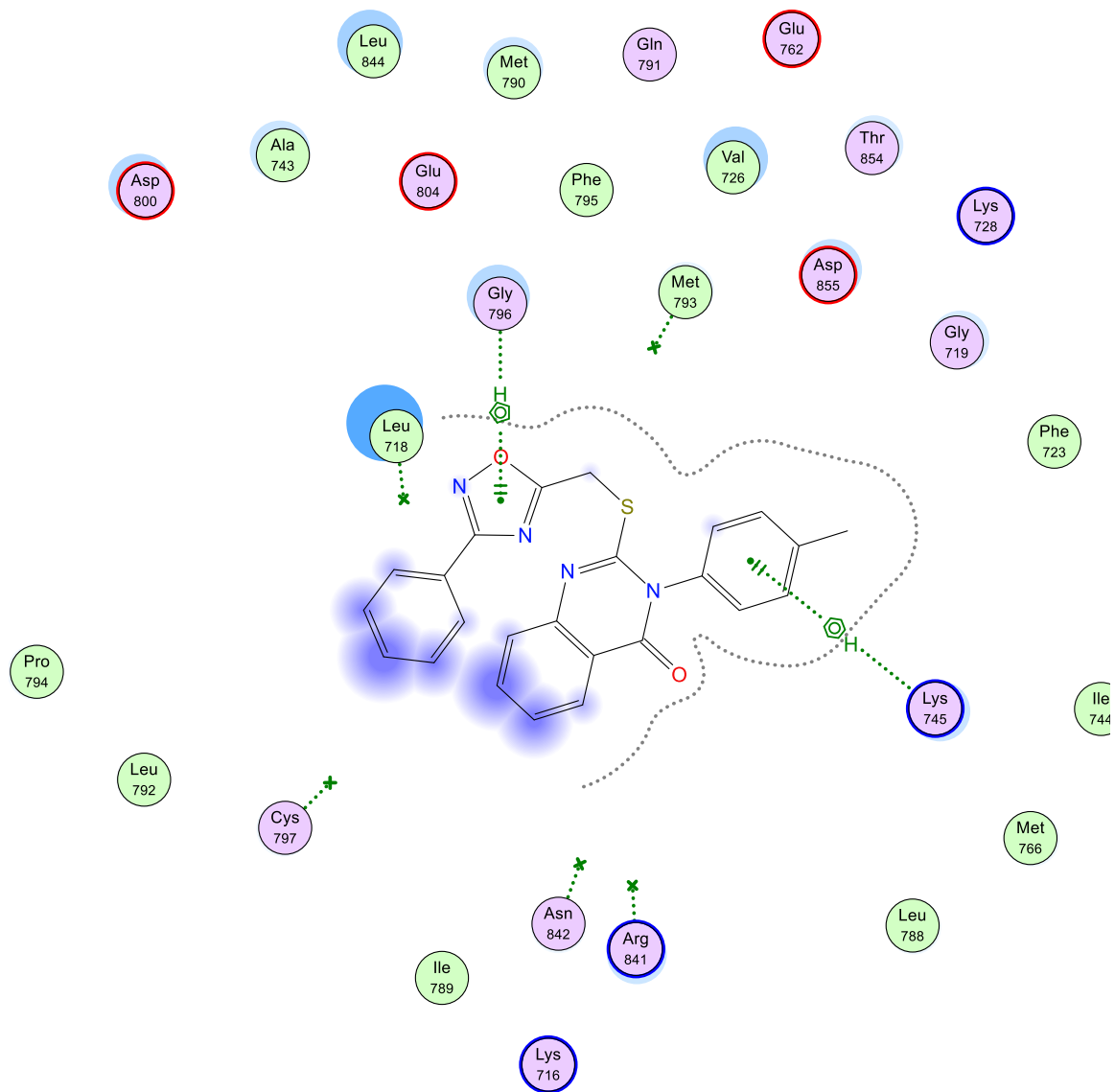
9b



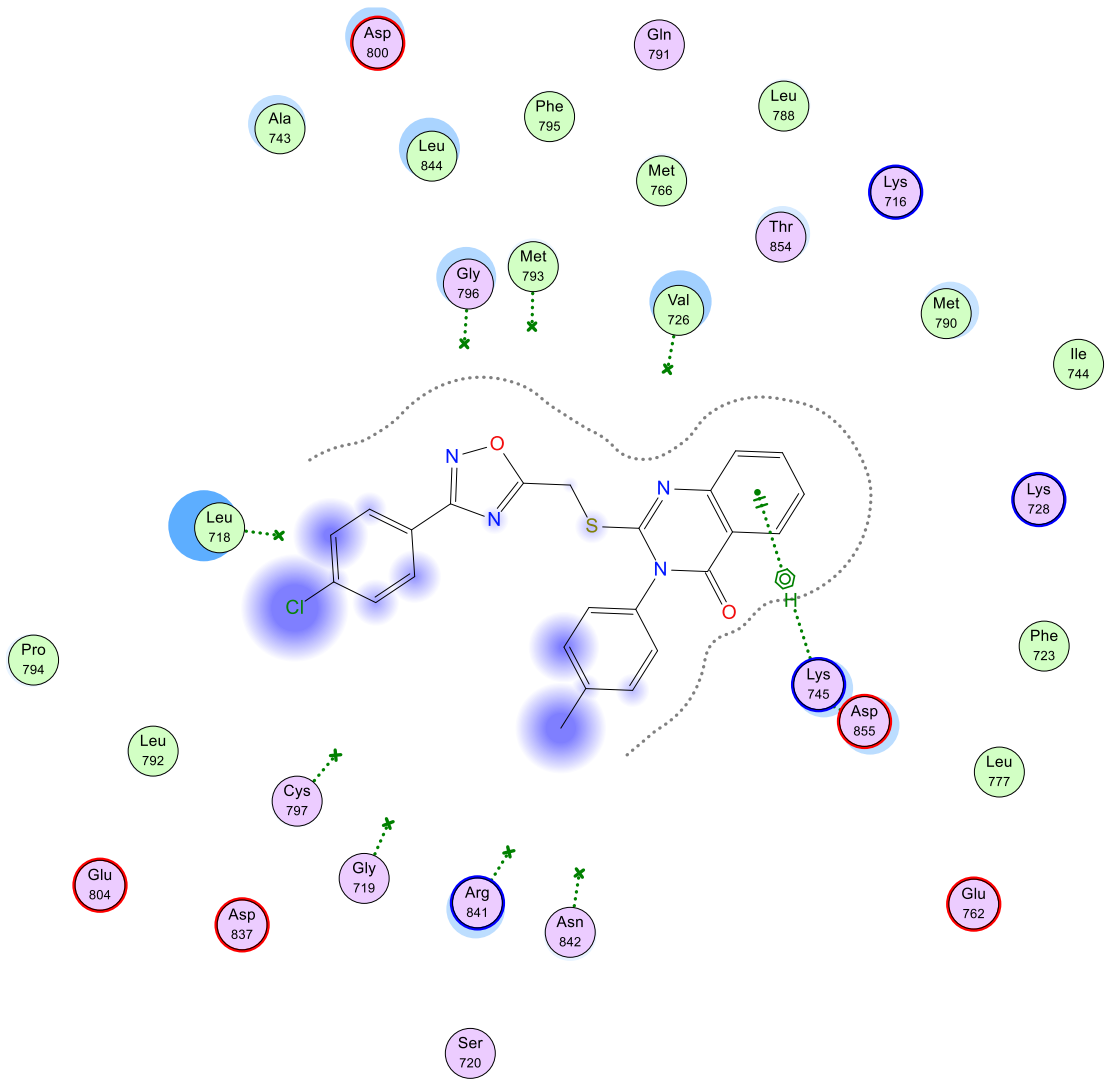
9c



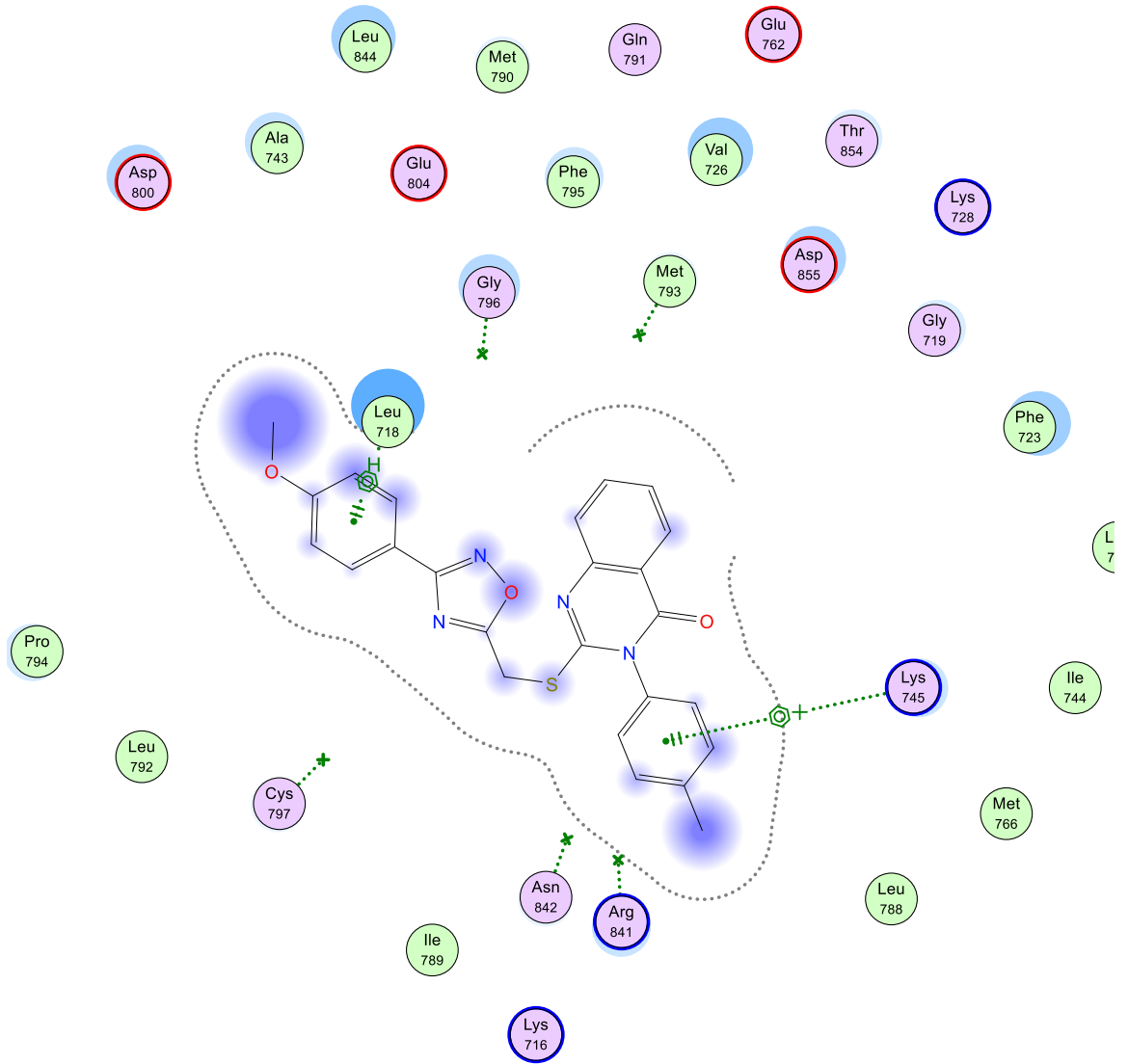
9d



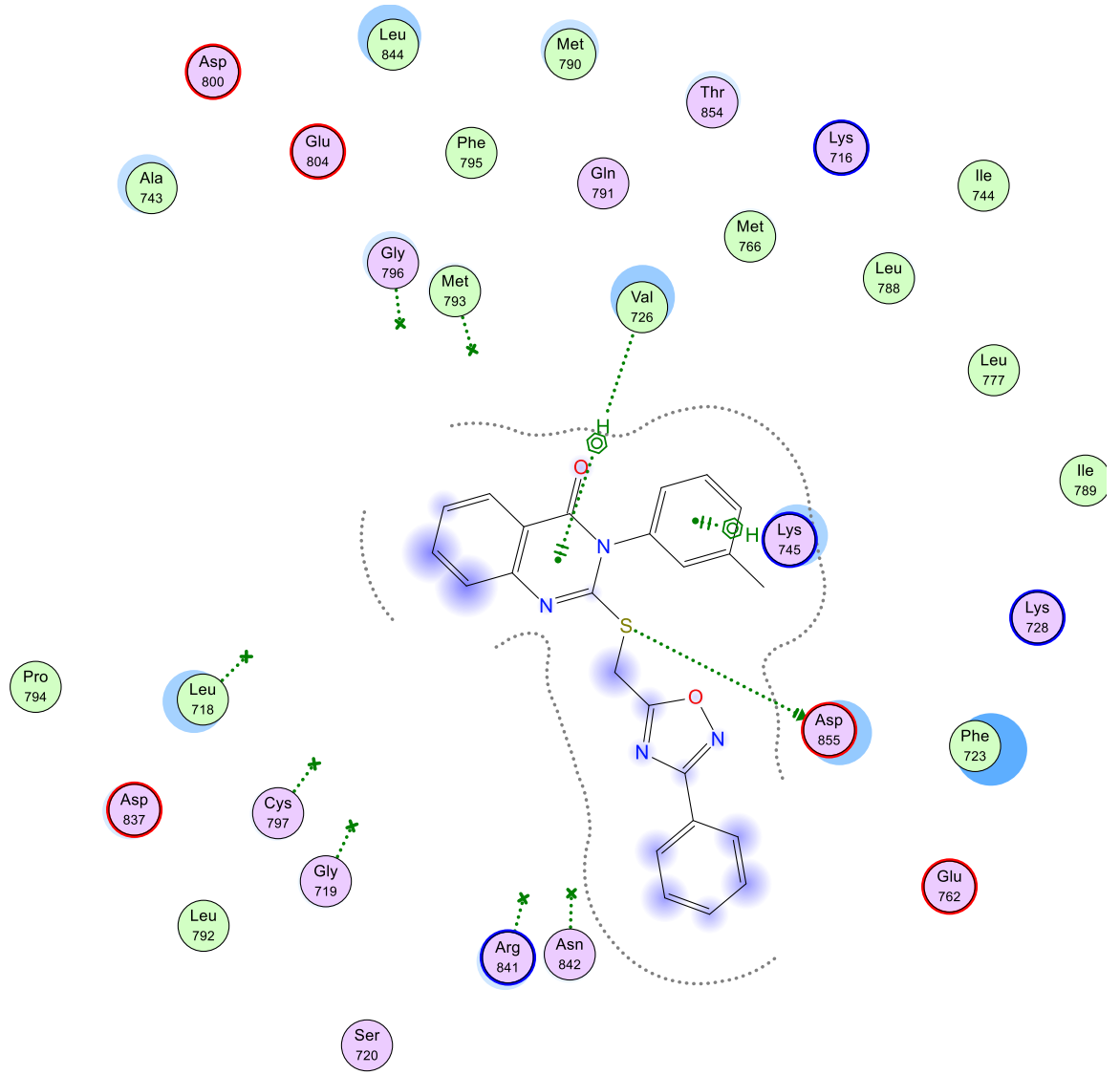
9e



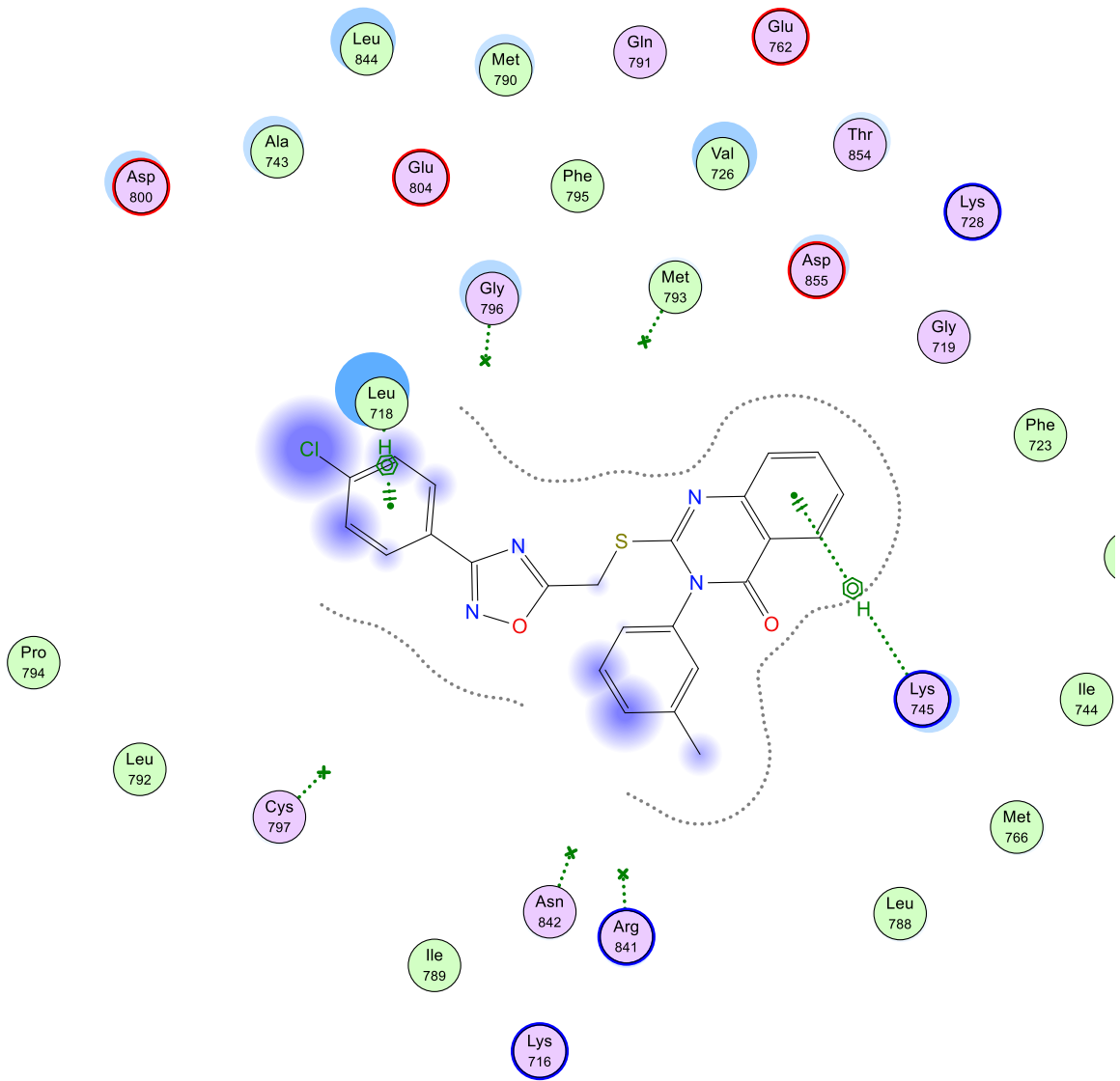
9f



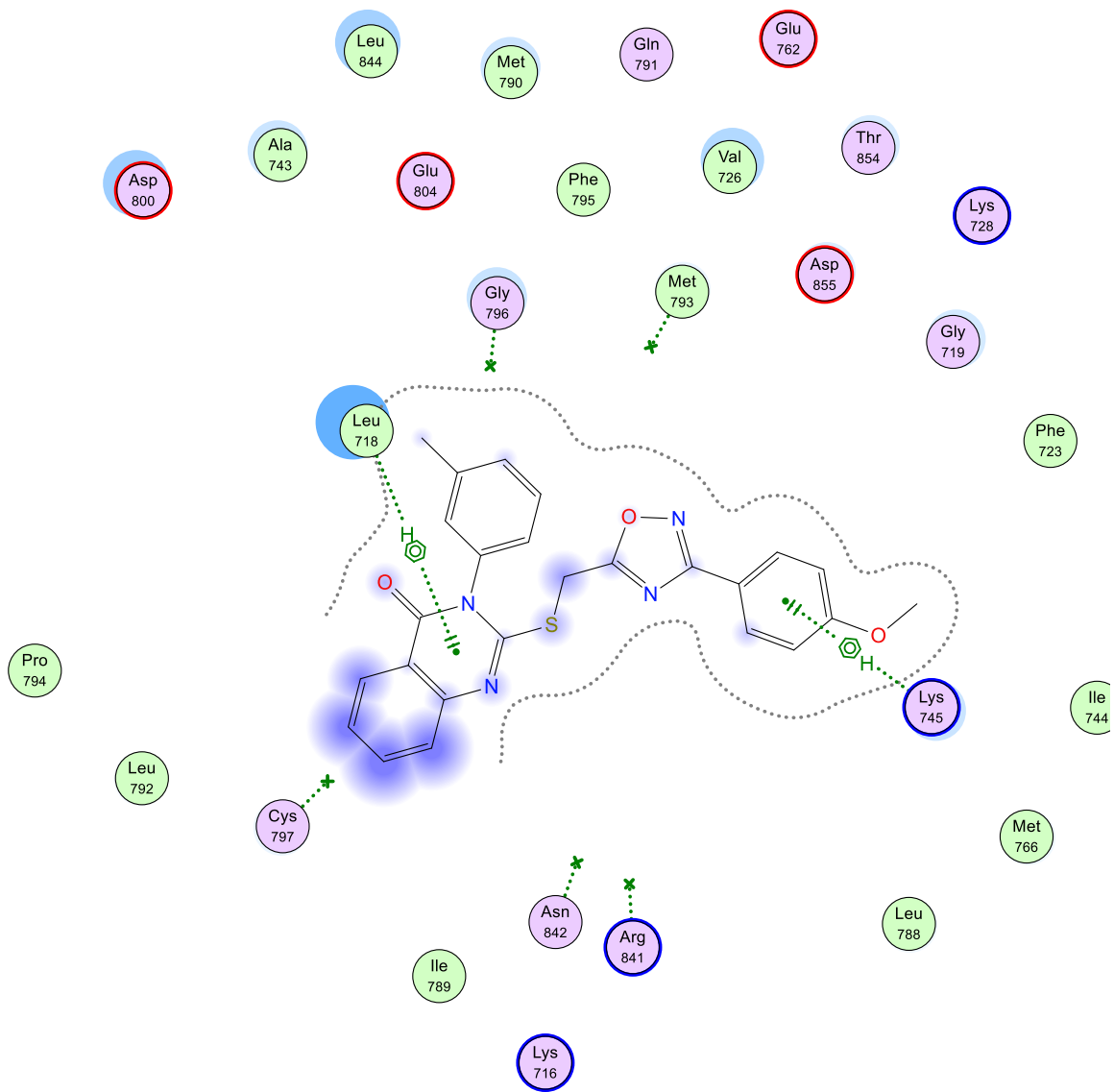
9g



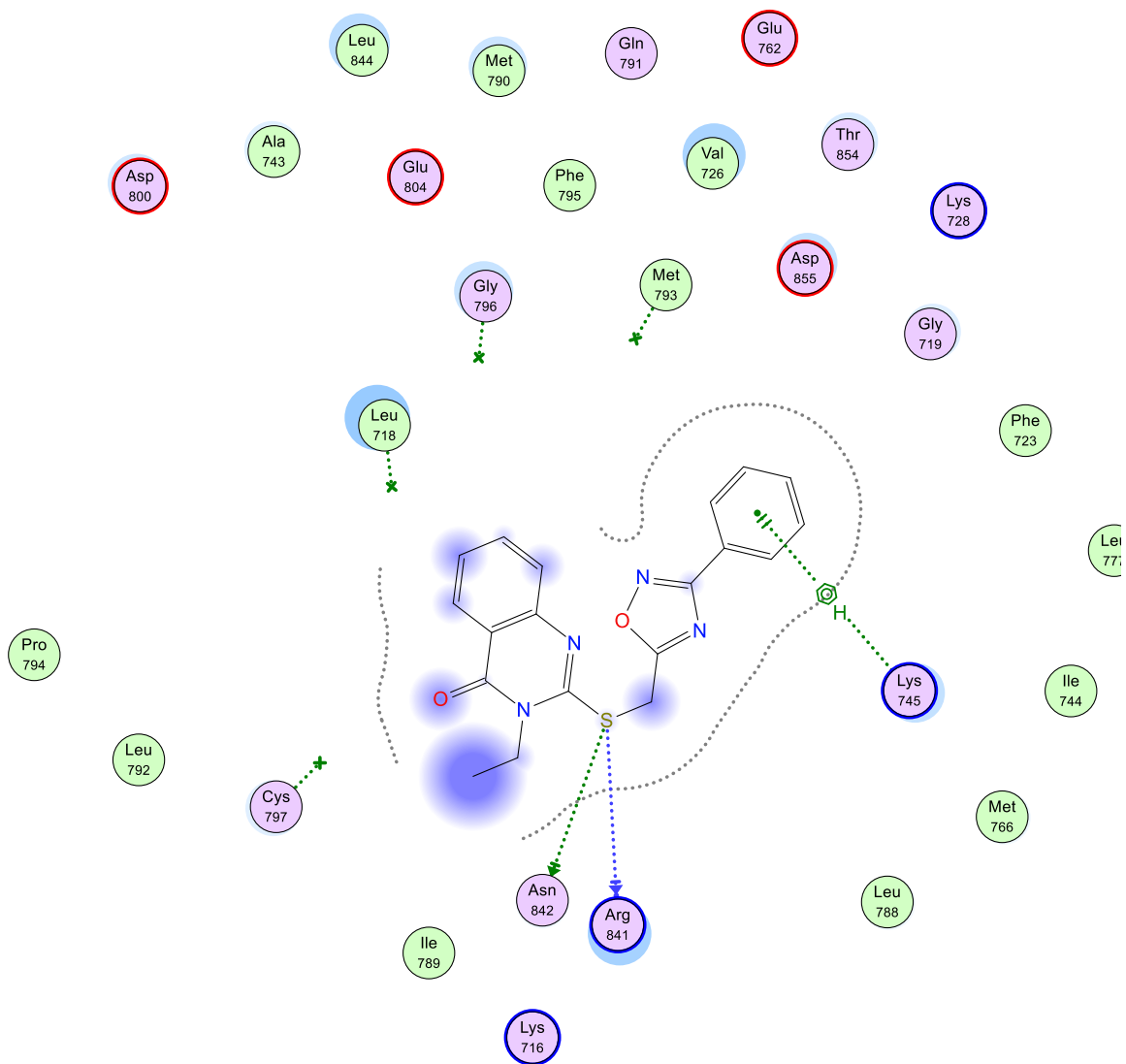
9h



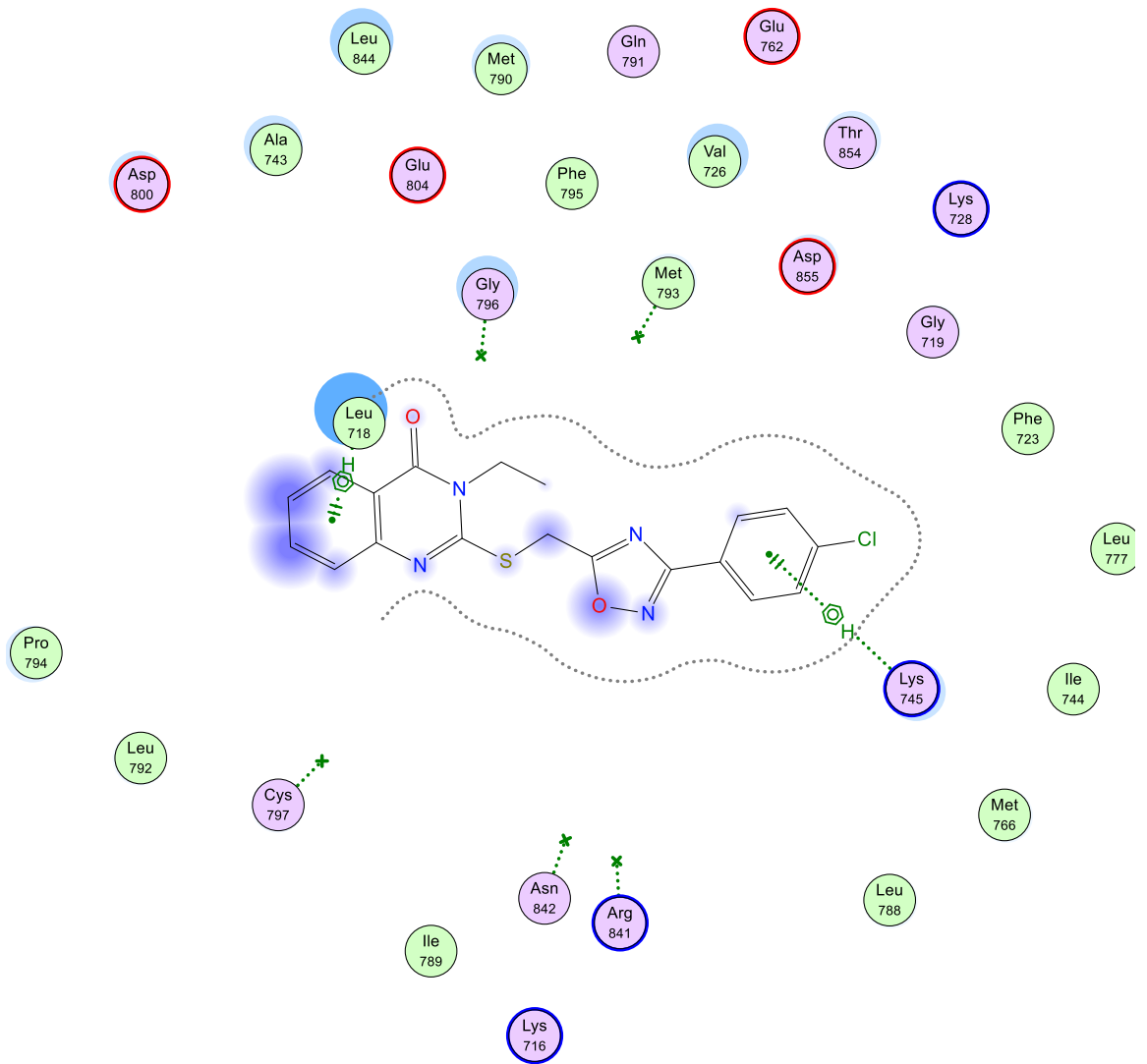
9i



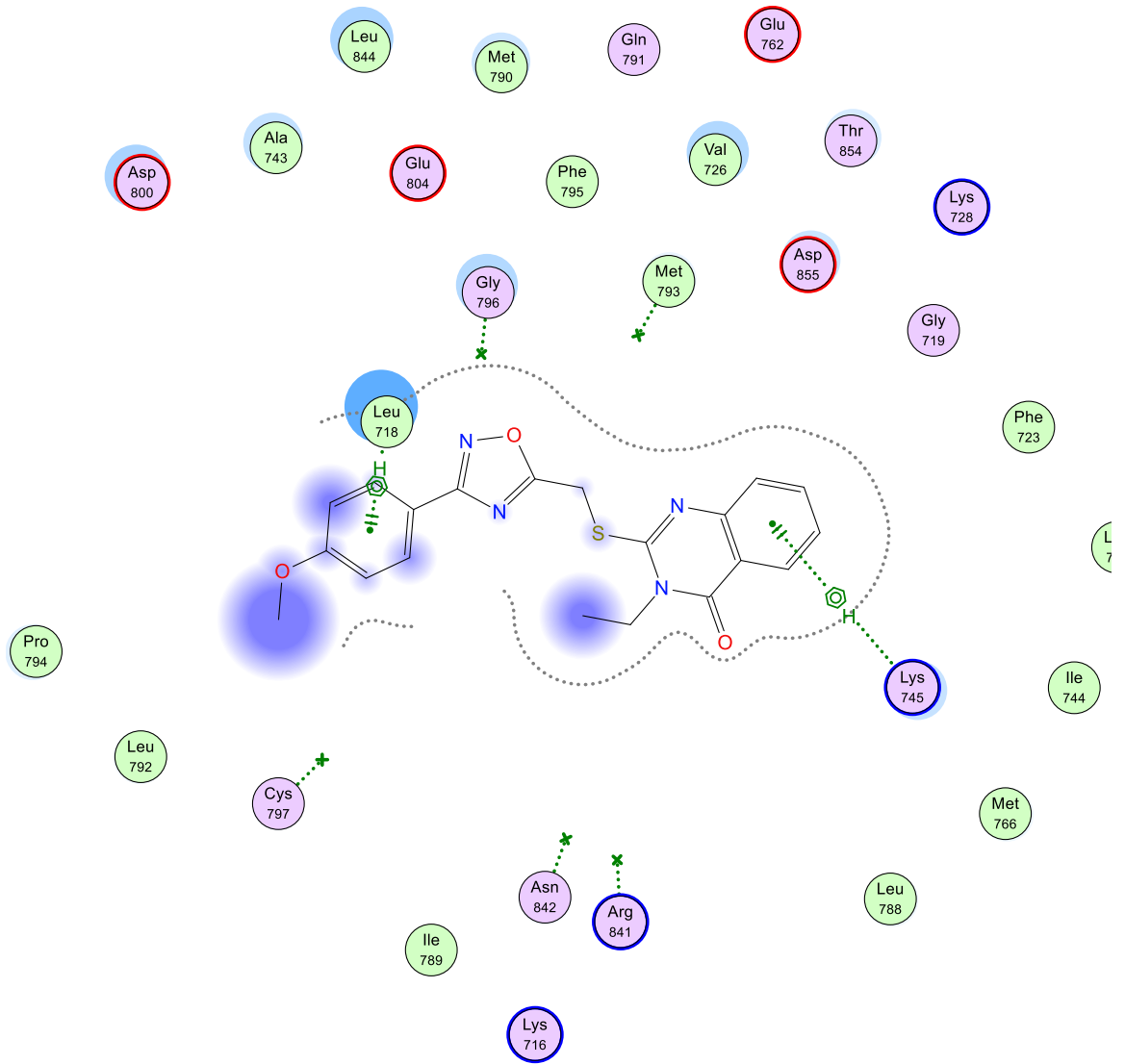
9j



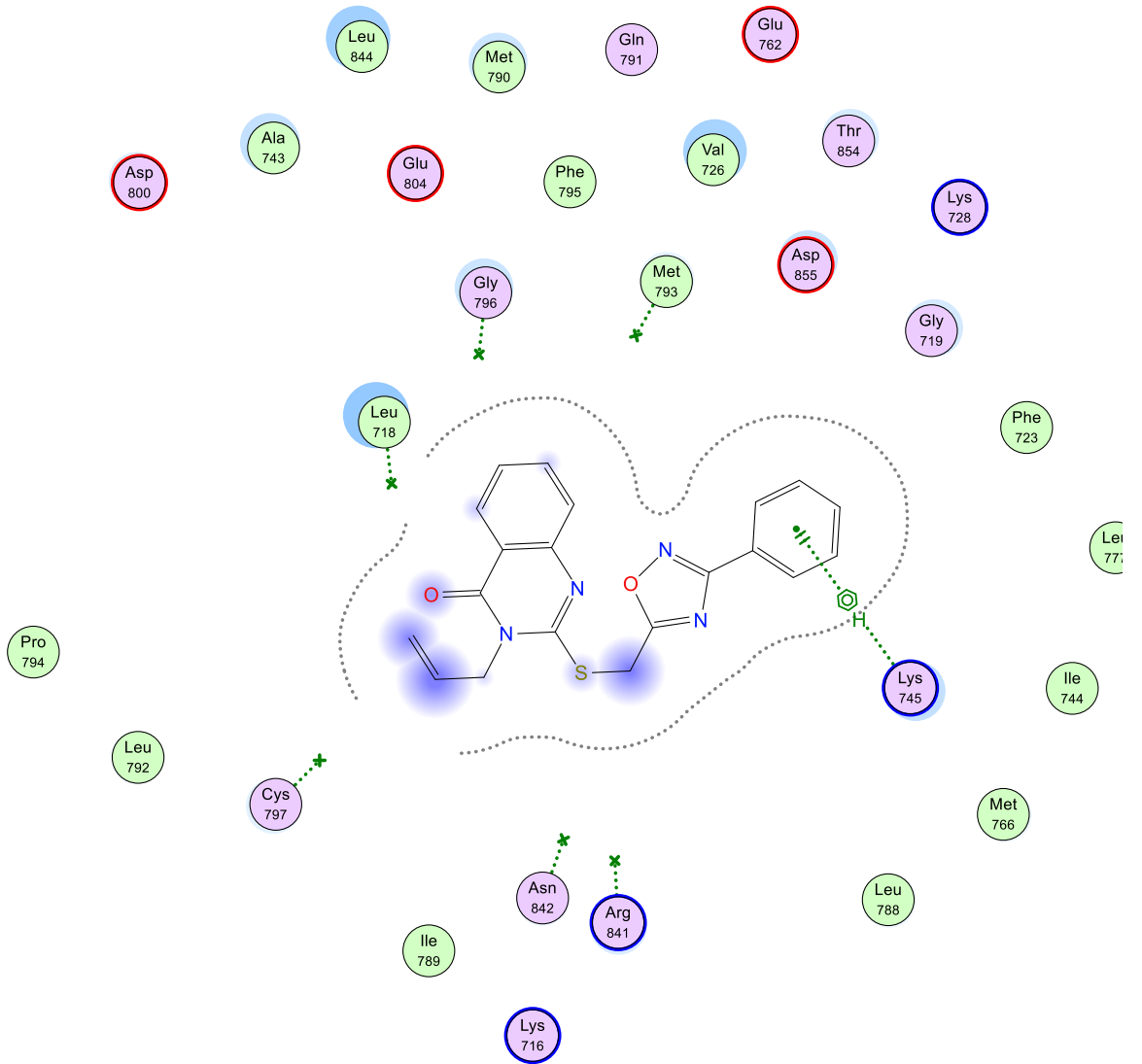
9k



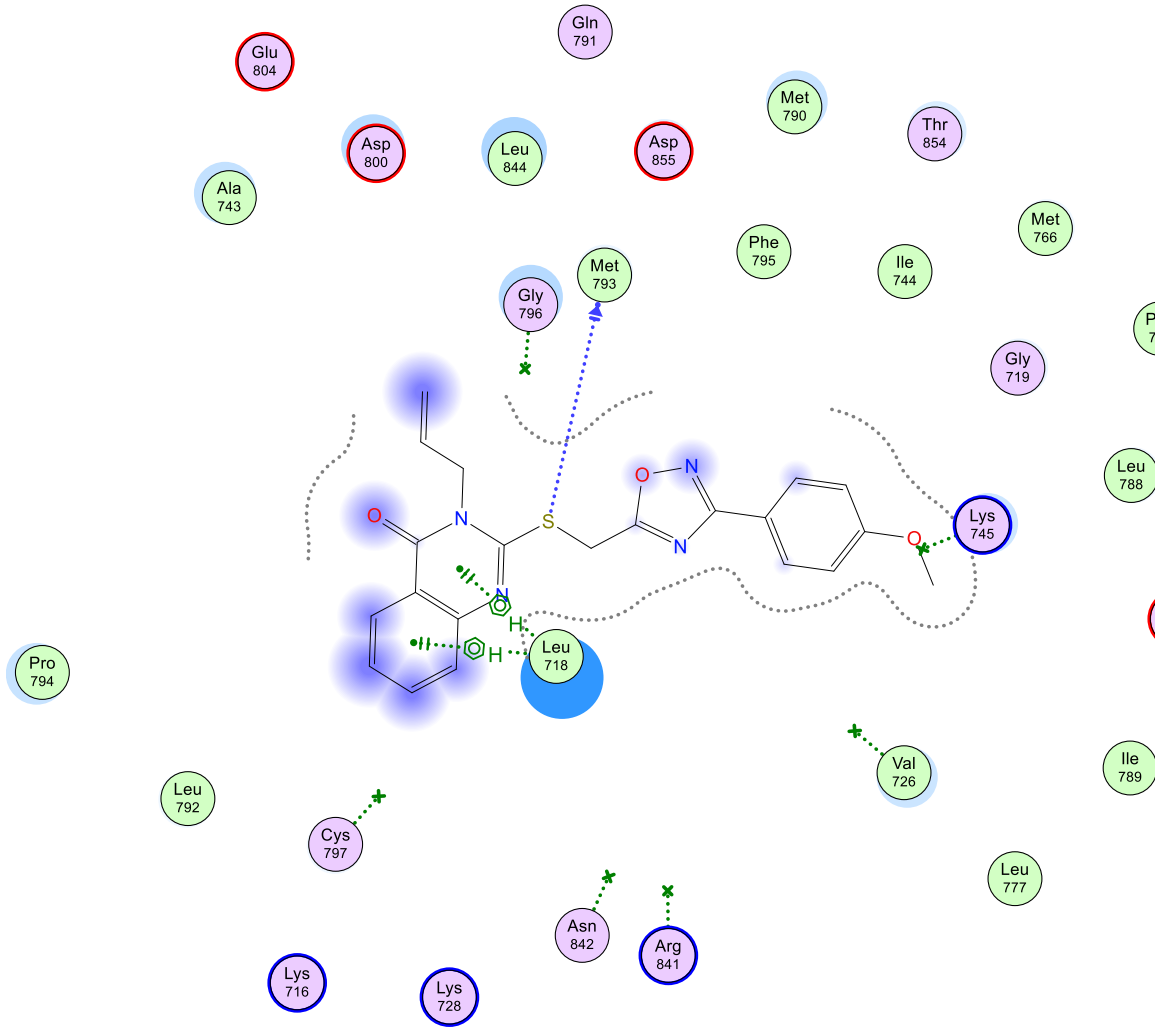
91



9m



90



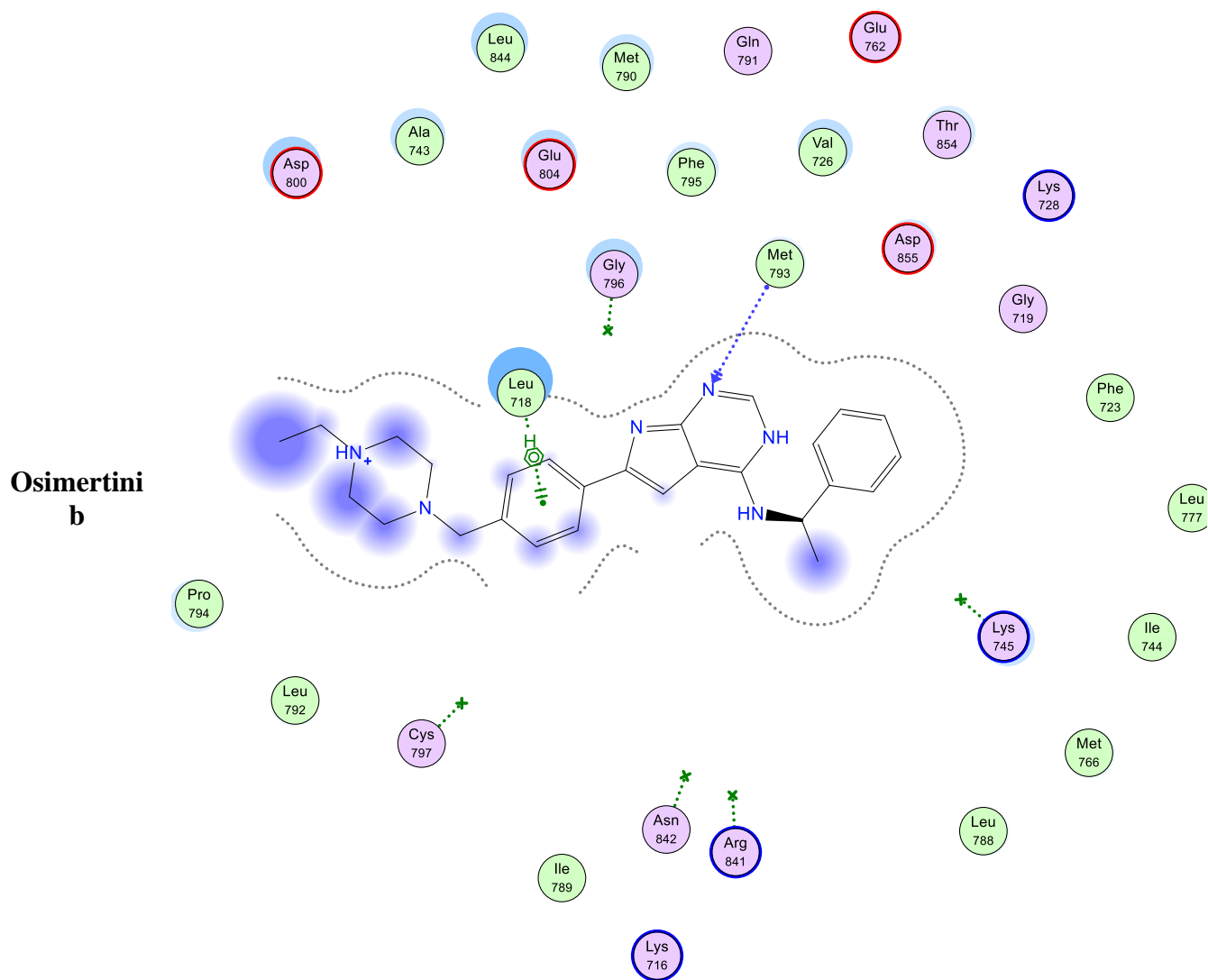
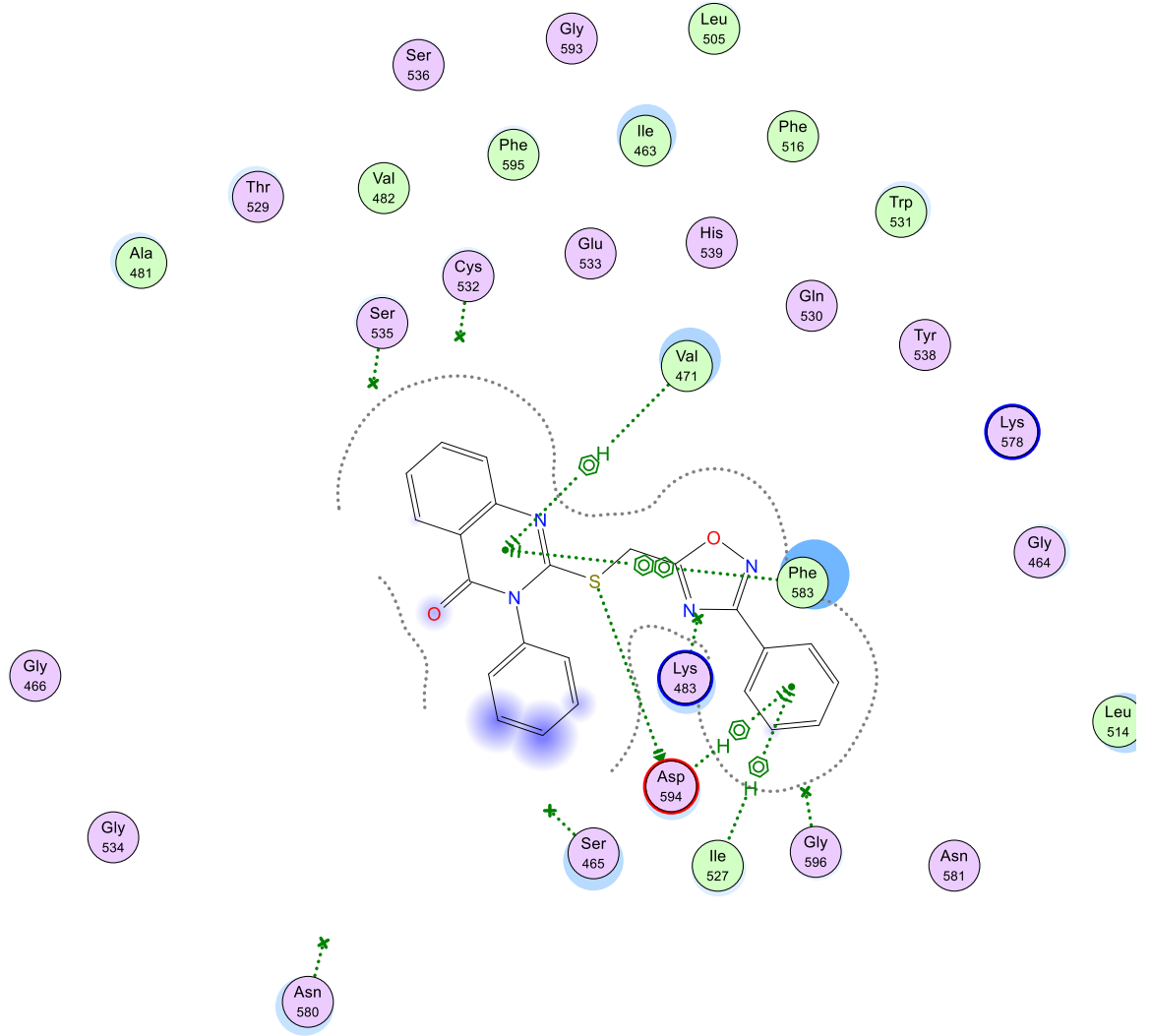
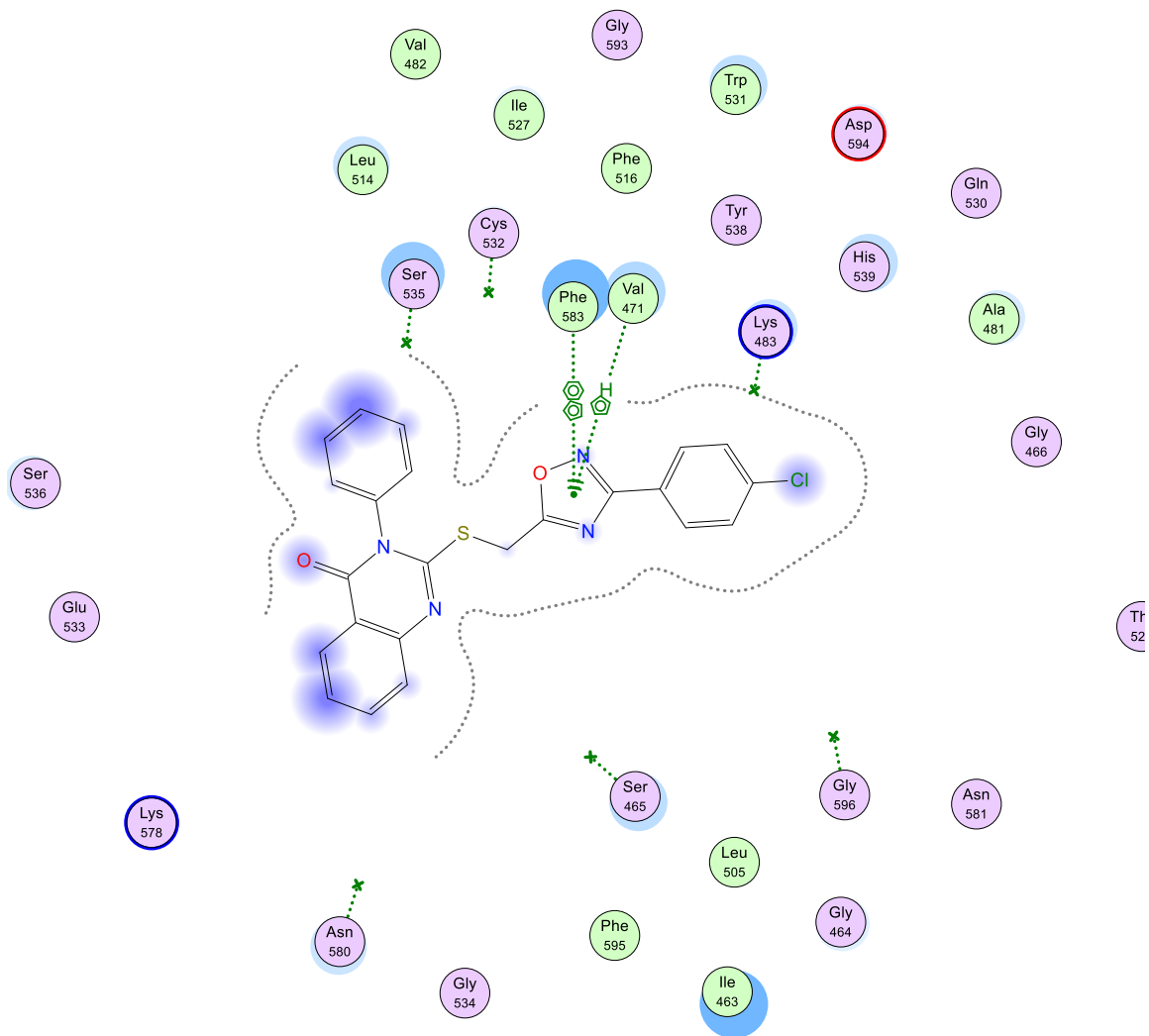


Fig. SI. 2 Docking poses of derivatives (**9a-o**) within EGFR^{T790M} (PDB ID: 2JIU) active site.

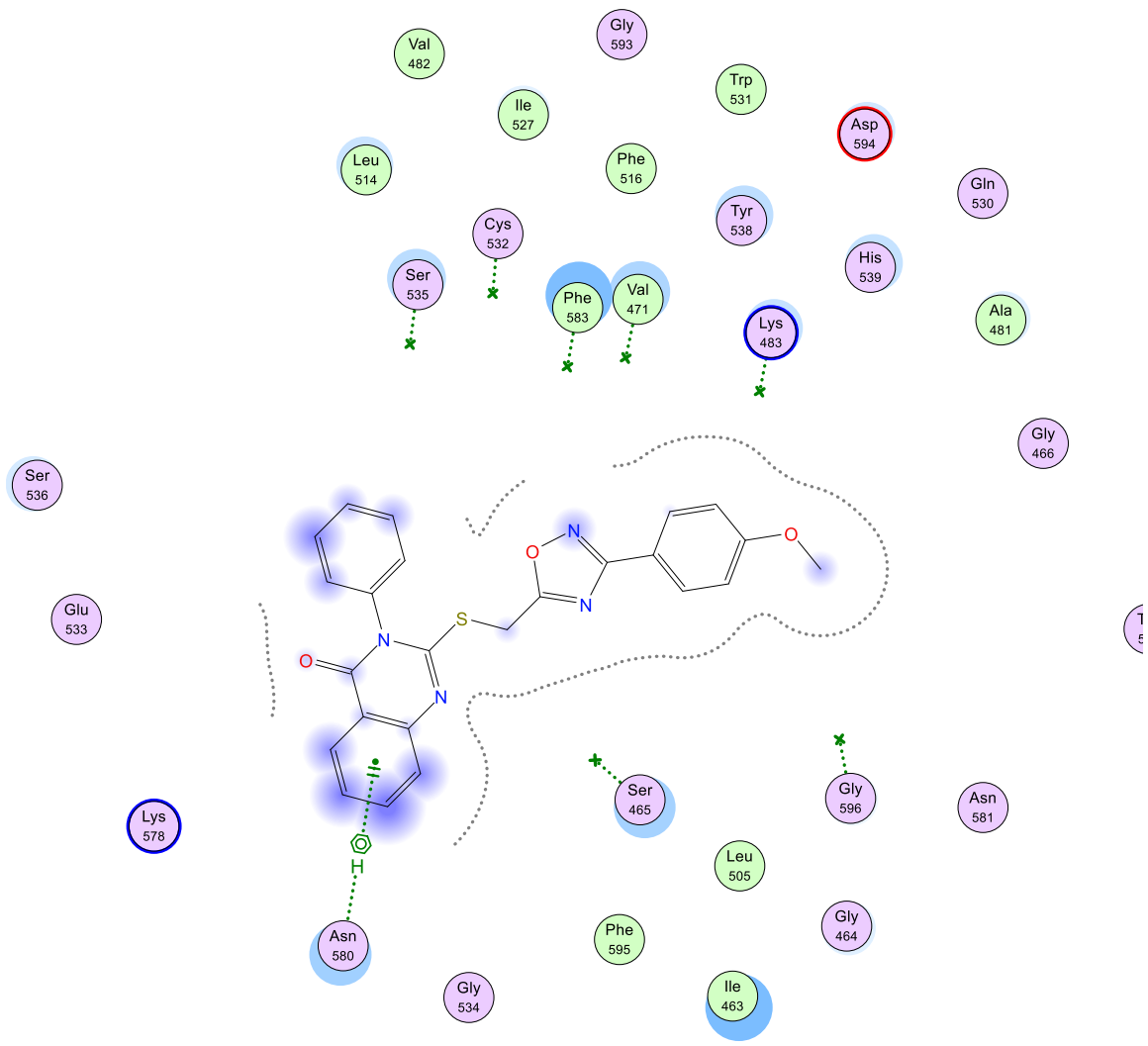
9a



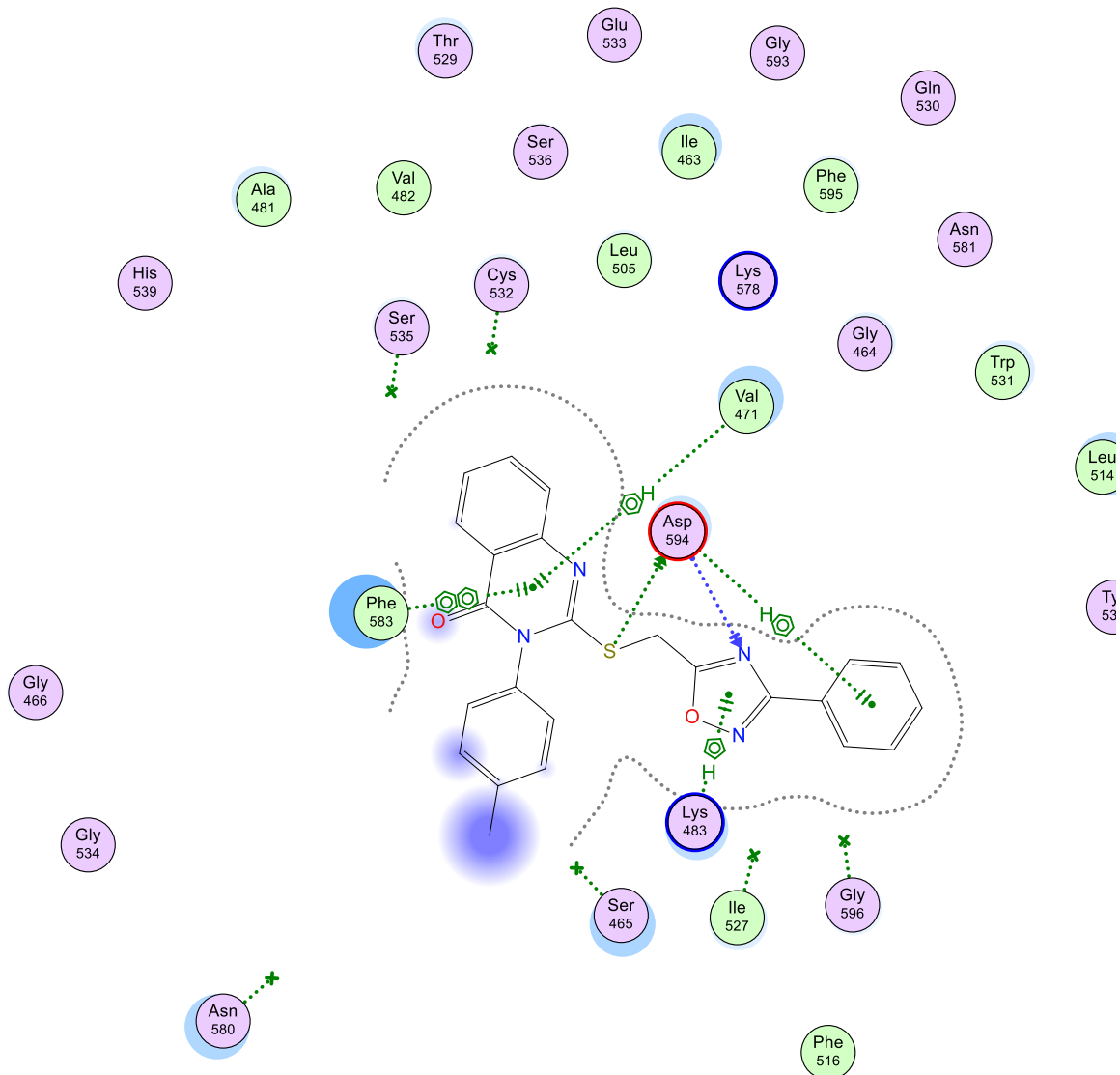
9b



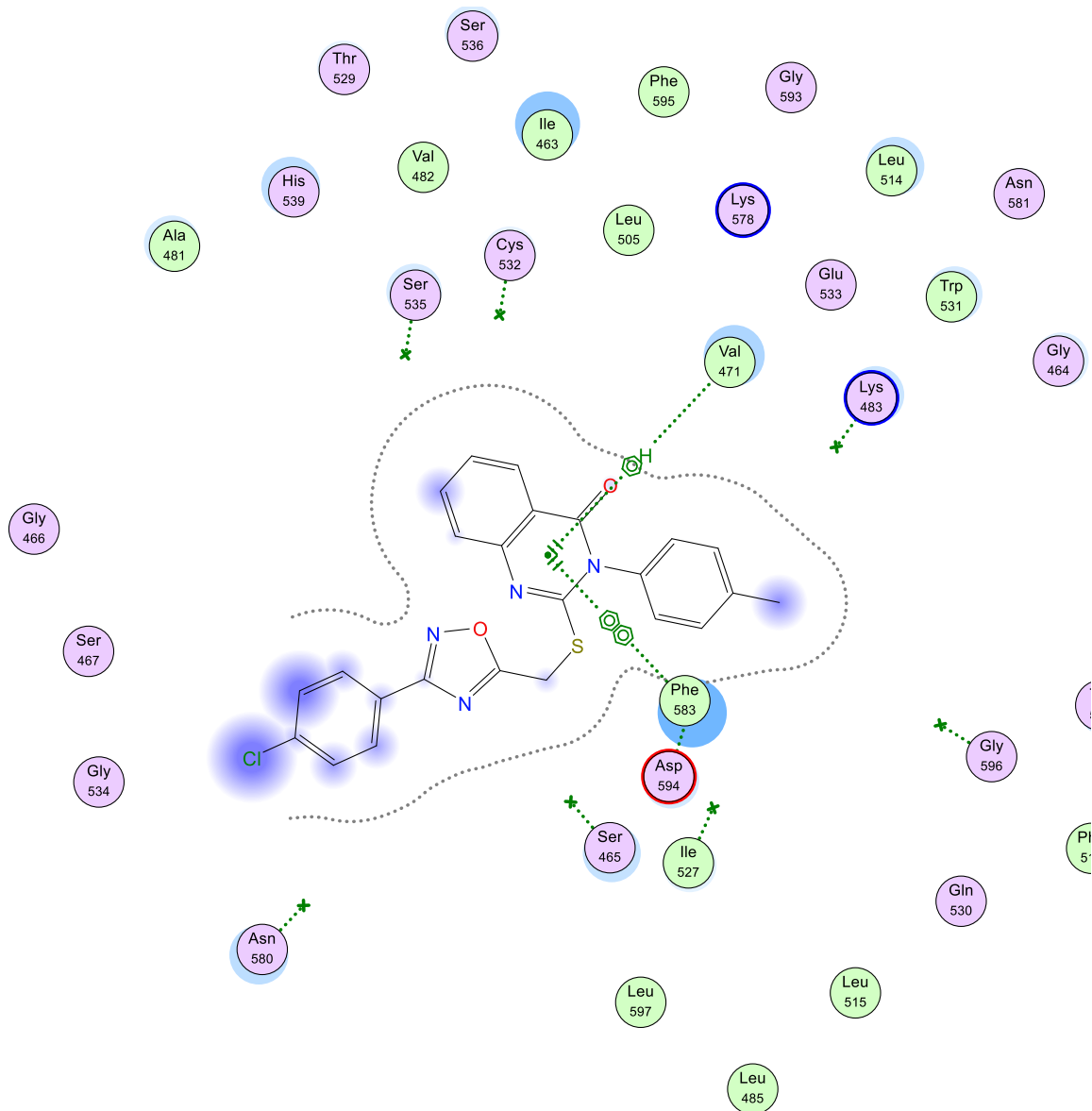
9c



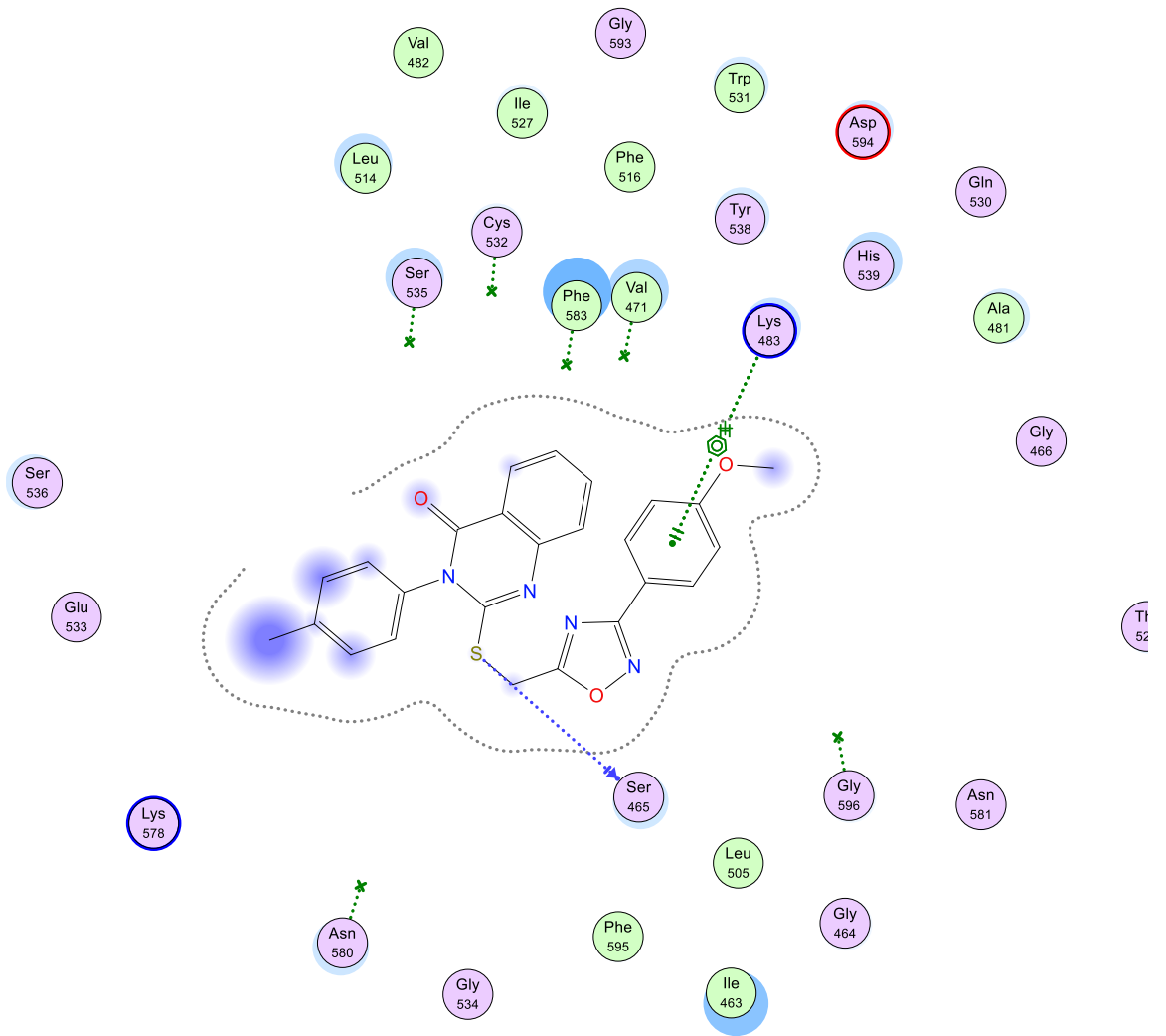
9d



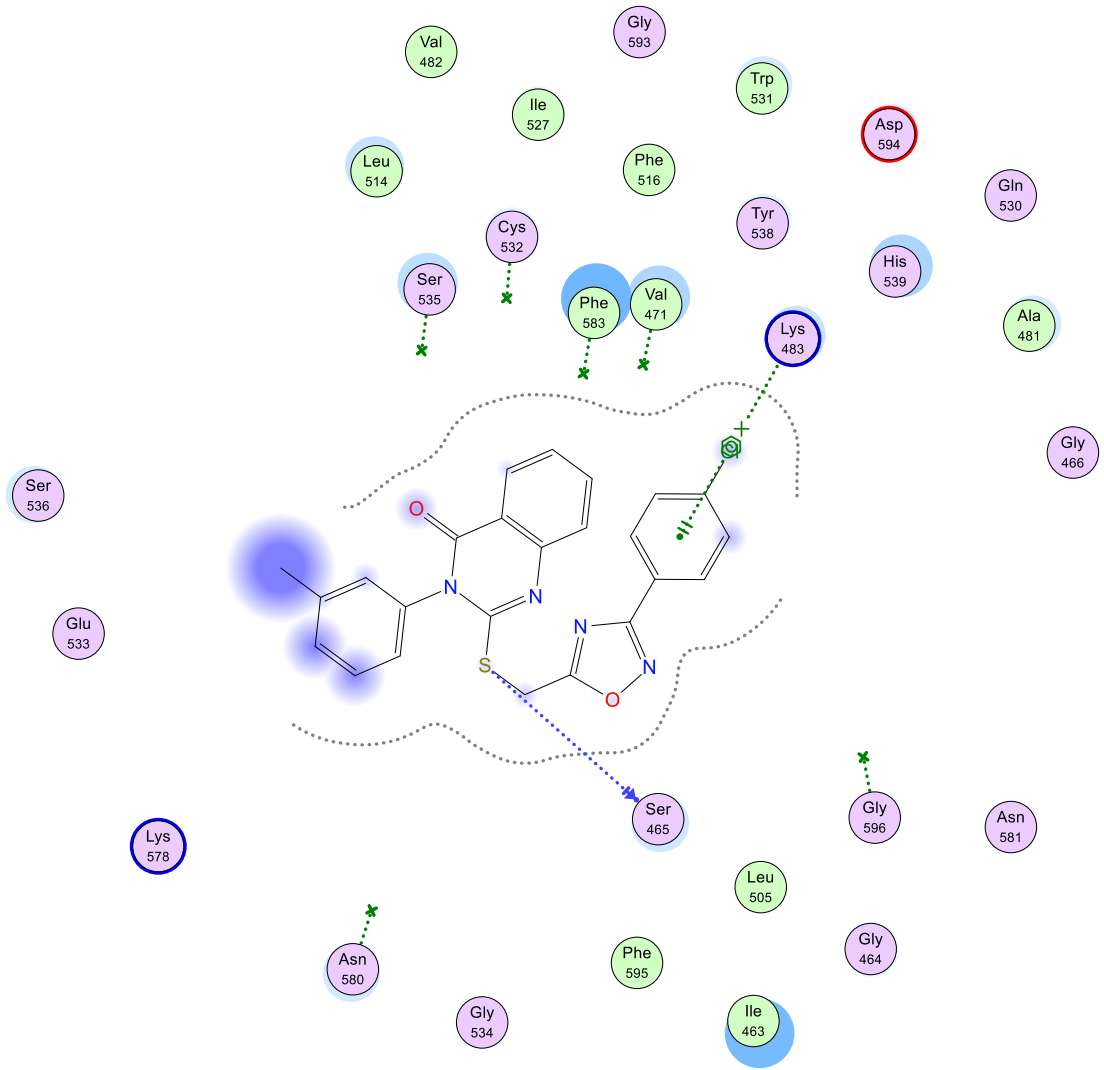
9e



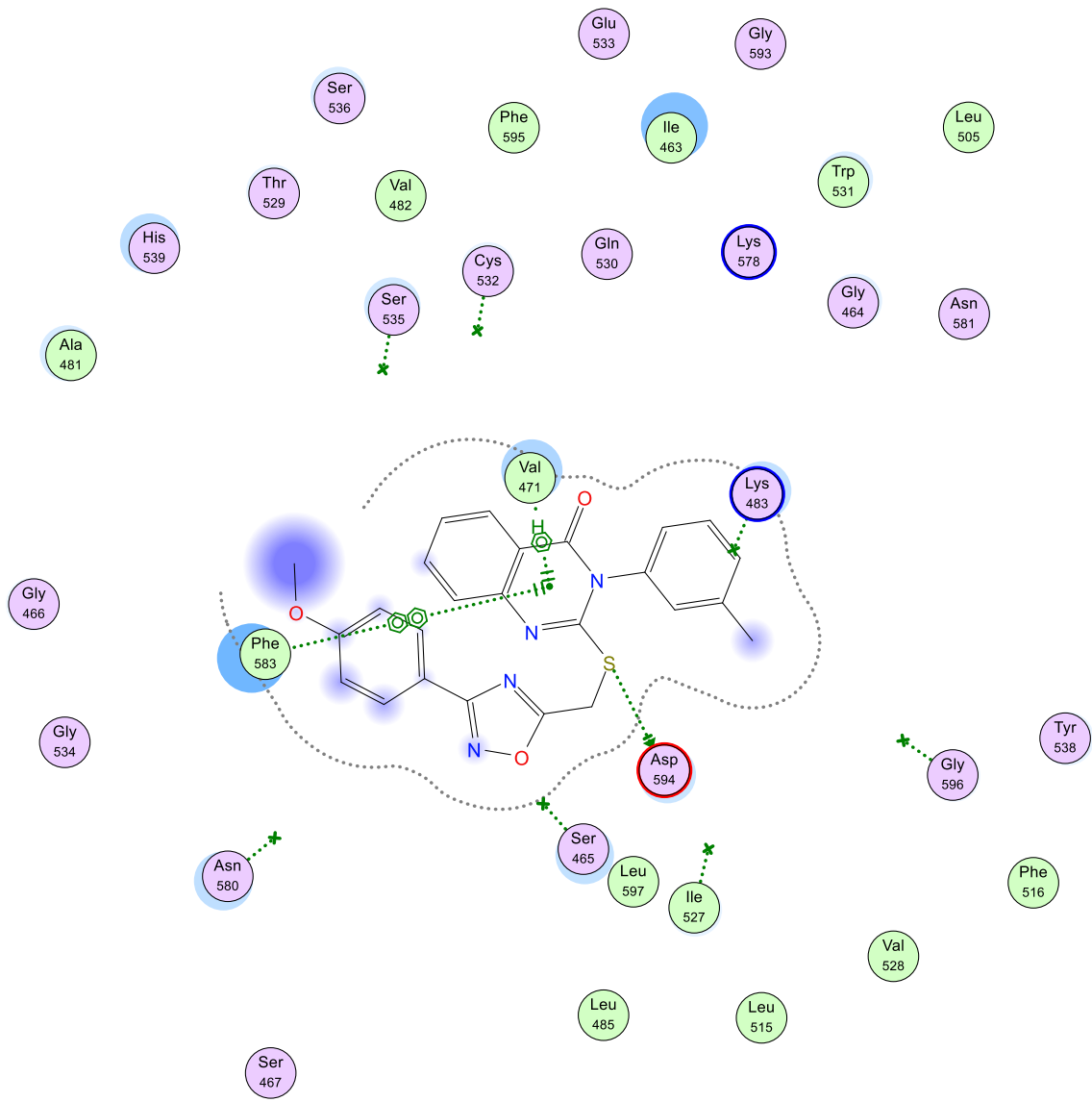
9f



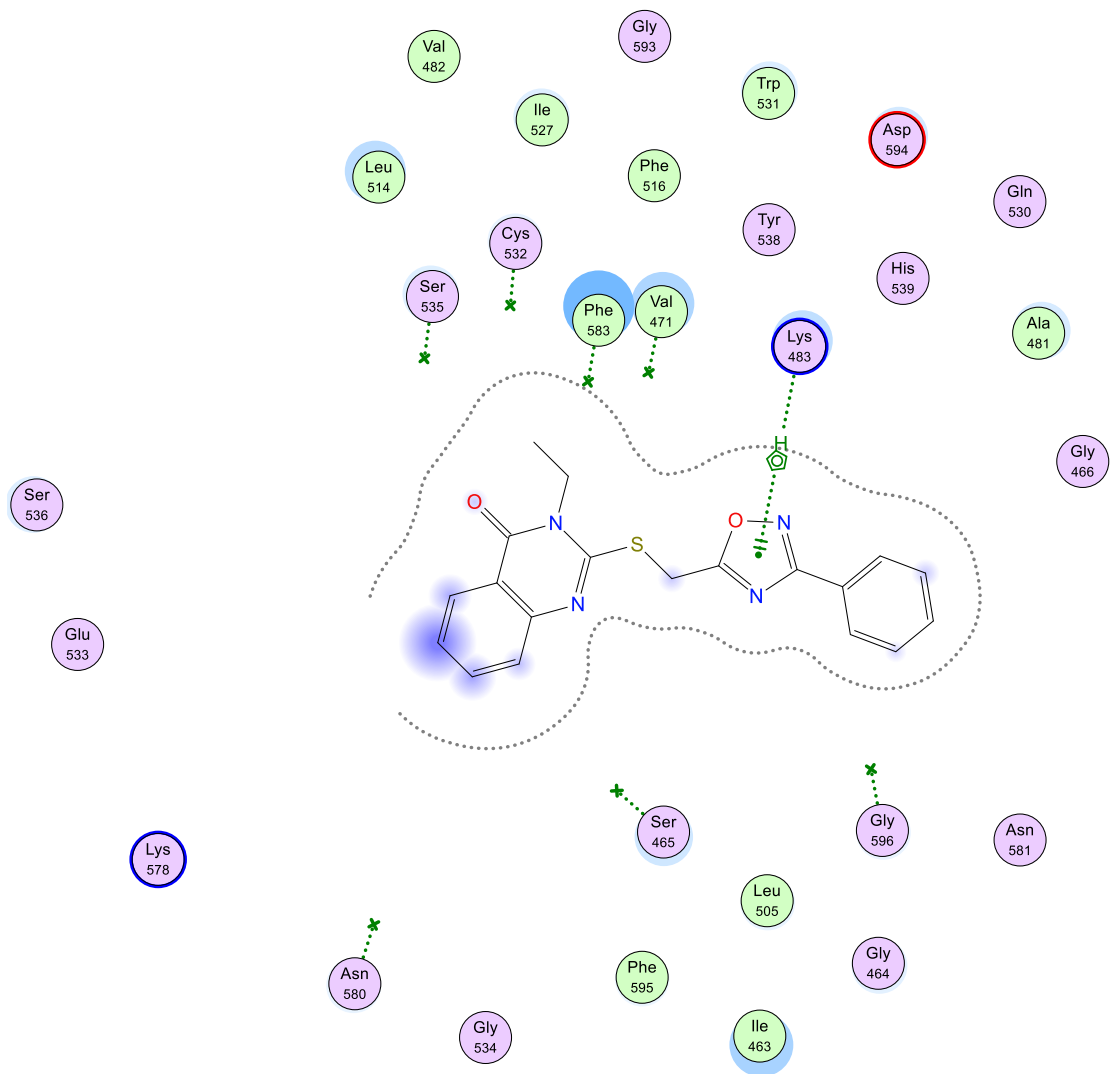
9h



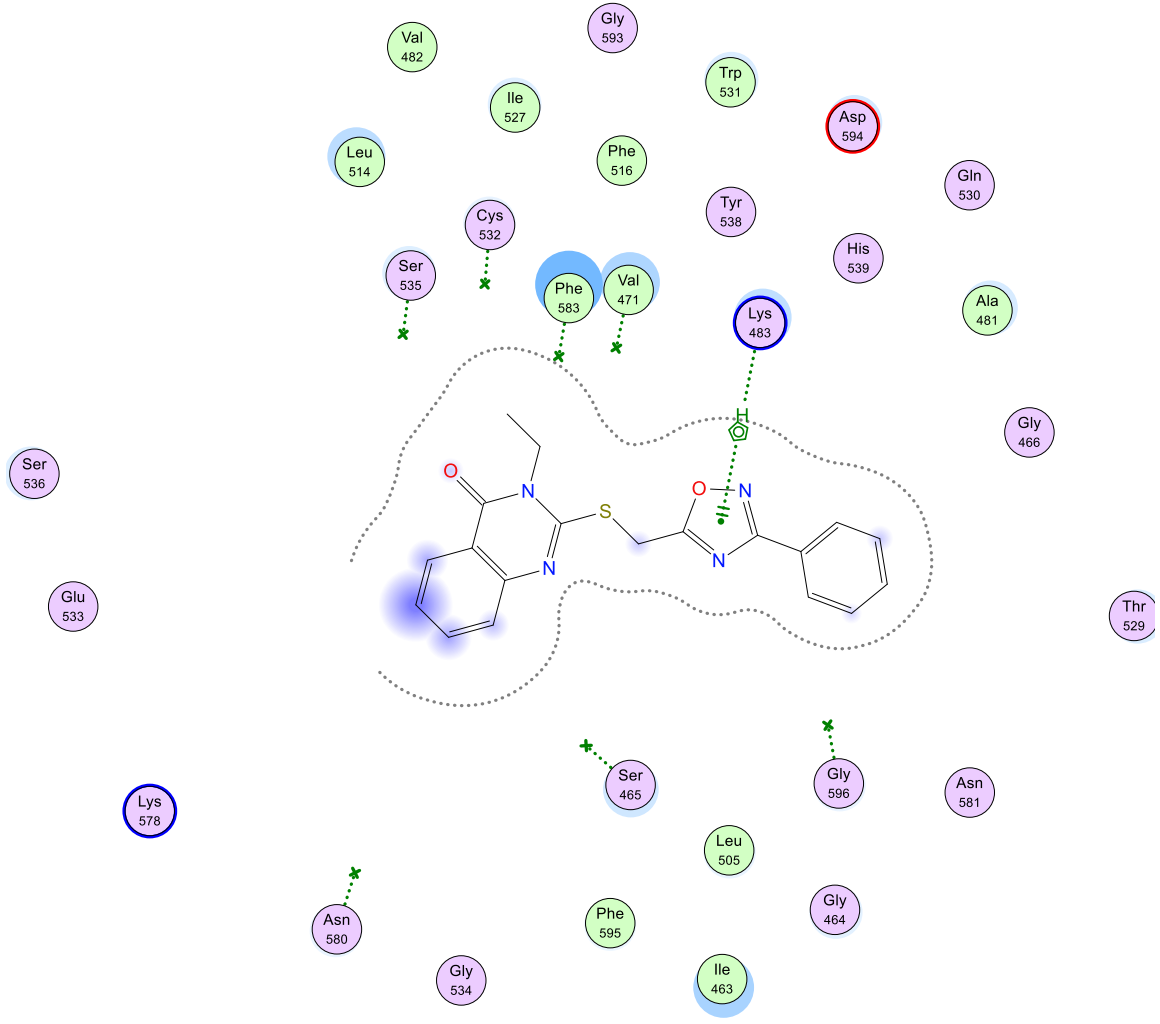
9i



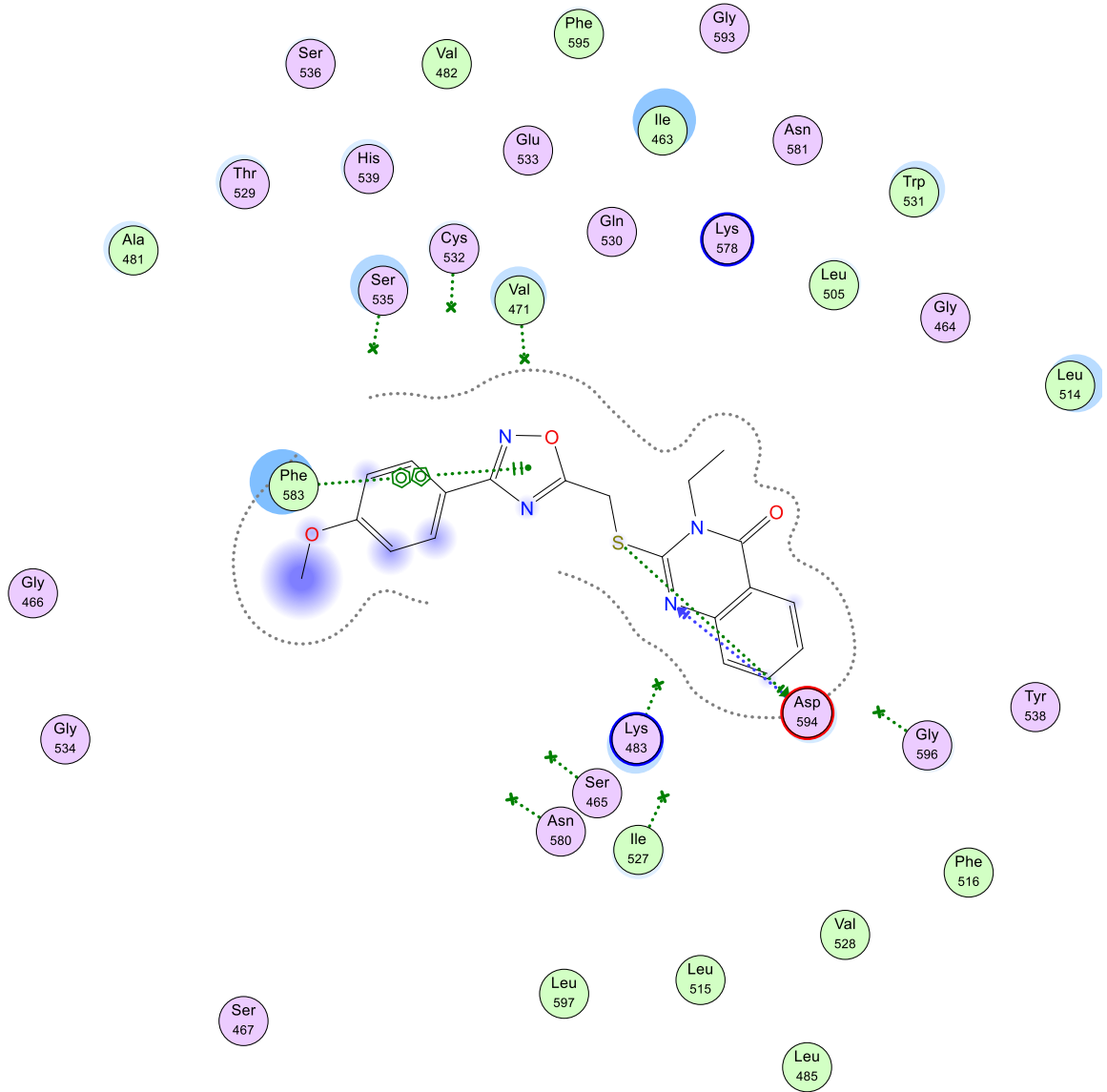
9j



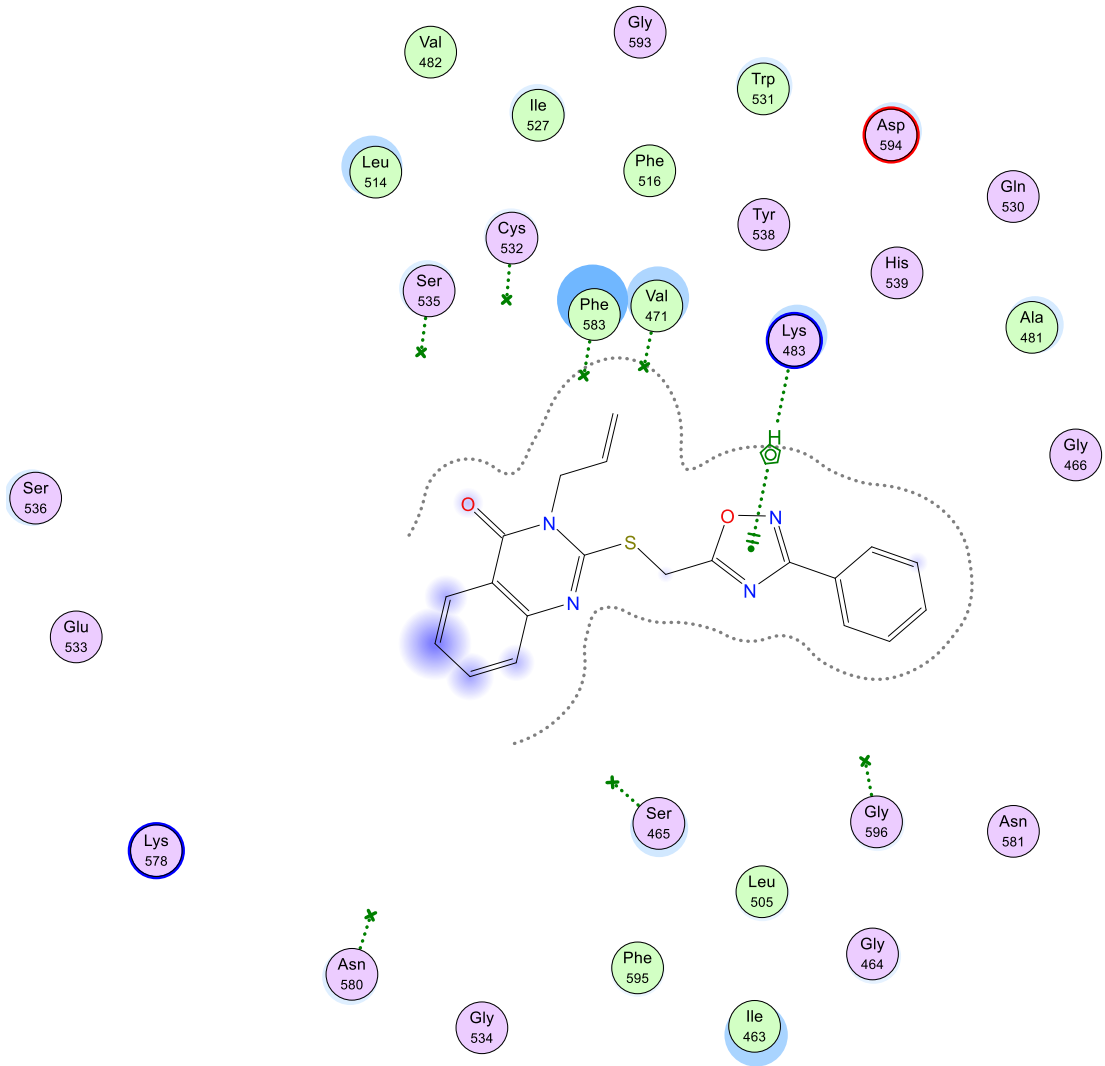
9k



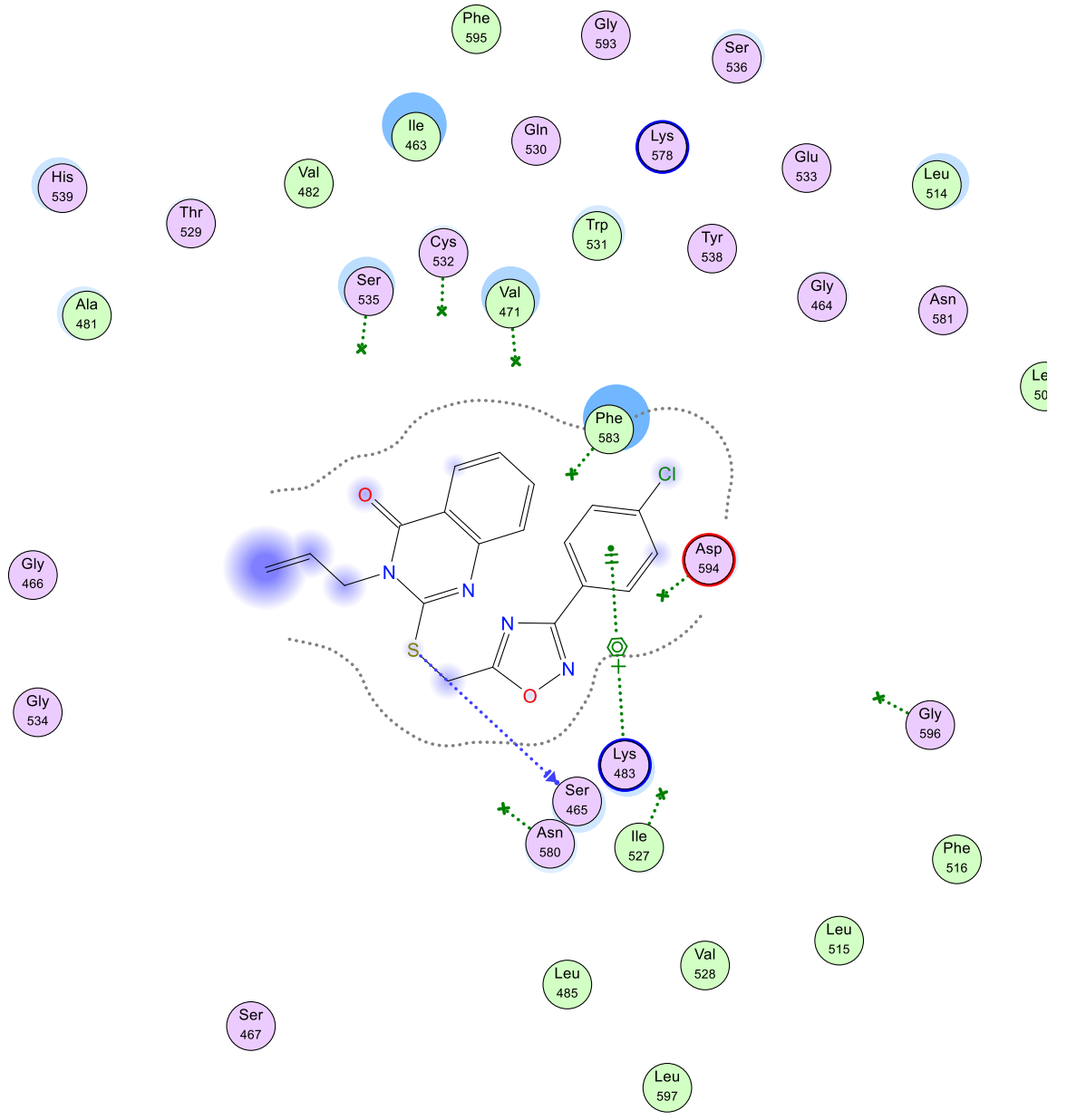
91



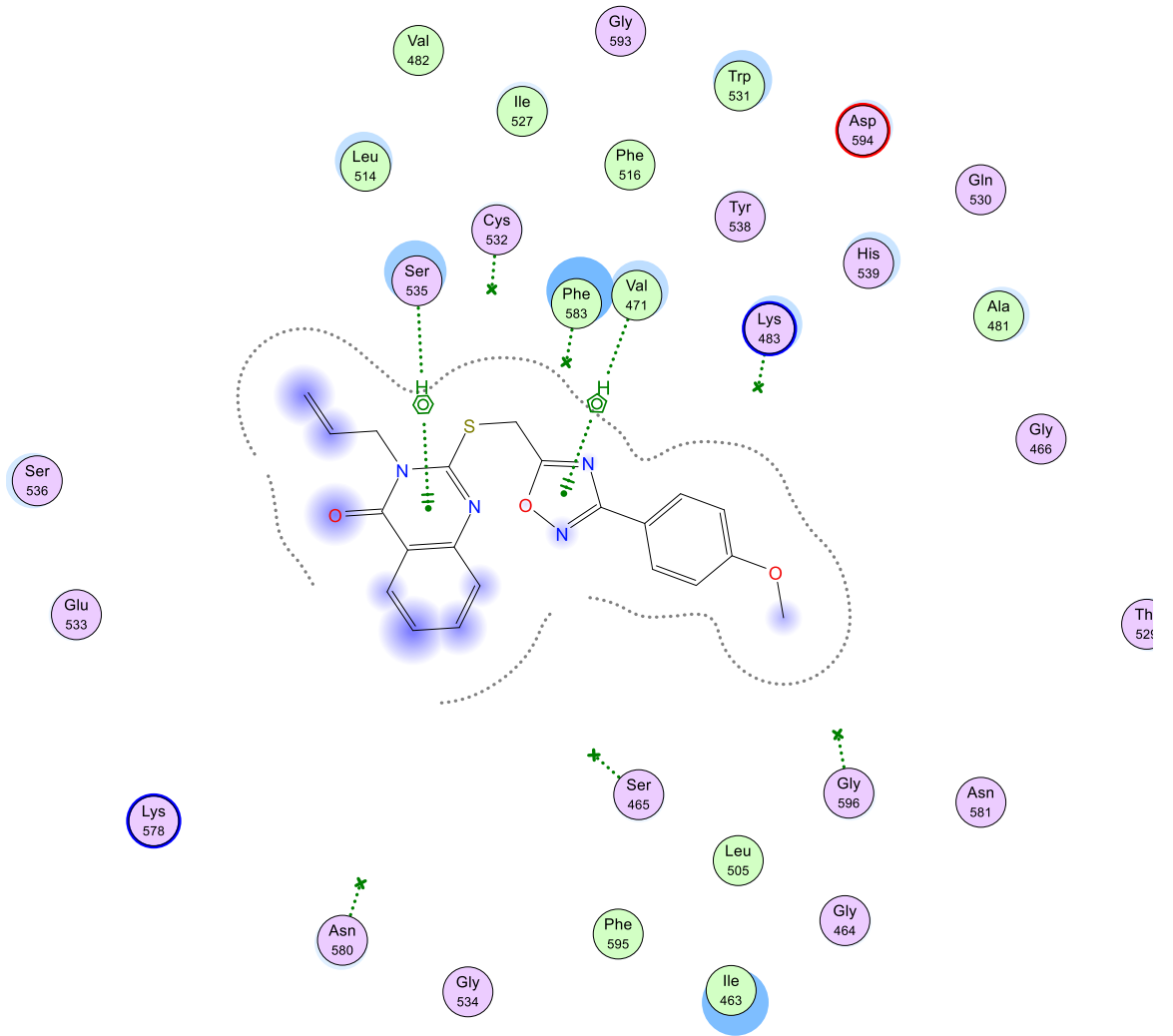
9m



9n



90



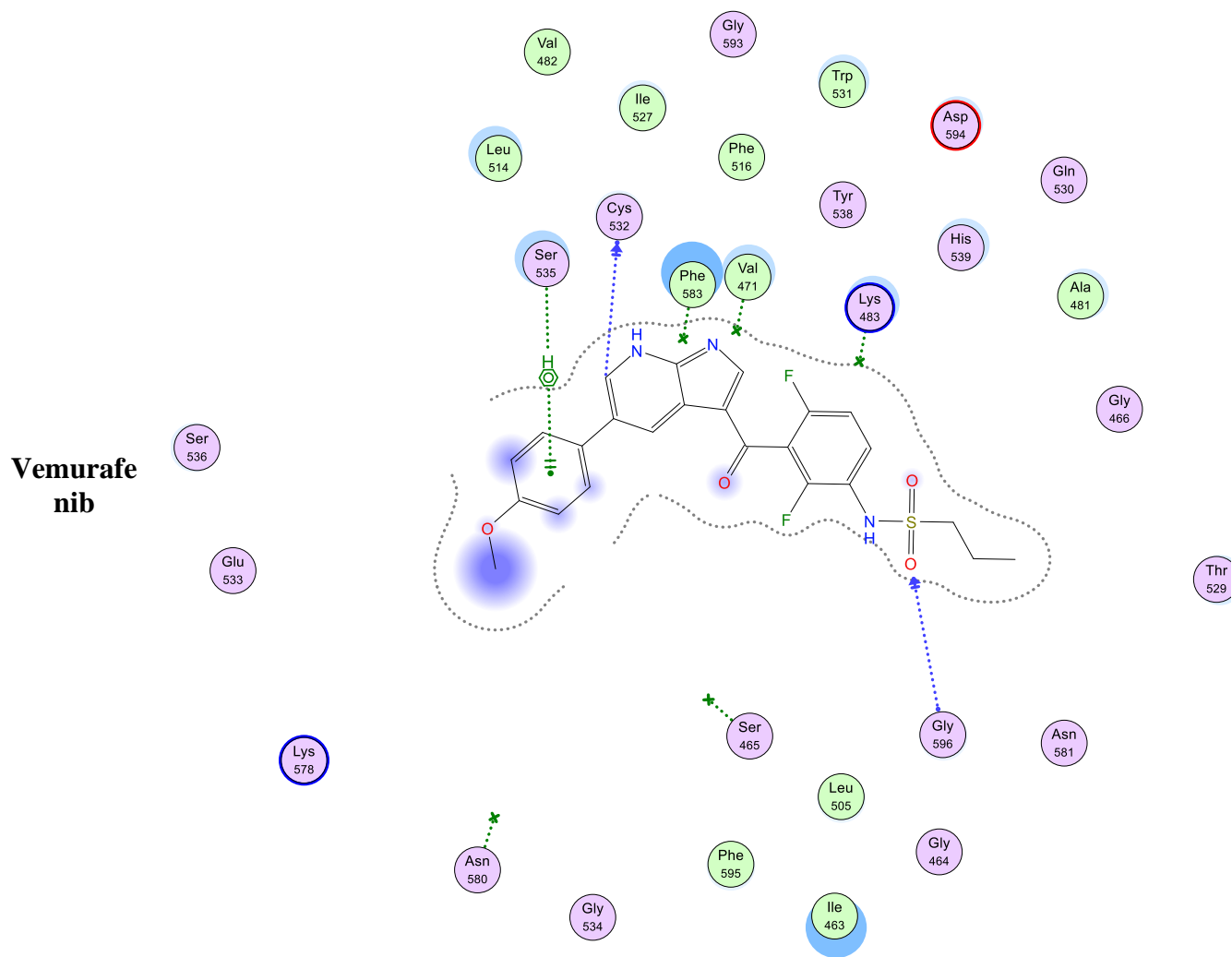


Fig. S.I. 3 Docking poses of derivatives (**9a-o**) within BRAF^{V600E} (PDB ID: 5JRQ) active site showing H-bonding and H-Pi interactions with key amino acid residues.

Appendix A

4. EXPERIMENTAL

4.1. Chemistry

General details

All the reactions progress were monitored with TLC (thin-layer chromatography) on Merck alumina-backed TLC plates and visualized under UV light. All spectral data were measured in DMSO-d₆ on a Bruker AV-300 spectrometer (300 MHz for ¹H and 75 MHz for ¹³C) in the Micro Analytical Center, Cairo University, Egypt. Chemical shifts are expressed in δ (ppm) versus internal Tetramethylsilane (TMS) = 0 ppm for ¹H and ¹³C. Also, the chemical shifts (δ) are reported in parts per million (ppm) relative to Tetramethylsilane (TMS) as internal standard, and the coupling constants (*J*) are reported in Hertz (Hz). Splitting patterns are denoted as follows: singlet (s), doublet (d), multiplet (m), triplet (t), quartet (q) and doublet of doublets (dd). Melting points (mp) were determined with a Stuart melting point instrument and are expressed in °C. Elemental analyses were carried out on Perkin device at the Microanalytical Center, Azhar University, Egypt.

4.2. Biological evaluation

4.2.1. Cytotoxic activity using MTT Assay and evaluation of IC₅₀

4.2.1.1. MTT assay

MTT assay was carried out to study the effect of compounds on mammary epithelial cells (MCF-10A). The medium in which cells were propagated contained Dulbecco's modified Eagle's medium (DMEM)/ Ham's F-12 medium (1:1) supplemented with epidermal growth factor (20 ng/mL), hydrocortisone (500 ng/mL), insulin (10 µg/mL), 2 mM glutamine and 10% foetal calf serum. After every 2-3 days, the cells were passaged using trypsin ethylenediamine tetra acetic acid (EDTA). The cells were seeded at a density of 10^4 cells mL⁻¹ in flat-bottomed culture plates containing 96 wells each. After 24 h, medium was removed from the plates and the compounds in (in 0.1% DMSO) were added (in 200 µL medium to yield a final concentration of 0.1% v/v) to the wells of plates. A single compound was designated with four wells followed by incubation of plates for 96h at 37°C. After incubation, medium was removed completely from the plates followed by addition of MTT (0.4 mg/mL in medium) to each well and subsequent incubation of plates for 3h. MTT (along with the medium) was removed and DMSO (150µL) was added to each well of the culture plates, followed by vertexing and subsequent measurement of absorbance (at 540 nm) using microplate reader. The data are shown as percentage inhibition of proliferation in comparison with controls containing 0.1% DMSO.

4.2.1.2. Assay for antiproliferative effect

To explore the antiproliferative potential of compounds MTT assay was performed according to previously reported procedure using different cell lines to explore the antiproliferative potential of compounds propidium iodide fluorescence assay was performed using different cell lines. To calculate the total nuclear DNA, a fluorescent dye (propidium iodide, PI) is used which can attach to the DNA, thus offering a quick and precise technique. PI cannot pass through the cell membrane and its signal intensity can be considered as directly proportional to quantity of cellular DNA. Cells whose cell membranes are damaged or have changed permeability are counted as dead ones. The assay was performed by seeding the cells of different cell lines at a density of 3000-7500 cells/well (in 200µl medium) in culture plates followed by incubation for 24h at 37 °C in humidified 5% CO₂/95% air atmospheric conditions. The medium was removed; the compounds were added to the plates at 10 µM concentrations (in 0.1% DMSO) in triplicates, followed by incubation for 48 h. DMSO (0.1%) was used as control. After incubation, medium was removed followed by the addition of PI (25 µl, 50µg/mL in water/medium) to each well of the plates. At -80 °C, the plates were allowed to freeze for 24 h, followed by thawing at 25°C. A fluorometer (Polar-Star BMG Tech) was used to record the readings at excitation and emission wavelengths of 530 and 620 nm for each well. The percentage cytotoxicity of compounds was calculated using the following formula:

$$\% \text{ Cytotoxicity} = \frac{A_C - A_{TC}}{A_C} \times 100$$

Where A_{TC} = Absorbance of treated cells and A_C = Absorbance of control. Erlotinib was used as positive control in the assay.

4.2.1.3. EGFR inhibitory assay

EGFR-TK assay was performed to evaluate the inhibitory potency of the most potent compounds against EGFR. Baculoviral expression vectors including pBlueBacHis2B and pFASTBacHTc were used separately to clone 1.6 kb cDNA coding for EGFR cytoplasmic domain (EGFR-CD, amino acids 645–1186). 5' upstream to the EGFR sequence comprised a sequence that encoded (His)₆. Sf-9 cells were infected for 72h for protein expression. The pellets of Sf-9 cells were solubilized in a buffer containing sodium vanadate (100 μM), aprotinin (10 μg/mL), triton (1%), HEPES buffer (50mM), ammonium molybdate (10 μM), benzamidine HCl (16 μg/mL), NaCl (10 mM), leupeptin (10 μg/mL) and pepstatin (10 μg/mL) at 0°C for 20 min at pH 7.4, followed by centrifugation for 20 min. To eliminate the non-specifically bound material, a Ni-NTA super flow packed column was used to pass through and wash the crude extract supernatant first with 10 mM and then with 100 mM imidazole. Histidine-linked proteins were first eluted with 250 and then with 500 mM imidazole subsequent to dialysis against NaCl (50 mM), HEPES (20 mM), glycerol (10%) and 1 μg/mL each of aprotinin, leupeptin and pepstatin for 120 min. The purification was performed either at 4 °C or on ice. To record autophosphorylation level, EGFR kinase assay was carried out on the basis of DELFIA/Time-Resolved Fluorometry. The compounds were first dissolved in DMSO absolute, subsequent to dilution to appropriate concentration using HEPES (25 mM) at pH 7.4. Each compound (10 μL) was incubated with recombinant enzyme (10 μL, 5 ng for EGFR, 1:80 dilution in 100 mM HEPES) for 10 min at 25°C, subsequent to the addition of 5X buffer (10 μL, containing 2 mM MnCl₂, 100 μM Na₃VO₄, 20 mM HEPES and 1 mM DTT) and ATP-MgCl₂ (20 μL, containing 0.1 mM ATP and 50 mM MgCl₂) and incubation for 1h. The negative and positive controls were included in each plate by the incubation of enzyme either with or without ATP-MgCl₂. The liquid was removed after incubation and the plates were washed thrice

using wash buffer. Europium-tagged antiphosphotyrosine antibody (75 μ L, 400 ng) was added to each well followed by incubation of 1h and then washing of the plates using buffer. The enhancement solution was added to each well and the signal was recorded at excitation and emission wavelengths of 340 at 615 nm. The autophosphorylation percentage inhibition by compounds was calculated using the following equation:

$$100\% - [(negative\ control)/(positive\ control) - (negative\ control)]$$

Using the curves of percentage inhibition of eight concentrations of each compound, IC₅₀ was calculated. Majority of signals detected by antiphosphotyrosine antibody were from EGFR because the enzyme preparation contained low impurities.

4.2.1.4. BRAF kinase assay

V^{600E} mutant BRAF kinase assay was performed to investigate the activity of tested compounds against BRAF. Mouse full-length GST-tagged BRAF^{V600E} (7.5 ng, Invitrogen, PV3849) was pre-incubated with drug (1 μ L) and assay dilution buffer (4 μ L) for 60 min at 25°C. In assay dilution buffer, a solution (5 μ L) containing MgCl₂ (30 mM), ATP (200 μ M), recombinant human full length (200 ng) and N-terminal His-tagged MEK1 (Invitrogen) was added to start the assay, subsequent to incubation for 25 min at 25°C. The assay was stopped using 5X protein denaturing buffer (LDS) solution (5 μ L). To further denature the protein, heat (70° C) was applied for 5 min. 4-12% precast NuPage gel plates (Invitrogen) were used to carry out electrophoresis (at 200 V). 10 μ L of each reaction was loaded into the precast plates and electrophoresis was allowed to proceed. After completion of electrophoresis, the front part of the precast gel plate (holding hot ATP) was cut and afterwards cast-off. The dried gel was developed using a phosphor screen. A reaction without active enzyme was used as negative control while that containing no inhibitor

served as positive control. To study the effect of compounds on cell-based pERK1/2 activity in cancer cells, commercially available ELISA kits (Invitrogen) were used according to manufacturer's instructions.

4.2.1.6. Cell apoptosis assay

Apoptosis was determined by flow cytometry based on the Annexin-V-fluoresce in isothiocyanate (FITC) and propidium iodide (PI) staining kit (BD Pharmingen, San Diego, USA) [25, 26]. Apoptosis was determined by flow cytometry based on the Annexin-V-fluoresce in isothiocyanate (FITC) and propidium iodide (PI) staining kit (BD Pharmingen, San Diego, USA). Apoptotic cells were defined as Annexin-V-positive. Cells were grown to approximately ~70% confluence and exposed to different concentrations of compounds (0, 2, 4, 6 and 8 $\mu\text{mol/L}$) for 24 h. Treated cells were trypsinized, washed twice with PBS and transferred into micro centrifuge tubes for centrifugation at 1000 rpm for 5 min at room temperature, then resuspended in binding buffer, 5 μL of FITC and PI were added to Eppendorf tube, cells were vortexed, incubated for 15 min at room temperature in dark. Subsequently, cells were analyzed by flow cytometry (Becton Dickinson, Franklin Lakes, and USA).

4.3. Statistical analysis

Computerized Prism 5 program was used to statistically analyzed data using one-way ANOVA test followed by Tukey's as post ANOVA for multiple comparison at $P \leq 0.05$. Data were presented as mean \pm SEM.